Developmental Studies of a Ground Louse, *Zorotypus caudelli* Karny, 1927 (Insecta: Zoraptera, Zorotypidae)

January 2014

Yuta MASHIMO

Developmental Studies of a Ground Louse, *Zorotypus caudelli* Karny, 1927 (Insecta: Zoraptera, Zorotypidae)

A Dissertation Submitted to

the Graduate School of Life and Environmental Sciences,

the University of Tsukuba

in Partial Fulfillment of the Requirements

for the Degree of Doctor of Philosophy in Science

(Doctoral Program in Biological Sciences)

Yuta MASHIMO

CONTENTS

ABSTRACT ---------- 1

INTRODUCTION ---------- 3

MATERIALS AND METHODS ---------- 8

1. Materials ---------- 8

2. Fixation ---------- 8

3. External morphology ---------- 9

4. Histology ---------- 11

5. Terminology ---------- 12

RESULTS ---------- 13

1. Mating and oviposition ---------- 13

2. Egg structure ---------- 13

3. Embryonic development ---------- 15

3.1. Stage 1 ---------- 16

3.2. Stage 2 ---------- 16

3.3. Stage 3 ---------- 16

3.4. Stage 4 ---------- 17

3.5. Stage 5 ---------- 17

3.6. Stage 6 ---------- 17

3.7. Stage 7 ---------- 18

3.8. Stage 8 ---------- 19

3.9. Stage 9 ---------- 20

3.10. Stage 10 ---------- 20

3.11. Stage 11 ---------- 21

3.12. Stage 12 ---------- 21

3.13. Hatching ---------- 23
4. Postembryonic development ---------- 23
4.1. Determination of the number of larval instars ---------- 23
4.2 Duration of larval instars ---------- 24
4.3. Morphological features in each larval instar ---------- 24
4.3.1. Instar I ---------- 25
4.3.2. Instar II ---------- 27
4.3.3. Instar III ---------- 28
4.3.4. Instar IV ---------- 28
4.3.5. Instar V ---------- 29
DISCUSSION ---------- 33
1. Egg structure ---------- 33
2. Formation of appendages ---------- 34
3. Egg tooth---------- 35
4. Formation of Embryo and blastokinesis ---------- 36
5. Recognition of larval instars ---------- 38
6. Wing dimorphism ---------- 40
7. Sexual dimorphism ---------- 42
8. Antennal development ---------- 43
9. Homology of thoracic sclerite ---------- 45
10. Phylogenetic implications of comparative embryology -------- 47
10.1. Affiliation of Zoraptera: Polyneoptera or Acercaria? ----- 47
10.2. Affinity of Zoraptera within Polyneoptera ---------- 52
ACKNOWLEDGMENTS ---------- 60
LITERATURE CITED ---------- 62

TABLES ---------- 84
FIGURES ---------- 88

ABSTRACT

Zoraptera is a poorly understood insect group and remains a systematic enigma, even in the “age of phylogenomics”. Despite greatly increased knowledge about Zoraptera, the information on their development is still totally lacking. The present study is the first developmental study of Zoraptera. The purpose of the present study is 1) to provide detailed documentation of the egg structure, the embryonic and postembryonic development of Zorapteran, 2) to reconstruct the groundplan of Zoraptera as well as of Neoptera, and 3) to extend the phylogenetic discussion on Neoptera and Pterygota.

The egg structure and embryonic and postembryonic developments in the ground louse *Zorotypus caudelli* Karny, 1927 (Zoraptera, Zorotypidae) were examined and described in detail. The eggs of *Z. caudelli* are: 1) elliptic and pale in color, 2) honeycomb pattern on their surface, 3) with the egg membranes composed of an exochorion perforated by numerous aeropyles, an endochorion with columnar structures on its outer surface and an extremely thin vitelline membrane, 4) with a pair of micropyles at the equator on the ventral side of the egg, 5) and without any structures specialized for hatching (e.g., operculum, hatching line). The embryonic development of *Z. caudelli* is characterized by: 6) the formation of an embryo by the fusion of paired blastoderm regions with higher cellular density, 7) differentiation of the embryo on the dorsal side of the egg, 8) embryogenesis of the short germ band type, 9) full elongation of the

embryo and the amnioserosal fold formation on the egg surface, 10) immersion of the embryo into the yolk after its full elongation, 11) katatrepsis accompanied by the reversion of the embryo's anteroposterior axis, and 12) an extremely long egg tooth on the head. The postembryonic development of *Z. caudelli* was also examined: 13) the postembryonic life comprises five larval instars, 14) the annular addition of antennae once occurs at the second molting by the division of the third annulus (meriston), and 15) the wing dimorphism occurs in the fourth larval instar.

The placement of Zoraptera among the "lower neopteran" or polyneopteran lineage is strongly suggested by the fusion of paired regions with higher cellular density and blastokinesis accompanied by full elongation of the embryo on the egg surface, both features of which are regarded as the embryonic autapomorphies of Polyneoptera. The extraordinarily long egg tooth may be a potential synapomorphy of Zoraptera and Eukinolabia (= Embioptera + Phasmatodea). Integrative discussion of the egg structure, male reproductive system and spermatozoa suggests a close affinity of Zoraptera with Eukinolabia and proposes a formulation "Zoraptera + (Embioptera + Phasmatodea [= Timematodea + Euphasmatodea])".

INTRODUCTION

Zoraptera, also known as ground louse or angel insects (e.g., Grimaldi and Engel, 2005), are small (less than 4 mm), and still enigmatic group of insects. They live in subcortical spaces in decaying logs in tropical and subtropical zones. The order is one of the smallest in terms of species diversity. So far, 39 extant and 9 fossil species have been described (e.g., Engel, 2009; Terry and Whiting, 2012). All species except for fossil *Xenozorotypus burmiticus* are classified in the single genus *Zorotypus* Silvestri (Engel and Grimaldi, 2000). However, the true diversity of these cryptic insects is apparently insufficiently explored. The scientific name given to the order ("purely apterous ones", Greek: zoros = pure, strong; aptera = apterous) is a misnomer, as zorapterans are primarily winged (Caudell, 1920). The wing dimorphism is one of few autapomorphies of the order, correlated with the presence or absence of compound eyes and ocelli, and the presence or absence of a distinct pigmentation.

The systematic position of Zoraptera is one of the most controversial and persistent problems in higher level phylogeny of insects since their discovery 100 years ago (Silvestri, 1913). More than 10 different phylogenetic hypotheses have been proposed and its placement in neopteran insects remains an open question (Engel and Grimaldi, 2002; Beutel and Weide, 2005; Yoshizawa 2007, 2011; Ishiwata et al., 2011; Trautwein et al., 2012). Consequently, the term "Zoraptera problem" was coined by Beutel and Weide (2005) to

highlight this controversial phylogenetic status, analogous to the "Strepsiptera problem" earlier introduced by Kristensen (1991). However, unlike Strepsiptera, which have recently been identified as a sister group of monophyletic Coleoptera (Niehuis et al., 2012; Pohl and Beutel, 2013), Zoraptera remain a systematic enigma, even in the "age of phylogenomics" (Letsch et al., 2012; Simon et al., 2012; Letsch and Simon, 2013; B. Misof, pers. comm.). Groups that have recently been proposed as sister group candidates are Paraneoptera, or Acercaria (to avoid confusion, in the present study I use the term "Acercaria" instead of Paraneoptera, which often includes Zoraptera; Hennig, 1969; Kristensen, 1975; Beutel and Weide, 2005; Beutel and Gorb, 2006), Holometabola (Rasnitsyn, 1998), Eumetabola (Acercaria + Holometabola, Beutel and Gorb, 2001; Blanke et al., 2012), Dermaptera (Carpenter and Wheeler, 1999; Jarvis et al., 2005; Terry and Whiting, 2005), Dictyoptera (Boudreaux, 1979; Wheeler et al., 2001; Yoshizawa and Johnson, 2005; Ishiwata et al., 2011; Wang et al., 2013), Plecoptera (Letsch and Simon, 2013), Embioptera (Minet and Bourgoin, 1986; Engel and Grimaldi, 2000, 2002; Grimaldi and Engel, 2005; Yoshizawa, 2007, 2011), Eukinolabia (Dallai et al., 2011) and remaining all polyneopteran (Simon et al., 2012; Letsch and Simon, 2013).

In the last decade, the investigation of Zoraptera has greatly accelerated, with different approaches and a focus on different character systems. The skeleto-muscular system of the head was studied by Beutel and Weide (2005), the thoracic skeleto-muscular

system by Friedrich and Beutel (2008), wing venation by Kukalová-Peck and Peck (1993), wing base structures by Yoshizawa (2007, 2011), the postabdomen by Hünefeld (2007), the reproductive systems by Dallai et al. (2011, 2012a,b, 2013b), fossil species by Engel and Grimaldi (2002), and mating by Dallai et al. (2013a).

However, despite greatly increased knowledge about Zoraptera, the embryonic development remains completely unknown, although the comparative embryological approach is one of the most promising ways for reconstructing groundplan of the group and solving phylogenetic problems. This results in an apparently serious gap in the growing body of evidence and a major impediment to attempts to place the group phylogenetically.

Besides, the biology of Zoraptera has also received scant attention and remains still enigmatic. Although there are several previous studies on the life history (Gurney, 1938; Riegel and Eytalis, 1974; Shetlar, 1978), their descriptions are fragmentary and insufficient. The mating behavior is relatively well studied, and three types of mating have been hitherto reported (Shetlar, 1978; Choe, 1994a,b, 1995, 1997; Dallai et al., 2013a): first is of the end-to-end type with the male supine and dragged around by the female and without any pre-copulatory courtship. This is the case observed in *Zorotypus hubbardi*, *Zorotypus gurneyi*, and *Zorotypus magnicaudelli* (Shetlar, 1978; Choe, 1995; Dallai et al., 2013) and also generally in pterygote insects (Dallai et al., 2013). Second is of the end-to-end type with a sequence of pre-copulatory courtship, during which the male

secretes a liquid substance from his cephalic gland as a gift for female to mate, observed in *Zorotypus barberi* (Choe, 1995, 1997). Third is of remarkable external sperm transfer type that male dose not copulate but deposit spermatophores externally on the abdomen of the female, observed in *Zorotypus impolitus* (Dallai et al., 2013a). Besides, dominance hierarchy established by the males to gain considerable control over mating has been reported from *Z. gurneyi* (Choe, 1994a,b, 1997). In this case, body size and age (order of emergence) are important in determining dominance and reproductive success among males (Choe, 1997). In contrast to the mating behavior, the biological information of Zoraptera such as life history and postembryonic development is virtually unknown. Gurney (1938) has given a little biological information such their food and habitat, and Valentin (1986) reported about grooming behavior. While Shetlar (1974, 1978) suggested that the total number of larval instars is four based on only head width using *Z. hubbardi*, which is widely distributed through the North America, Riegel & Eytalis (1974) estimated the total number of larval instars of the same species is five, examining the lengths of prothorax, profemur, metafemur and metatibia. However, both of these studies are highly speculative, paying little attention to morphological features of each instar.

Consequently, I have undertaken the developmental study of Zoraptera, with *Zorotypus caudelli* Karny, 1927 as material (Fig. 1A, B). The aim of the present study is: 1) to provide detailed documentation of the egg structure, the embryonic and postembryonic

developments of *Z. caudelli*, 2) to develop the comparative embryological arguments, comparing the embryogeneses of other neopterans, 3) to reconstruct the groundplan of Zoraptera as well as of Neoptera, and 4) to extend the phylogenetic arguments on Neoptera and Pterygota.

MATERIALS AND METHODS

1. Materials

Zorotypus caudelli adults and larvae were collected from under the bark of decaying logs in Ul Gombak (Selangor, Peninsular Malaysia). They were kept in plastic cases (15 cm × 8 cm × 3 cm) with a bottom of moist soil at room temperature (ca. 24°C), and fed on dry yeast, powdered dried *Bombyx* pupae (commercially sold fishing bait) and live springtails (*Folsomia* sp.). Collected eggs were transferred to other plastic cases containing wet tissue paper and incubated at ca. 24°C for rearing.

In order to identify larval instar and examine duration of each instar, more than100 individuals of first or second larval instar were separately kept in plastic cases (3.6 cm × 3.6 cm × 1.4 cm) with a bottom of moist soil at 26°C. I inspected the morphological changes of larvae, checking them under a stereomicroscope SZ61 (Olympus, Tokyo, Japan) every day.

2. Fixation

Prior to fixation, eggs were cleaned with a soft brush in commercial bleach (Seven premium kitchen bleach) for 30 sec, and rinsed in distilled water. The eggs were soaked in Karnovsky's fixative (2% paraformaldehyde + 2.5% glutaraldehyde 0.1 mol/l HCl-sodium cacodylate buffer solution, pH 7.2 [SCB]) for 1 min, punctured with a fine needle and fixed for 1 h. After making a small opening in the

chorion with sharpened forceps, the eggs were further fixed with the same mixture at 4°C for 24 h and then stored in SCB at 4°C.

For detailed observations of external features of embryos, they were dissected out of living eggs with fine forceps and a razor blade in Ephrussi-Beadle's solution (0.75% NaCl, 0.035% KCl, 0.021% $CaCl_2$) containing detergent (0.1% Triton X-100), rinsed in new solution, and then fixed with Karnovsky's fixative for 12 h. Fixed embryos were also stored in SCB at 4°C.

A part of larvae were anesthetized by CO_2, fixed with FAA fixative (ethyl alcohol : formalin : acetic acid = 15 : 5 : 1) for 10 h and stored in 80% ethyl alcohol. The fixed specimens were measured for: (1) antenna lengths, (2) head width, (3) prothoracic notum length and (4) width, (5) profemur length and (6) width, (7) protibia length, (8) mesofemur length and (9) width, (10) mesotibia length, (11) metafemur length and (12) width, and (13) metatibia length.

3. External morphology

General features of the eggs were observed under a stereomicroscope MZ12 (Leica, Heerbrugg, Switzerland). To observe the micropyles, the egg membranes were mounted in a polyvinyl-lactophenol medium, Heinz liquid (polyvinyl-alcohol 10 g + distilled water 80 ml + lactic acid 35 ml + glycerin 10 ml + phenol 25 ml + chloral hydrate 20 g), and examined under a biological microscope OPTIPHOT-2 (Nikon, Tokyo, Japan) equipped with Plan Apo objectives (Nikon, Tokyo, Japan) for light field images or a

DM6000B (Leica, Wetzlar, Germany) for differential interference contrast images.

Fixed eggs and embryos were stained with DAPI solution (4', 6-diamidino-2-phenylindole dihydrochloride, diluted about 10 µg/ l with SCB) for several days and 20-30 min, respectively. Specimens stained with DAPI were observed with a fluorescence stereomicroscope MZ FL III (Leica, Heerbrugg, Switzerland) under UV light excitation at 360 nm. Some fixed embryos, stained with 1% Delafield's hematoxylin, were observed with a biological microscope OPTIPHOT-2 equipped with a long working distance objective ELWD 20X (Nikon, Tokyo, Japan). Drawings were made using a camera lucida.

For scanning electron microscopy (SEM), some eggs and embryos fixed with Karnovsky's fixative were post-fixed with 1% OsO_4 for 1 h. Fixed embryos were dehydrated in a graded ethanol series, dried with a critical point dryer Samdri-PVT-3D (tousimis, Rockville, Maryland), coated with gold, and then observed with an SEM SM-300 (TOPCON, Tokyo, Japan) at 15 kV. The embryonic cuticle secreted over the entire surface of the embryo is often swollen at later developmental stages and separated from the embryo or wrinkled. In coated specimens this impedes accurate observation of the surface of the embryo in the usual high-vacuum SEM mode (Machida, 2000b). Consequently, some embryos were observed without coating using a low-vacuum SEM SM-300 Wet-4 (TOPCON, Tokyo, Japan) at 13 Pa at 15-30 kV.

General features of the juveniles and adults were observed under stereomicroscopes MZ12 or a SZ61 (Olympus, Tokyo, Japan). Living and slide-mounted specimens in Euparal were photographed with a Digital Sight DS-Fi2 camera (Nikon, Tokyo, Japan), under a stereomicroscope MZ12 and a biological microscope Optiphot-2, respectively. For SEM, fixed specimens were dehydrated in a graded ethanol series, dried with a critical point dryer tousimis Samdri-PVT-3D, coated with gold, and then observed with an SEM SM-300 SEM at 15 kV.

4. Histology

Fixed specimens were dehydrated in a graded ethanol series and embedded in a methacrylate resin Technovit 7100 (Külzer, Wehrheim, Germany), as described by Machida et al. (1994a,b). Semithin sectioning was performed at a thickness of 2 µm using a semithin microtome H-1500 (Bio-Rad, Hercules, California) equipped with a tungsten carbide knife Superhard Knife (Meiwafosis, Tokyo, Japan). Sections were stained with 0.5% Delafield's hematoxylin for 12 h, 0.5% eosin gelblich or eosin bläulich for 1h, and 0.5% fast green FCF 80% ethanol solution for 1 min.

For transmission electron microscopy (TEM), eggs were fixed with Karnovsky's fixative containing 1% tannic acid at 4°C for 24 h and post-fixed with 1% OsO_4 for 1h. Fixed eggs were dehydrated in a graded acetone series, embedded in water-miscible epoxy resin Quetol 651 (Nisshin EM, Tokyo, Japan), and processed into sections 0.1 µm

thick with an ultramicrotome MT-XL (RMC, Tucson, Arizona), equipped with a diamond knife. Sections were stained with uranyl acetate and lead citrate and observed under a TEM LEM-2000 (TOPCON, Tokyo, Japan) at 90 kV.

5. Terminology

As for the terminology of the sclerites I followed Snodgrass (1935) and Matsuda (1970), and in the interpretation of the prothoracic sclerites which are highly modified and difficult to identify I referred to also Friedrich and Beutel (2008) (see DISCUSSION 9).

RESULTS

1. Mating and oviposition

Pairs were often observed to mate under rearing conditions. Mating in *Zorotypus caudelli* is of the end-to-end type with the male supine and dragged around by the female (Fig. 1C) as reported for other zorapterans (Shetlar, 1978; Choe, 1997; Dallai et al., 2013a). Every few days, the eggs are deposited on substrates such as bark or in galleries formed in rotting wood.

2. Egg structure

In the designation of egg axes, I followed the conventional concept (see e.g., Wheeler, 1893), which is based on the position of the embryo just before hatching. Consequently, the side of the egg facing the substrate is considered dorsal, the side with the micropyles as ventral, the slightly narrowed end as anterior, and the slightly broadened end as posterior (Figs. 2A, B, 3A, B).

Eggs of *Zorotypus caudelli* are elliptic with a length of around 0.6 mm long and a diameter of about 0.3 mm (Figs. 2A, B, 3A, B). The surface shows a hexagonal or less frequently pentagonal, honeycomb pattern made of an exochorionic ridge. The single compartments measure about 50 μm in diameter (Fig. 2C). The honeycomb pattern is more distinct on the ventral side (Fig. 3B-D). Each honeycomb contains about 50 aeropyles about 1 μm in diameter (Figs. 2C, 3C, D). A fringe formed by a fibrillar substance encircles

the lateral surface of the egg a little biased ventrally (Fig. 3A, B, D). The surface at both poles is featureless (Fig. 3F, G). At the equator on the ventral side of the egg, a pair of small polygons 20 μm in diameter is found (Figs. 2C, 3A, B, E): occasionally an additional polygon is present (Fig. 4A, B). Each small polygon contains 30 to 40 aeropyles and one micropyle about 2 μm in diameter (Fig. 2C); the aeropyles are not recognizable in Figure 3E as they are concealed by an extrinsic substance secreted at the oviposition. In eggs with fringe structures developed the small polygons are often covered by the fringe structure and difficult to observe.

The egg membranes are composed of a two-layered chorion comprising an exochorion and endochorion, and additionally an extremely thin vitelline membrane. The exochorion is about 5 μm thick, electron-dense and homogeneous in structure (Fig. 5A). The exochorion forms a ridge which shows a honeycomb pattern on the egg surface: the height of the ridge is various, e.g., about 3 μm on the ventral side and less than 1 μm on the dorsal side (Fig. 3C, D). The fringe is independent of the chorion, and probably secreted on to the egg after the completion of the chorion: there is a discontinuity between the exochorion and fringe, and a difference in stainability, i.e., the latter shows greater affinity for fast green FCF and is more electron-dense than the former (Fig. 5B, C). The aeropylar canals run through the exochorion, branching themselves, and reach the space formed between the exochorion and endochorion.

The endochorion is about 1 μm thick and homogeneous in

structure, with a slightly less electron-density than the exochorion (Fig. 5A). The endochorion yields numerous short columnar structures, about 1 μm in height and 0.2-0.4 μm in diameter, on its outer surface. The exochorion and endochorion are in contact with these columns, being spaced by about 1 μm (Fig. 5A). The vitelline membrane is an extremely thin layer adhering to the endochorion, less than 0.1 μm thick, and with a high electron density (Fig. 5A).

From each micropyle a micropylar canal of about 15 μm length penetrates the chorion and runs obliquely through it in lateral direction (Fig. 4C). Around the micropylar canal, the small columnar structures on the outer surface of the endochorion are lacking, and the exochorion and endochorion are fused (Fig. 4E). At the inner opening of the micropylar canal the endochorion forms a flap, which covers the micropylar inner opening (Fig. 4D, E). The lumen of the micropylar canals is filled with a substance more basophilic and electron-dense (Fig. 4C, E).

3. Embryonic development

The egg period of *Zorotypus caudelli* is about 40 days under incubation at 28°C. Based on the changes in external embryonic features, this period is divided into 12 stages (Figs. 6, 7), expressed as a percentage of total developmental time (DT), with 0% at oviposition and 100% at hatching (cf. Bentley et al., 1979) (Table 1).

3.1. Stage 1: 12-15% DT

Paired lateral regions with higher cellular density form on the dorsal side of the blastoderm close to the equator, only slightly posterior to the middle region (Fig. 8B-E). These areas migrate medially and fuse into a small heart-shaped embryo at the equator of the dorsal side of the egg (Figs. 8F, G, 9A). The anterior end of the embryo faces toward the posterior pole of the egg: the anteroposterior axes of the embryo and egg are reversed (Fig. 8F, G). Secondary yolk cells are observed to be segregated from the serosa (Fig. 8A).

3.2. Stage 2: 15-20% DT

The embryo extends along the dorsal surface of the egg, and the anterior protocephalon and posterior protocorm differentiate (Figs. 8H, I, 9B). The amnion starts to emerge from the embryonic margin. It forms the amnioserosal fold (Fig. 9B, C), which extends over the ventral surface of the embryo. The margins fuse with each other above the central area of the protocephalon, thus completing the anatrepsis. Further elongation of the embryo follows (Fig. 9D).

3.3. Stage 3: 20-22% DT

The protocephalon is enlarged laterally and a distinct head lobe differentiates. Segmentation starts almost simultaneously from the antennal segment to the prospective metathorax (Fig. 9E). The neural groove appears along the median line (Fig. 9E).

3.4. Stage 4: 22-25% DT

In the antennal, mandibular, maxillary, labial and thoracic segments, the appendages differentiate as lateral swellings (Fig. 10A, C). The prospective mandibles are considerably smaller than the other appendages (Fig. 10A, C). No appendicular structure develops in the intercalary segment throughout embryonic development. The neural groove becomes distinct. At its anterior end, the stomodaeum differentiates as a shallow pit (Fig. 10C). The caudal end of the embryo elongates and starts to bend ventrally (Fig. 10B, D).

3.5. Stage 5: 25-28% DT

The prospective antennae, maxillae, labium, and legs elongate, whereas the mandibles remain short (Fig. 11A, C). The anlage of the clypeolabrum develops as a median swelling anterior to the stomodaeum (Fig. 11A, C). Segmentation proceeds posteriorly, reaching abdominal segment III (Fig. 11D), and appendages develop in the newly differentiated segments. Caudal flexure is increased (Fig. 11B, D).

3.6. Stage 6: 28-30% DT

The embryo, which has been greatly elongated on the egg surface during the preceding stages, migrates in parallel into the central yolk mass (Fig. 12A, B). The clypeolabrum develops above the stomodaeum (Fig. 12A, C). The length of the antennae increases. They turn toward the median line and divide into the scapus, pedicellus, and

flagellum (Fig. 12C). The mandibles remain smaller than the other appendages (Fig. 12C). The appendages of the maxillary, labial, and thoracic segments elongate and divide into two subcomponents, the proximal coxopodite and the distal telopodite (Fig. 12C, D). In the mesal regions of the maxillary and labial coxopodites, prospective endite lobes appear as swellings (Fig. 12C). Segmentation proceeds posteriorly and reaches abdominal segment VI. Appendages develop on each abdominal segment (Fig. 12D). The abdomen begins to curve to the ventral side (Fig. 12B, D).

3.7. Stage 7: 30-40% DT

The embryo immerses more deeply into the central yolk mass and as a consequence the visibility of its details decreases (Fig. 13A, B). The antennal flagellum subdivides into four segments (Fig. 13C). The differentiation of the maxillae and labium continues: their endites enlarge and elongation of the telopodites, i.e., the palps, continues. The maxillary palp divides into five segments and the labial palp into three (Fig.13C). Elongation of the thoracic telopodites also continues and they divide into the trochanter, femur, tibia, tarsus, and pretarsus (Fig. 13D). The abdominal segments VII-XI differentiate and appendages develop on each as slight swellings (Fig. 13E, F). The segmental appendages of abdominal segment I or the pleuropodia differentiate into coxopodites and telopodites (Fig.13E), whereas those of abdominal segments II-X remain undivided. Cerci differentiate as distinct paired appendages of abdominal segment XI (Fig. 13E). The

proctodaeum with its Y-shaped opening invaginates between the cerci (Fig. 13G). The ventral curvature of the abdomen becomes more distinct and the embryo assumes an S-shaped body form (Fig. 13B, D). The thickness of abdominal segments VII-X increases compared to the anterior abdominal segments (Fig. 13F).

3.8. Stage 8: 40-50% DT

The embryo migrates still deeper into the yolk mass (Fig. 14A,B). The formation of the clypeolabrum continues. It divides into the clypeus and labrum, and a lateral external rim divides the former into the anteclypeus and postclypeus (Fig. 14C). The coxopodites of the gnathal and thoracic appendages divide into two parts, the proximal subcoxae and the distal coxae (Fig. 14D). The endites of maxilla and labium differentiate into two parts, the mesal lacinia and lateral galea, and the mesal glossa and lateral paraglossa, respectively (Fig. 14C). The labial appendages of both sides begin to migrate toward the median line (Fig. 14C) and are hardly visible from the lateral view, as shown in Figure 14D. The thoracic appendages assume a mesal orientation (Fig. 14C, cf. Fig. 13C). The cerci subdivide into two segments, a proximal coxopodite and a distal telopodite (Fig. 14E). Paired tracheal pits or spiracles invaginate in the meso- and metathoracic regions and also in abdominal segments I-VIII (Fig. 14D-F). A pair of ectodermal invaginations forms at the mesal bases of the thoracic appendages, developing into sternal apophyses, i.e., furcae (Fig. 21A). Abdominal equivalents of these apophyses could not be

observed throughout embryonic development. The size of the stomodaeum and proctodaeum increases distinctly during this stage (Fig. 14D, F)

3.9. Stage 9: 50-60% DT

During this stage the embryo develops within the yolk mass (Fig. 15A, B). In the anterior head region the precursor of the egg tooth appears as a very long median longitudinal ridge (Fig. 15C). A pair of shallow longitudinal depressions appears anterior to the antennal bases (arrows in Fig. 15C, D). Microtome sections reveal that the formation of these concavities is related to strong inflation of the adjacent protocerebral lobes, probably between lobes 1 and 2. The mandibles become flattened anteroposteriorly, and their teeth differentiate on the mesal side (asterisk in Fig. 15C). The hypopharynx appears as a single swelling between the mandibles (Fig. 15C). The thoracic appendages fold, with each femur overlapping the coxa and trochanter, and the tarsi subdivide into two segments (Fig. 15D). In the pleuropodia, the telopodite region collapses into the coxopodite (Fig. 15E). In the posterior abdomen the definitive dorsal closure proceeds from the posterior (Fig. 15F).

3.10. Stage 10: 60-65% DT

The amnioserosal fold ruptures near the gnathal region, and katatrepsis occurs, involving marked movement of the embryo. After being deeply immersed within the yolk mass in the previous stages, the

embryo re-appears on the egg surface. The head follows the movement of the amnion around the posterior pole, then along the ventral surface of the egg toward the anterior pole (Fig. 16A, C). Accordingly, the anteroposterior axis of the embryo reverses to correspond with that of the egg. Serosal cells move toward the anterodoral region of the egg and form the secondary dorsal organ there (Fig. 16B, D). With the progressive condensation and withdrawal of serosal cells, the amnion replaces the serosa and spreads over the dorsal yolk as the provisional dorsal closure (Fig. 16B, D).

3.11. Stage 11: 65-80% DT

The embryo, which has undergone katatrepsis, takes its position on the ventral side of the egg with its abdomen flexed (Fig. 17A, B). The head lobes extend dorsally and fuse to form the head capsule. The cerci develop as conical structures (Fig. 17E, F). The definitive dorsal closure proceeds toward the posterior thoracic region and anterior abdomen, replacing the provisional dorsal closure or the amnion (Fig. 17B, D). The secondary dorsal organ starts degenerating and sinks into the developing midgut. The embryonic cuticle is secreted, and the long blade-like egg tooth forms along the median line of the anterior head capsule (Fig. 17C, D).

3.12. Stage 12: 85-100% DT

The definitive dorsal closure is completed (Fig. 18B, D). The larval cuticle is secreted beneath the embryonic cuticle, with the setae

inserted into its surface (Fig. 18A, B). The egg tooth is sclerotized and strongly pigmented (Fig. 18A). The egg tooth appears to attain the labral territory (Fig. 20A), but a sagittal section reveals that it only protrudes above the proximal part of the labrum (Fig. 20C). SEM observations of embryos with the embryonic cuticle removed clarify the boundaries between the frons and postclypeus (epistomal suture) and between the ante- and postclypeus (Fig. 20B): the origin of the egg tooth lies in the territory from the frons to the anteclypeus (Fig. 18C). Compound eyes, which develop only in winged forms, are formed in the postembryonic stage. The tips of mandibular teeth become sclerotized and pigmented. The differentiation of thoracic appendages is completed and they acquire their definitive form (Fig. 18D), including the pair of pretarsal claws (Fig. 18D). In each thoracic segment, the sternal apophyses on both sides are shifted towards the median line and fuse to form the furcae (Fig. 21B). Friedrich and Beutel (2008) reported thoracic spinae. However, they are poorly developed in adults of *Zorotypus hubbardi* and *Zorotypus weidneri*. Throughout the embryonic development of *Z. caudelli* mesal ectodermal invaginations representing prospective spinae do not develop. It is conceivable that they emerge during postembryonic development. The strongly retracted abdominal sternum X is hardly visible externally (Figs. 18E, F, 21C). A sagittal section shows that it is in fact invaginated between the sterna IX and XI and concealed beneath the former (Fig. 21D). The coxopodites of cerci extend and almost completely occupy the ventral side of abdominal segment IX

(Fig. 18E). Later in this stage, a long and strong seta forms at the tip of the cercus (Fig. 18E, F): from externally, the cerci appear elongated.

3.13. Hatching: 100% DT

The embryo has acquired its definitive shape when the prelarva medially severs the chorion with the egg tooth and hatches. The head emerges first, followed by the thorax and abdomen. Peristaltic movements are involved in the process. The distal parts of the thoracic legs remain within the egg, whereas the proximal region is exposed. The former function as anchors for the prelarva to enable it to shed the embryonic cuticle (Fig. 19A, B). Emerging from the egg and the embryonic cuticle, the prelarva becomes the first instar larva. Shortly after hatching it starts to move actively. The embryonic cuticle with the egg tooth visible as a dark structure is left on the egg surface (Fig. 19C).

4. Postembryonic development

4.1. Determination of the number of larval instars

With daily checking of exuviae and appearance of chaetotaxy for the next instar under the cuticle in the individuals separately reared (Fig. 23A), I could distinguish five larval instars in *Zorotypus caudelli* (Fig. 22). A part of the individuals separately reared were fixed for each instar. On these instar-identified samples together with the fixed individuals from the group rearing, I made the morphological observation, measurement and/or counting of several features (Tables

2, 3, Figs. 22-30).

4.2 Duration of larval instars

To examine the duration of each instar, more than 100 larvae of the first or second instar were separately kept in plastic cases. However, I succeeded in measuring the duration of the third to fifth larval instars, but failed in measuring for the first and second larval instars because of a considerable high mortality of the first instar larva. Therefore, I tried to rear the larvae which hatched out on the same date in a group (10-20 individuals) and to measure the duration again. I do not know the reason but I succeeded in significantly lowering the mortality of the first instar larvae, and consequently measuring the duration of the first and second instars. The durations of each instar were as follows and summarized in Table 2: the first instar, 14.98 ± 2.82 days (n = 46); the second instar, 13.48 ± 5.74 days (n = 21); the third instar, 12.12 ± 3.07 days (n = 33); the fourth instar of apterous form, 14.58 ± 3.66 days (n = 12); the fourth instar of winged form, 17.51 ± 5.33 days (n = 35); the fifth instar of apterous form, 16.44 ± 3.10 days (n = 18); the fifth instar of winged form, 24.88 ± 4.64 days (n = 32). The adults continued living for several months but exact records are not available.

4.3. Morphological features in each larval instar

I made SEM observation of external morphology of instar-identified larvae. Measurements data of some morphological

characters are summarized in Table 3.

4.3.1. Instar I

The antenna is composed of eight antennomeres (Fig. 24B). The first antennomere or the scapus is elongate, approximately twice longer than wide. The second and third antennomeres or pedicellus and the first annuli of flagellum are small, spherical and half the length of the first antennomere (Fig. 24B'). The fourth to seventh antennomeres are spherical. The eighth antennomere is large, and one and half the length of the first antennomere, with its tip pointed (Fig. 24B). The head is orthognathous and subtriangular (Fig. 24A). The prothoracic notum is subrectangular. The meso- and metathoracic nota are trapezoidal and slightly wider toward the posterior. Lateral margins of each thoracic notum are scarcely overhung (Fig. 24A, C, D). In the propleurite, the slender anterior propleural sclerite, small and subrectangular middle and posterior propleural sclerites, and the triangular trochantin located anterior to the procoxa are discernible (Fig. 24C). Although the dorsal parts of the anterior and middle propleural sclerites are fused with each other, the membranous region separates the posterior propleural sclerite from them (Fig. 24C). The invagination line of the propleural apophysis along the lower margin of the posterior propleural sclerite is represented by a pleural suture. In each of meso- and metathorax, the pleurite is divided into the anterior episternum and posterior epimeron by the pleural suture between the lateral margin of the thoracic notum and the pleuro-coxal joint. The

sutures separating the anepisternum, katepisternum and preepisternum, and that separating the anepimeron and katepimeron could not be found (Fig. 24D). According to the interpretation by Friedrich and Beutel (2008), the region anterior to the trochantin represents the preepisternum. The subtriangular trochantines are located anterior to the meso- and metacoxa (Fig. 24D). In the mesothorax, a small sclerite anterior to the episternum is discernible (black star in Fig. 24D) and apparently larger than that of metathorax (white star in Fig. 24D). The femur of each leg is relatively slender (Fig. 29A). The profemur is wider than mesofemur. The bristles arranged as comb are found in the ventral side of the distal half of protibia. The metafemur is longer than the pro- and mesofermora, approximately three and half times longer than wide, and slightly swollen proximally (Fig. 29A). The first to eighth abdominal terga are uniformly sclerotized and with a row of setae along the posterior margin (Fig. 24A, E). The ninth abdominal tergum is short with a medial pair of setae (Fig. 24F). The 10th abdominal tergum is subtriangular with a pair of slender setae (Fig. 24F). The 11th abdominal tergum is short and membranous. A pair of spiracles is located on the membranous pleurites in each of the first to eighth abdominal segments (Fig. 24E). The spiracles of the first abdominal segment take more dorsal position. The first and second abdominal sterna are not sclerotized (Fig. 24G). The third to seventh abdominal sterna are partly sclerotized (arrows in Fig. 24G), with a pair of setae on each of ventral restricted, sclerotized regions. The eighth abdominal sternum is wide and approximately twice longer than

the other abdominal sclerites. The ninth abdominal sternum is shorter than the eighth abdominal sternum. Externally, the 10th abdominal sternum is not recognized. The ventral side of the 11th abdominal segment is occupied by coxopodites of cerci (asterisks in Fig. 24F). The cerci are unisegmented and approximately conical with one long apical seta, several subapical moderate-length setae and very long and fine setae (Fig. 24A, F). The cerci are closely located and directed posteriorly (slightly laterally), and their surface is covered with numerous minute cuticular spicules (Fig. 24F).

4.3.2. Instar II

The antenna is composed of eight antennomeres (Fig. 25B). The third antennomere become egg-shaped and approximately twice longer than the second antennomere (Fig. 25B'). The cephalic features including the chaetotaxy are basically the same as those of the first instar larvae. The thoracic nota develop, being slightly overhung to the lateral (Fig. 25A). The metafemur is swollen proximally and three times longer than wide (Fig. 29B). The abdominal terga extend laterally and fuse with pleurites to form the tergopleurites (Fig. 25C). Therefore, the position of the spiracles (black arrowheads in Fig. 25C) which are originally formed on the abdominal pleura, are seemingly shifted on to the territory of "tergum" or the tergopleurite s.str. In the posterior abdominal segments, however, sclerotization of the tergopleurites is yet to complete (cf. asterisk in Fig. 25C). The 10th abdominal tergum slightly extends to the posterior (Fig. 25D). The

second abdominal sternum is slightly sclerotized (asterisk in Fig. 30A), but the third to seventh abdominal sterna become uniformly sclerotized with two pairs of setae (Fig. 30A). The eighth and ninth abdominal sterna become longer and shorter, respectively (Fig. 30A). The cerci show little morphological changes, but become somewhat apart from each other (Fig. 25D).

4.3.3. Instar III

The antenna is composed of eight antennomeres (Fig. 26B). The third antennomere is constricted in the middle. This constriction is a sign of subdivision of meriston. Other antennomeres become slightly elongate (Fig. 26B, B'). A few short setae newly differentiate lateral to the antennal bases (Fig. 26A). One small seta appears on each of meso- and metaepimeron (Fig. 26C). The metafemur become further swollen and as shown in Figure 29C. In the posterior abdominal segments, sclerotization of the tergopleurites completes (Fig. 26D). The 10th abdominal tergum further extends posteriorly (Fig. 26E). The abdominal sterna are as shown in Fig. 30B.

4.3.4. Instar IV

The antenna becomes nine-segmented by division of the third antennomere (Fig. 27B). The fourth antennomere is newly differentiated and subequal to the length of the third antennomere, with several small setae in the subapical region (Fig. 27B'). The other antennomeres become slightly elongate (Fig. 27B). The morphological

difference between apterous and winged form arises in this stage (Fig. 22D, G). In winged form, the prospective compound eyes appear as small black spots at the posterolateral corners of the head (Figs. 22G, 23B), although the cuticle around the ocular black spots shows no changes (Fig. 27A vs. C). The cephalic chaetotaxy is, irrespective of apterous or winged, basically the same as that of the previous instar (Fig. 27A). Small wing pads differentiate at the posterolateral corners of the pterothoracic nota in the winged form (Figs. 22G, 27D). One small seta appears on the posterior area of the meso- and metaepisternum (Fig. 27D). The metafemur is as shown in Figure 29D. The 10 and 11th abdominal terga are fused and uniformly sclerotized (Fig. 27E). One additional pair of setae appears on the 10- 11th abdominal tergum (Fig. 27E). The setae of the posterior row in each of the third to seventh abdominal sterna increases in number (Fig. 30C). A few pairs of setae are newly differentiated on the eighth abdominal sternum (Fig. 30C).

4.3.5. Instar V

The antenna is composed of nine antennomeres (Fig. 28B). The third and fourth antennomeres elongate and become one and half times longer than the second antennomere (Fig. 28B’). Numerous short setae occur on the subapical region of the fourth antennomere (Fig. 28B’). In the winged form, the ocular black spots on the posterolateral corners of the head extend (Figs. 22H, 23C), but the cuticle over the ocular spots shows no changes (Fig. 28C). Toward the emergence, the black spots

become gradually extensive and intensive, and three prospective ocelli are visible between the compound eyes (Figs. 22H', 23C). In the heads of both apterous and winged forms, a few additional setae are added lateral to the antennal bases (Fig. 28A, C). The morphological difference in thoraces becomes more distinct between the apterous and winged forms. In the winged form, transparent and thin wing pads of pterothoraces are enlarged, and those of metathorax reach the fourth abdominal segment (Figs. 22H, 28F). Around the time the prospective ocelli become visible, the wing pads become thickened and whitish (Fig. 22H'). The wing pads turn black just before the emergence due to numerous short setae on the adult wings being formed and darkened (Figs. 22H'', 23D). Very rarely larvae with a smaller ocular spots are found, of which the posterolateral corners of pterothoraces little protrude (Fig. 23E). They become adults with a similar body color to the apterous adults and the black ocular spots conspicuous, and they have a pair of sclerotized projections at the posterolateral corners of pterothoracic nota. In contrast to that the remarkable difference appears in the tergal region of pterothoraces between the apterous and winged forms, practically no difference arises in the pleural region of the segments, as shown in Figure 28D and E. The metafemur is as shown in Figure 29E, which is basically the same as the definitive form of adults (Fig. 29F). A few setae are newly added on the lateral region of tergum in each of the first to seventh abdominal segments (Fig. 28A). Two different patterns in chaetotaxy of the ninth and 10-11th abdominal terga are recognized (Fig. 28G, H). Under SEM, a

small posteromedial swelling could be found on the 10-11th abdominal tergum in a part of larvae (white arrow in Fig. 28G): the individuals of this projection are masculine, so the difference in the chaetotaxy in the ninth and 10-11th abdominal terga is a sexual diagnosis. A few of setae are added anterior to the posterior row of setae on the fourth to seventh abdominal sterna (Fig. 30D). The eighth abdominal sternum enlarges, with several short setae added (Fig. 30D).

***Key to larval instars of* Zorotypus caudelli**

1. Wing pads and prospective compound eyes present ……. 2
—. Wing pads and prospective compound eyes absent ……..……. 3
2. Small wing pads, small black ocular pigment at the posterolateral corners of the head, the third antennomere subequal to the second antennomere ……..……. fourth instar of winged form
—. Long wing pads, prospective compound eyes as large black spots present, occasionally prospective ocelli present, the third antennomere around twice longer than the second antennomere……. fifth instar of winged form
3. Nine-segmented antennae ……..……... 4
—. Eight-segmented antennae …… 5
4. The third antennomere subequal to the second antennomere …… fourth instar of apterous form

—. The third antennomere around twice longer than the second antennomere ……. fifth instar of apterous form

5. The third antennomere constricted in the middle, meso- and metathoracic notum angular ……. third instar

—. The third antennomere not constricted, meso- and metathoracic notum rotundate …… 6

6. The third antennomere oval, the cerci located slightly apart …… second instar

—. The third antennomere spherical, the cerci located very closely …… first instar

DISCUSSION

1. Egg structure

The structural features of zorapteran eggs have been described in four species, *Zorotypus snyderi* (Caudell, 1920), *Zorotypus hubbardi* (Gurney, 1938), *Zorotypus brasiliensis* (Silvestri, 1946), *Zorotypus gurneyi* and *Zorotypus barberi* (Choe, 1989). The information provided is based on light and/or scanning electron microscopic observations and is only fragmentary. I cannot find any difference between my observations of eggs of *Z. caudelli* and the structural features of the eggs of the other zorapterans. The eggs of Zoraptera can be characterized as follows (new findings presented here indicated by italics): 1) elliptic in shape and creamy white in color; 2) a honeycomb pattern in their surface; 3) *egg membranes composed of an exochorion, an endochorion and a vitelline membrane; the exochorion is electron-dense and homogeneous in structure with numerous branching aeropyles; the endochorion is electron-dense, homogeneous, and bears numerous small columnar structures on its outer surface;* 4) a pair of small polygons at the equator on the dorsal side of the egg; each polygon contains one micropyle; *the micropylar canal runs obliquely through the chorion in lateral direction; the exochorion and endochorion are fused together around the micropylar canal; the endochorion at the inner opening of the micropylar canal forms a flap;* 5) *no structures specialized for hatching (e.g. operculum, hatching line).* The eggs of *Z. caudelli* are equipped with a fringe

structure encircling the lateral surface. Similar features were documented in Choe's (1989) scanning electron micrographs for *Z. barberi* but not for *Z. gurneyi*. Such structures were neither described in the study on *Z. snyderi* (Caudell, 1920) nor depicted in those on *Z. hubbardi* and *Z. brasiliensis* (Gurney, 1938; Silvestri, 1946). The fringe is an extrinsic structure secreted onto the egg surface after the completion of the egg, and the secretion may differ among the species.

2. Formation of appendages

My observations confirm that, as in other insects, the development of the maxillae and labium differs distinctly from that of the mandibles, even though these appendages are apparently serial homologues belonging to the fourth, fifth and sixth head segments, respectively (Machida, 2000a; Uchifune and Machida, 2005). The former divide into two major subelements, whereas the anlage of the mandible neither shows distinct elongation nor division throughout embryonic development. Serial homology suggests that the proximal and distal parts of the developing maxillae and labium are equivalent to the coxopodite and telopodite of the thoracic appendages, whereas the mandible is only represented by the coxopodite, as suggested in other hexapods (cf. Machida, 2000a; Uchifune and Machida, 2005).

At 40-50% DT, the maxillary and labial coxopodites subdivide into proximal and distal parts, i.e., the stipes and cardo in the maxilla, and the prementum and postmentum in the labium. These proximal and distal parts of the coxopodites of the mouthparts may be serially

homologous to the thoracic subcoxa and coxa, respectively. The maxillary and labial telopodites differentiate into segmented elements, i.e., the palps. Likewise, at 40-50% DT the mandibles subdivide into two parts, similar to other gnathal and thoracic coxopodites, as described by Machida (2000a) for developing appendages of archaeognathan embryos. Machida identified the proximal and distal parts of archaeognathan mandibles as the mandibular subcoxa and coxa, respectively, and the mandibular parts in the embryo of *Zorotypus caudelli* apparently correspond with these subelements.

Generally, insect mandibles are approximately the same size as the other segmental appendages in their early stage of development. In Zoraptera, however, they appear as distinctly smaller swellings (Fig. 10A). This unusually small size is a potential autapomorphy of the order.

3. Egg teeth

In the apterygote orders, an egg tooth occurs only in zygentomans, which suggests that it is absent in the groundplan of Hexapoda. In zygentomans it is formed by the larval cuticle and persists during the first instar stage (Konopová and Zrzavý, 2005). In contrast to this, the egg teeth of most pterygotes including zorapterans are formed by the prelarval embryonic cuticle and are consequently absent after hatching.

The pterygote egg tooth is usually formed as a short longitudinal ridge or a small pointed projection (Sikes and Wigglesworth, 1931;

Kishimoto and Ando, 1985; Uchifune and Machida, 2005; Shimizu, 2013). The extremely elongate condition distinguishes Zoraptera from other pterygote orders with the notable exception of Embioptera (Jintsu, 2010). In *Aposthonia japonica*, a Japanese embiopteran species, a robust longitudinal egg tooth covers the entire length of the frons. The strong degree of elongation could be considered as a potential synapomorphy of both orders. However, the evolution of egg teeth in Pterygota is presently not well understood. They can be present or absent or occur in entirely different body regions, as it is for instance the case in Coleoptera (e.g., Beutel, 1997).

4. Formation of embryo and blastokinesis

In *Zorotypus caudelli*, a small heart-shaped embryo is formed. It gradually grows, with segments subsequently added from anterior to posterior. Thus, the embryo of *Z. caudelli* can be categorized as belonging to the short germ band type (cf. Krause, 1939; Sander, 1984). Two alternative varieties of this category occur in Insecta (= Ectognatha). In most groups of the lower neopteran insects, or Polyneoptera, the embryo is formed by a pair of blastoderm regions with higher cellular density (Bedford, 1970; Uchifune and Machida, 2002, 2005; Jintsu, 2010; Shimizu, 2013). In other groups, the cells near the posterior pole concentrate and proliferate to form the embryo. The latter type is known in Palaeoptera and Acercaria (Goss, 1952; Ando, 1962; Heming, 1979; Haga, 1985; Tojo and Machida, 1997, 1998), but also in the apterygote ectognathan orders Archaeognatha

(Machida et al., 1990) and Zygentoma (Masumoto and Machida, 2006). This strongly suggests that this type of embryo formation belongs to the groundplan of Ectognatha and Pterygota, whereas the former may be regarded as potential autapomorphy of Polyneoptera, which is still strongly disputed as a clade (e.g., Kristensen, 1995). The present study revealed that this developmental feature also occurs in Zoraptera.

It is noteworthy that the early embryo forms on the dorsal side in Zoraptera, with its anteroposterior axis diametrically opposed to that of the egg. In a typical case, the insect embryo forms on the ventral side with its anteroposterior axis corresponding with the orientation of the egg. However, it is also known that the position of the embryo can vary considerably, from around the equator to close to the posterior pole on the ventral side of the egg, even within a single order (Cobben, 1968; Warne, 1972). One explanation could be that the unusual position in Zoraptera just lies within this wide range in insects. Another possible interpretation is that the unusual position is due to "precocious migration of the embryo". It is conceivable that the migration of blastoderm cells toward the posterior region, which is the driving factor in the formation of the embryo, is accelerated in Zoraptera, leading finally to placement on the dorsal side of the egg with reversed orientation. In the embryonic development of the immersed type in hemimetabolous insects (see Johannsen and Butt, 1941; Anderson, 1972; Heming, 2003), progressive elongation along the egg surface also results in a shift of the embryo from the ventral to the dorsal surface, with a reversed anteroposterior axis. In the case of

Zoraptera, the unusual position of the early embryo might be caused by the unusually early start of cell migration, leading to “precocious migration of embryo to the dorsal side of the egg”. To our knowledge, the position of the early zorapteran embryo is unique and shows the potential autapomorphy of the order.

The embryo of *Z. caudelli* thus differentiated on the dorsal side of the egg develops there into its full elongation, undergoing embryogenesis of the short germ band type. The embryo then migrates in parallel with the egg surface deep in the yolk and develops for a short period. Katatrepsis then occurs, and the embryo appears again on to the egg surface, accompanied by the reversion of its anteroposterior axis, finally taking its position on the ventral side of the egg. As has been mentioned and discussed thus far, the formation of the embryo and blastokinesis of *Z. caudelli* (Zoraptera; Figs. 6, 7, 31D) may be characterized as follows: 1) the formation of an embryo by the fusion of paired blastoderm regions with higher cellular density, 2) differentiation of the embryo on the dorsal side of the egg, 3) embryogenesis of the short germ band type, 4) full elongation of the embryo on the egg surface, 5) immersion of the embryo into the yolk after its full elongation, and 6) katatrepsis accompanied by the reversion of the embryo’s anteroposterior axis.

5. Recognition of larval instars

The postembryonic development of Zoraptera remains little known. Although there are several studies on life history, the total

number of larval instars is disputable (Riegel and Eytalis 1974; Shetlar, 1974, 1978; Riegel, 1987). While Riegel and Eytalis (1974) and Riegel (1987) suggested that the total number of larval instars is four based on the head width of *Zorotypus hubbardi*, Shetlar (1974) suggested that the total number of larval instars is five based on the lengths of prothorax, profemur, metafemur and metatibia. However, the former studies scarcely showed measurement data, and that of the latter failed to present significant differences enough to distinguish instars (Shetlar, 1974: Tables 1, 2, Graphs 1, 2). Although these studies suggested the total number of larval instars, the conclusions are speculative.

For tiny insects like zorapterans, it may be very difficult to designate significant differences in measurements, and herewith to determine the number of instars. Therefore, only the measurement of few characters could not be a crucial clue for identification of instar numbers for Zoraptera. The present study succeeded in demonstrating that the total number of larval instars of *Zorotypus caudelli* is five, employing many morphological, not only quantitative but qualitative, features and directly counting the number of ecdysis. The total number of larval instars of *Z. caudelli* revealed in the present study “five” is the same as that of *Z. hubbardi* in the previous study by Shetlar (1974, 1978). In the present study, I not only described larval morphology of each instar, but also succeeded in designating the morphological keys to identify the larval instar, such as the antennomeres, thoracic nota and wind pads. Observation of these characters in combination enables the exact identification of larval instars. Detailed postembryological

studies, employing the critical methods as developed in the present study, are much required to be held in more species of Zoraptera, to test whether the total number of larval instars “five” can be regarded as groundplan of Zoraptera. Meanwhile, the sizes of the eggs and adults in *Z. hubbardi*, *Z. caudelli*, and other zorapteran species hitherto reported, which are respectively around 0.6-0.7 mm and 2 mm (cf. Silvestri, 1946; Choe, 1989; Dallai et al., 2012b), are roughly comparable with each other. It is likely that the number of larval instars is constant throughout the order.

6. Wing dimorphism

Dispersal wing dimorphism is widely known in insects (Ross, 1986; Simpson et al., 2011). This is often found in gregarious insects, and undoubtedly evolves independently in various lineages. Usually in wing dimorphism, the apterous (brachypterous) form with higher reproductive ability appears under stable and optimal environment condition. Meanwhile, in the face of deteriorating local environment conditions, winged form individuals with higher dispersal ability appear and move to new habitats (Ross, 1986; Simpson, et al. 2011). Although “Zoraptera” was established and described as a completely wingless insect order by Silvestri (1913), Caudell (1920) found that zorapterans are primarily winged. Until now both winged and apterous forms have been reported from many zorapteran species, and wing dimorphism is considered to be one of the potential autapomorphies of Zoraptera (Friedrich and Beutel, 2008).

In Zoraptera, developed compound eyes and three ocelli are present in winged form, but absent in apterous form. In *Zorotypus caudelli*, the morphological differences between apterous and winged forms become distinct from the fourth larval instar. In the fourth instar of the winged form, small wing pads and small ocular spots appear. In the fifth instar of the winged form, wing pads elongate and ocular spots are widened, and soon, three ocelli of the adult appear. The mechanism of wing dimorphism in Zoraptera has not been examined in detail. We have only fragmentary information on the zorapteran wing dimorphism from the breeding by Shetlar (1974, 1978). Shetlar could not clarify the key factor controlling the wing dimorphism, but mentioned “Crowding does not seem to have an effect on production of winged individuals” since no difference in numbers of winged form was found in the laboratory colonies of different densities ranging from 10 to 50 individuals (however, details of rearing experiments and the occurrence rate of winged form was not mentioned). In the present study, I reared around 150 individuals separately, most of which became winged form (data not shown). This may support Shetlar (1974, 1978) that the crowding should not always be a key factor controlling the wing dimorphism in Zoraptera. However, the young larvae examined in the present study were derived from the eggs laid by the females reared in high density of 100-200 individuals in a case of 15 cm × 8 cm × 3 cm, and a possible effect of crowding could not be completely rejected. Although I obtained relatively many winged males in the present study, it was reported that the winged males are

very rare in field, and that the majority of winged form is feminine (Gurney, 1938; Shetlar, 1974; Grimaldi and Engel, 2005). Shetlar (1974, 1978) suggested that the production of winged form may be not sex-determined, but sex-influenced or sex-relate. To understand the mechanism of wing dimorphism in Zoraptera, culture experiments over several generations are needed. I observed that in *Z. caudelli* very rarely appear the fifth instar larvae with the ill-developed ocular spots and wing pads roughly comparable to those of the fourth instar (Fig. 23E). These wing pads persist in the adults as small sclerotized projections at the posterolateral corners of pterothoracic nota. Similar report was made by Shetlar (1978). These cases of ill-developed wings may provide a hint in clarifying the key factor controlling the wing dimorphism in Zoraptera.

7. Sexual dimorphism

Zoraptera show no distinct difference in size between sexes, and lack the external genitalia such as ovipositor. In most zorapteran species, the abdominal terminalia show only subtle differences between sexes: in the male of *Zorotypus caudelli*, eight pairs of setae are arranged on the ninth abdominal and 10-11th abdominal terga (see RESULTS 4.3.5. Instar V) is equipped with a pair of lateral triangular sclerites (hemitergite) and small and upcurved mating hook (Fig. 28I); meanwhile, in the female only a few pairs of setae are arranged on the ninth abdominal tergum, and the 10-11th abdominal tergum is uniformly sclerotized (Fig. 28J); the eighth and ninth abdominal sterna

of the females are larger and shorter, respectively, than those of the males.

The present study revealed that the sexual dimorphism does not appear until the final or the fifth instar. In the prospective male fifth instar larva shown in Figure 28G, four pairs of setae are arranged on the ninth abdominal tergum, and small postmedian swelling is present on the 10-11th abdominal tergum (white arrow in Fig. 28G). Meanwhile, in the prospective female fifth instar larva, two pairs of setae are arranged on the ninth abdominal tergum, and no swelling as comparable to that in male fifth instar larva is found on the 10-11th abdominal tergum (Fig. 28H). The subtle postmedian swelling on the 10-11th abdominal tergum found in the prospective male fifth instar larva is considered to correspond to the mating hook of the male (black arrow in Fig. 28I). Because this swelling structure can be detected only under SEM, the chaetotaxy in the postabdomen is only available diagnosis for light-microscopical sexing in larval stage of *Z. caudelli*.

8. Antennal development

In the hemimetabolous insect groups, three modes of the antennal development are known (Hockman et al., 2009): the first mode is the simplest and involves exclusively the division of the first annulus of the flagellum (meriston) into two or three annuli at each molt; the second mode involves three types of annular zone of the flagellum, i.e., the basalmost meriston, meristal annulus which is derived from the meriston and undergoes once subdivision to produce

singleton(s), and singletons which never divide; in the third modes, the meristal annuli are not only derived from the division of the most basal annulus (meriston) but instead from several basal or even all annuli in the flagellum of the first instar (Hockman et al., 2009).

In *Zorotypus caudelli*, the annular addition occurs only once at the molting from the third to fourth instar. At the third instar larva, the third antennal annulus or the first flagellar annulus (meriston) becomes constricted in the middle at the third instar. The constricted meriston divides into two during the molting, and the number of the antennomeres increases from eight to nine. This mode of the antennal development shown in Zoraptera may be categorized in the first, simplest mode of antennal growth. The antennal growth of this mode is also known from Isoptera (Fuller, 1920), Blattaria, Plecoptera (Qadri, 1938) and Dermaptera (Davies, 1966; Shimizu and Machida, 2011). However, the number of the antennomeres in Zoraptera, which is the insect group characterized by “reduced characters” (cf. Beutel and Weide, 2005), increases only once by only one segment from eight to nine, and so it is very difficult to evaluate the zorapteran antennal growth and compare it with those of other insects. Besides, as Hockman et al. (2009) discussed, the flexibility of the antennal development such as the number of annuli produced from the one meriston at each molt even within one order may limit the phylogenetic value of this character for reconstructing interordinal relationships. Furthermore, the antennal development of some neopteran group such as Embioptera and Phasmatodea has not been

examined yet. To reconstruct the groundplan of antennal growth in Neoptera and Pterygota, more extensive and intensive examinations covering all major groups are required.

9. Homology of thoracic sclerite

The exoskeletal system of Zoraptera was investigated by Crampton (1920, 1926), Delamare-Debouteville (1947), Rasnitsyn (1998) and Friedrich and Beutel (2008). As in the case of other pterygote insects, the exoskeletal system of prothorax is uniform between winged and apterous forms, and likewise that of pterothoraces uniform between these two forms; but the exoskeletal systems of the prothorax and pterothoraces considerably differs from each other (Crampton, 1920, 1926; Friedrich and Beutel, 2008). In contrast to the pterothoraces with modifications related with flight, the prothoracic pleural sclerites are simple and less differentiated. However, the homology of prothoracic pleural sclerites between Zoraptera and other pterygote insects is highly problematic as well as the serial homology between the prothoracic and pterothoracic sclerites (Friedrich and Beutel, 2008).

In the previous studies, the posterior propleural sclerite has been interpreted as being comparable to the epimeron of the pterothorax (Crampton, 1920, 1926; Matsuda, 1970; Friedrich and Beutel, 2008), and the present study agrees with this interpretation, in light of the relative position of the structures concerned to the pleural sutures (cf. Fig. 24C vs. D). Friedrich and Beutel (2008) examined the

skeleto-muscular systems of *Zorotypus hubbardi* and *Zorotypus weidneri* in detail and designated several muscular features supportive of this interpretation. Delamare-Deboutteville (1947) described the paracoxal suture in the prothoracic pleuron (cf. Matsuda, 1970), but I could not find the suture as Crampton (1920, 1926) and Friedrich and Beutel (2008) failed.

The characterization of the anterior and middle propleural sclerites of Zoraptera remains controversial. The anterior propleural sclerite has been variously termed, i.e., the lateropleurite (Crampton, 1920; Delamare-Deboutteville, 1947), precoxale (Crampton, 1926), episternum/anapleurum (the proximal part representing preepisternum) (Matsuda, 1970), or preepisternum + anterior anaepisternum (Friedrich and Beutel, 2008). Meanwhile, the middle propleural sclerite was termed the episternum (Crampton, 1926; Delamare-Deboutteville, 1947), or posterior anaepisternum (Friedrich and Beutel, 2008). In the present study, I found that the anterior and middle propleural sclerites of *Zorotypus caudelli* keep a connection at their dorsal regions throughout the postembryonic development, although the ventral separation of them becomes gradually deepened and distinct. Crampton (1920, 1926) and Friedrich and Beutel (2008) depicted separately the anterior and middle propleural sclerites in Zoraptera, but the present study confirmed the anterior and middle propleural sclerites dorsally unified as Delamare-Deboutteville (1947) suggested. Based on the positional relationships of them to the ventral notch and trochantin (see Fig. 24C), the anterior and middle propleural sclerites

may be suggested to represent the preepisternum and anaepisternum, respectively, although they are not clearly demarcated by separating structures such as suture.

In contrast to the prothorax, there seem few controversial issues on the meso- and metathoracic pleurites of Zoraptera. However, in the present study I found new small sclerites with spiracles located anterior to the meso- and metathoracic anepisterna (cf. asterisks in Figs. 26C, 28D,E). Uchifune and Machida (2005) followed the formation of thoracic eusternal and pleural sclerites in a grylloblattid, *Galloisiana yuasai*, and discussed the origins of thoracic sclerites. According to their interpretation that spiracles attribute to the preepisternum, and the re-characterization of the meso- and metathoracic pleurites may have to be done, especially focusing on the origin of preepisternum.

10. Phylogenetic implications of comparative embryology

10.1. Affiliation of Zoraptera: Polyneoptera or Acercaria?

As already pointed out in the introduction, the systematic position of Zoraptera is apparently one of the few remaining enigmas in insect phylogeny (e.g., Hennig, 1969; Kristensen, 1975; Beutel and Gorb, 2001, 2006; Beutel and Weide, 2005; Yoshizawa, 2007, 2011; Ishiwata et al., 2011; Blanke et al., 2012; Trautwein et al., 2012; Letsch and Simon, 2013). Recent morphological and molecular studies tentatively support their placement in Polyneoptera (Engel and Grimaldi, 2000, 2002; Yoshizawa and Johnson, 2005; Yoshizawa, 2007, 2011; Ishiwata et al., 2011; Letsch and Simon, 2013). However,

even the monophyly of this lineage is a long debated problem (e.g., Boudreaux, 1979; Kristensen, 1991; Kjer, 2004; Grimaldi and Engel, 2005; Kjer et al., 2006; Misof et al., 2007; Klass, 2009; Ishiwata et al., 2011; Yoshizawa, 2011) and the neutral term "lower Neoptera" is often used (e.g., Kristensen, 1981, 1995), although I use the term “Polyneoptera” in the present study. The presence of euplantulae (Minet and Bourgoin, 1986; Beutel and Gorb, 2001) and a fan-like anal lobe of the hindwing (Grimaldi and Engel, 2005; Beutel and Gorb, 2006) have been proposed as autapomorphies of Polyneoptera. However, these features are not present in some polyneopteran orders, and both are missing in Zoraptera (Minet and Bourgoin, 1986; Grimaldi and Engel, 2005; Yoshizawa, 2011). So far, the most conclusive evidence has been provided by Yoshizawa (2011), who proposed four potential apomorphies of the wing base in support of Polyneoptera, including Zoraptera.

The main alternative hypothesis, the “Paraneoptera concept” with Zoraptera as a sister group of Acercaria (e.g., Hennig 1969; Beutel and Weide 2005; Beutel and Gorb, 2006), has gained no support in more recent studies, and morphological arguments were discussed critically by Yoshizawa (2011). Nevertheless, with the present knowledge, this option cannot be ruled out with certainty.

In insect comparative embryology it is well known that Polyneoptera and Acercaria show a profound contrast in the process of the embryo’s migration into the yolk (Fig. 31A, C). Blastokinesis has been examined in all polyneopteran orders, although the data are

fragmentary in some cases (Plecoptera: Miller, 1939, 1940; Kishimoto and Ando, 1985; Dermaptera: Heymons, 1895; Fuse and Ando, 1983; Shimizu, 2013; Orthoptera: Roonwal, 1936, 1937; Rakshpal, 1962; Warne, 1972; Pétavy, 1985; Grylloblattodea: Ando and Nagashima, 1982; Uchifune and Machida, 2005; Mantophasmatodea: Machida et al., 2004; Phasmatodea: Thomas, 1936; Bedford, 1970; Embioptera: Melander, 1903; Kershaw, 1914; Jintsu, 2010; Mantodea: Hagan, 1917; Blattodea: Wheeler, 1889; Heymons, 1895; Lenoir-Rousseaux and Lender, 1970; Ando, 1971; Tanaka, 1976; Isoptera: Knower, 1900; Striebel, 1960; Mukerji and Chowdhuri, 1962; Kawanishi, 1975; Hu and Xu, 2005). In Polyneoptera, two distinctly different varieties of blastokinesis were distinguished by Anderson (1972), the immersed type and the superficial type. The first is found in Plecoptera, Grylloblattodea, Mantophasmatodea, Embioptera, Isoptera, and Blattoidea. In these groups, the embryo is formed on the ventral side of the egg and covered with the thin amnioserosal fold (Fig. 31A). It extends and moves along the dorsal egg surface and migrates into the yolk after reaching its full elongation. The second type occurs in Dermaptera, Phasmatodea, Mantodea, and Blaberoidea. The embryo is also formed on the ventral side and is covered by the thin amnioserosal fold (Fig. 31B), but without a shift to the dorsal side of the egg and without immersion into the yolk. The embryo maintains its original superficial position on the ventral side and reaches its full length there.

Blastokinesis was also described for members of all acercarian orders, although with a clear bias towards Hemiptera (Psocoptera:

Goss, 1952, 1953; Seeger, 1979; Phthiraptera: Schölzel, 1937; Thysanoptera: Heming, 1979; Haga, 1985; Moritz, 1988; Hemiptera: Mellanby, 1935, 1936; Butt, 1949; Cobben, 1968; Heming and Huebner, 1994). A small embryo forms on the ventral side. It gradually elongates and migrates into the yolk from its rear, accompanied by the production of amnion. At the end of the process the embryo is deeply immersed in the yolk mass (Fig. 31C).

Blastokinesis in the two palaeopteran orders strongly resembles what is described for acercarian groups (Ephemeroptera: Tojo and Machida, 1997, 1998; Odonata: Ando, 1962), with a very similar pattern of embryo formation, elongation and migration into the yolk. The phylogenetic pattern of Palaeoptera outside of Neoptera (outgroup), and Acercaria as a monophyletic neopteran subunit clearly shows that the palaeopteran-acercarian type is a groundplan feature of Pterygota and of Neoptera. The immersed and superficial types occurring in polyneopterans seem to differ greatly, but both share a marked common feature. That is, full elongation of the embryo and formation of amnioserosal fold occur on the egg surface in these groups (Fig. 31A, B). This feature may be an autapomorphy of Polyneoptera, which are not supported by a single non-homoplastic morphological feature at present (see above), and has not unequivocally confirmed by molecular data (Letsch et al., 2012).

Above, I enumerated six features characterizing the embryogenesis of Zoraptera. Among these features, the first, fourth and fifth features are especially significant in discussing the zorapteran

affiliation. Namely, the first feature, "formation" as already discussed and the fourth, "full elongation of the embryo on the egg surface" as mentioned just above can be proposed as potential autapomorphies of Polyneoptera, including Zoraptera. The fifth feature, "immersion of the embryo into the yolk after its full elongation" should be also noticed, being typical of polyneopteran blastokinesis of the immersed type. Consequently, embryological data strongly suggest the placement of Zoraptera among the Polyneoptera.

The embryonic membranes which are crucially involved with the blastokinesis have been largely ignored among insect developmental geneticists, as the model system *Drosophila melanogaster* has an extremely reduced extraembryonic component, the amnioserosa (Panfilio, 2008). However, recently available molecular developmental information focusing on embryonic membranes has gradually increased (Panfilio, 2009; Panfilio and Roth, 2010; Sharma et al. 2013). For example, it has been suggested that embryonic membrane system has taken a great part in the spectacular radiation of insects on land (Anderson, 1972; Zeh et al., 1989), and the significant role of serosa was eventually demonstrated from the recent molecular developmental approach by Jacob et al. (2013). To experimentally test the protective function of the serosa and serosal cuticle, Jacob et al. (2013) investigated the function of a serosal marker *zerknüllt* (*zen*) and a key enzyme in cuticle synthesis, *chitin-synthase1* (*chs1*), using in situ hybridization and RNAi in *Tribolium castaneum,* and revealed a critical role for the insect serosa

in desiccation resistance. So far molecular developmental data on embryonic membranes is strongly biased toward a few orders such as Diptera (*Drosophila*), Coleoptera (*Tribolium*) and Hemiptera (*Oncopeltus*) (Panfilio et al., 2006, 2013; Jacob et al., 2013). EvoDevo approaches on the embryonic membranes covering major insect lineages will provide new insights in the evolutionary understanding of insects.

10.2. Affinities of Zoraptera within Polyneoptera

Closer affinity between Zoraptera and Dermaptera has been suggested based on morphological and molecular data sets (Carpenter and Wheeler, 1999; Terry and Whiting, 2005; the assemblage of them was named the “Haplocercata” by Terry and Whiting [2005]), but this is in contrast to the developmental features discussed above (immersed versus superficial type). According to Chauvin et al. (1991), the eggs of Dermaptera are characterized by a five-layered chorion, aeropyles arranged in a circle, and the presence of one micropyle at the anterior pole of the egg. Shimizu (2013) compared eight dermapteran families and proposed a revised interpretation of micropyle and aeropyle, and concluded that the openings arranged in a circle and that at the anterior pole of the egg as the micropyles and the aeropyle or hydropyle, respectively. The egg structures do not show any resemblances between Zoraptera and Dermaptera. Moreover, inherent problems with the direct optimization (POY) used in molecular analyses supporting this affinity (Carpenter and Wheeler, 1999; Jarvis et al., 2005; Terry

and Whiting, 2005) were pointed out by Simmons (2004), Kjer et al. (2007), Morgan and Kelchner (2010), Yoshizawa (2010), and Simmons et al. (2011), and it was shown in an empirical study (Ogden and Rosenberg, 2007) that POY performs less well than other approaches. In addition, Yoshizawa (2010) pointed out that the specific 18S rRNA sequence was erroneously assigned to Zoraptera (*Zorotypus hubbardi*) by Terry and Whiting (2005) as a result of contamination. This was shown by BLAST search analysis, which assigned this sequence to the dermapteran genus *Tagalina*.

A sister group relationship between Zoraptera and Dictyoptera has been suggested based on morphological characteristics, molecular data, and combined evidence (Silvestri, 1913; Caudell, 1918; Crampton, 1920; Weidner, 1969, 1970; Boudreaux, 1979; Wheeler et al., 2001; Yoshizawa and Johnson, 2005; Ishiwata et al., 2011; Wang et al., 2013). Four morphological characteristics, i.e., a disc-shaped pronotum, a forward-slanting pleural suture, ill-developed indirect flight muscles, and posteriorly directed coxa, have been suggested as potential synapomorphies (Boudreaux, 1979; Wheeler et al., 2001). However, Beutel and Weide (2005) and Friedrich and Beutel (2008) pointed out that the indirect flight muscles are well developed in winged forms, that the other three arguments are greatly weakened by superficial character definition, and that they are obviously either subject to homoplasy or are plesiomorphic. A forward-slanting pleural suture for instance is found in most if not all groups of pterygote insects. Analyses of 18S (Yoshizawa and Johnson, 2005), 28S RNA

(Wang et al., 2013) and three protein-coding genes (Ishiwata et al., 2011) suggested a close affinity between Zoraptera and Dictyoptera. However, Yoshizawa and Johnson (2005) pointed out that this result might be affected by the unusual characteristics of these genes, such as a markedly accelerated substitution rate, resulting in very long branches, modifications of the secondary structure, and long insertions. According to Ishiwata et al. (2011), the close affinity between Zoraptera and Dictyoptera suggested by sequences of protein-coding genes (*DPD1*, *RPB1*, *RPB2*) has only low support in maximum likelihood (ML) analyses, even though it appears well supported by Bayesian analysis. In it, Zoraptera were shown in an unresolved polyneopteran polytomy in a summary tree (Ishiwata et al. 2011). The features of embryonic development discussed above (immersed versus superficial type) and of egg structure also do not suggest the affinity between Zoraptera and Dictyoptera. We have several studies on the egg structures of Dictyoptera such as: Iwaikawa and Ogi (1982) on Mantodea, Hinton (1981) and Bellés et al. (1994) on Blattodea, and Knower (1900), Mukerji (1970), and Grandi (1990), and Grandi and Chicca (1999) on Isoptera. Although the information is still fragmentary, Fujita and Machida (2014) examined available information on the dictyopteran egg structure, and proposed the numerous micropyles localized on the ventral surface as an autapomorphy of Dictyoptera. In the eggs of Mantodea and Blattodea, which are protected by the ootheca, the chorion is very fragile, and the endochorion is laminal. Thus, I cannot find any common features of

the egg structure suggesting phylogenetic affinities between Zoraptera and Dictyoptera. However, it has to be taken into consideration that a hypothetical ancestral condition is likely secondarily modified in extant members of the Dictyoptera due to the presence of the ootheca in the groundplan of this lineage.

A clade Zoraptera + Embioptera ("Mystroptera": Rafael and Engel, 2006) is suggested by the largest number of potential synapomorphies, including a reduced number of tarsomeres, paddle-shaped wings, a metafemur with a unique musculature, wing base structures, and ecology-related characteristics such as wing dimorphism and a gregarious lifestyle (Minet and Bourgoin, 1986; Engel and Grimaldi, 2000, 2002; Yoshizawa, 2007, 2011). The present study revealed a marked developmental feature shared by embryos of members of both orders, i.e., an extraordinarily long egg tooth. Embioptera have a unique set of features concerning the egg structures, such as a specialized micropyle-related chorion structure, a micropylar tube, an operculum, and a polar mound, while all these features are lacking in zorapteran eggs (cf. Jintsu et al., 2007; Jintsu and Machida, 2009). As an alternative evolutionary scenario of Embioptera, a close affinity between Embioptera and Phasmatodea has been suggested based on morphological and molecular evidence (Rähle, 1970; Tilgner, 2002; Kjer, 2004; Terry and Whiting, 2005; Bradler, 2009; Jintsu et al., 2007, 2010; Ishiwata et al., 2011; Wipfler et al., 2011; Friedemann et al., 2012; Letsch and Simon, 2013), and the name "Eukinolabia" was proposed for this clade by Terry and Whiting (2005). Embryological

studies also support the affinity of Embioptera and Phasmatodea and proposed some potential autapomorphies in the egg structure (Jintsu et al., 2007, 2010; Jintsu and Machida, 2009). In this context, there is one thing worth mentioning. The present study revealed that unique egg structure among polyneopteran eggs, i.e., a pair of micropyles, occurs in eggs of Zoraptera. This peculiar character is found in basalmost phasmatodean Timematodea and also in Euphasmatodea, in the latter of which micropyles are located very closely as if they could be a single micropyle (Godeke and Pijnacker, 1984; Jintsu et al., 2010). Consequently, this was suggested as potential autapomorphy of a clade comprising Zoraptera + Eukinolabia (=Embioptera + Phasmatodea), with secondary modification (reduction into one) in Embioptera. A clade comprising Zoraptera, Embioptera and Phasmatodea was first suggested based on wing base structures by Yoshizawa (2007), but after performing formal cladistic analysis, he suggested the close affinity between Phasmatodea and Orthoptera (Yoshizawa, 2011). A monophyletic unit, Zoraptera + Embioptera + Phasmatodea, was again tentatively supported by the results of recent studies on sperm ultrastructure. Dallai et al. (2011, 2012b) provided a detailed description of the male reproductive system and sperm ultrastructure, and also suggested the close affinity of these three orders based on two apomorphic characteristics, 17 protofilaments comprising accessory tubules of axonomes and L-shaped electron-dense lamellae accompanying microtubular triplets in the centriole adjunct.

The interpretation of the elongated egg tooth occurring in

Zoraptera remains ambiguous in the scenario with Zoraptera as the sister group of Eukinolabia. While an extremely long egg tooth is shared with Zoraptera and Embioptera, egg tooth itself is considered to be absent in Phasmatodea, which possess tough egg shells and an operculum (Thomas, 1936; Bedford, 1970). This suggests that the specialized egg teeth of Zoraptera and Embioptera have either evolved independently or that is secondarily absent in phasmatodean embryos.

The prelarvae of Zoraptera use an egg tooth to penetrate the chorion of the egg, which lacks an operculum (Fig. 19A, B). In contrast, an operculum is used for hatching by the prelarvae of Embioptera and also of Phasmatodea. It is noteworthy that an egg tooth is preserved in embryos of the former group, but apparently does not interact with the chorion. The operculum-detaching mechanism is less elaborate in eggs of Embioptera than those of Phasmatodea, which lack a perforating device. The phasmatodean egg is characterized by a distinct detachment line between the operculum and the egg body (Hinton, 1981; Jintsu et al., 2010), whereas in embiopteran eggs a less well-defined spongy zone of weakness forms an opening mechanism (Jintsu and Machida, 2009; Jintsu, 2010). It is conceivable that a longer evolutionary pathway led to the typical condition of the phasmatodean operculum and opening mechanism, along with increasing reduction of the primarily present egg tooth. This interpretation is tentatively supported by an interesting finding in timematodean eggs. A discontinuous and ill-defined but long egg tooth is identified in the frontal region of the prelarvae of *Timema*

monikensis (Y. Uchifune-Jintsu and R. Machida, pers. obs.). This suggests that an elongated egg tooth is groundplan apomorphy of the Zoraptera-Eukinolabia clade, with partial secondary reduction in Phasmatodea (groundplan) and complete loss as autapomorphy of Euphasmatodea. That Phasmatodea is more closely related with Embioptera is clearly supported by several derived features of the egg: 1) a detachable operculum, 2) a specialized micropylar structure on the ventral side of the egg, i.e., micropylar plate or tube, 3) a small number of micropyles (one or two) associated with the specialized micropylar structure, and 4) a specialized chorionic structure at the posterior pole of the egg, i.e., a polar mound or projection. Consequently, an evolutionary scenario for the egg tooth and egg structures is shown in Figure 32.

The systematic problem of Zoraptera has been long standing phylogenetic mystery since their discovery 100 years ago, which has been called the “Zoraptera problem” (Beutel and Weide, 2005). Proposing two potential embryological autapomorphies for Polyneoptera of which monophyly has been much argued, the present study strongly supported the monophyletic Polyneoptera and affiliated Zoraptera to Polyneoptera. The careful comparative embryological analysis simultaneously proposed a close affinity of Zoraptera with Eukinolabia, and figured out a phylogenetic hypothesis formulated as “Zoraptera + (Embioptera + Phasmatodea [= Timematodea + Euphasmatodea])”, integrating data from various sources such as the male reproductive system and spermatozoa. The present results could

afford a deep insight to the long standing “Zoraptera problem”, providing a plausible, phylogenetic hypothesis on the placement of Zoraptera. Different follow-up investigations such as detailed documentation of organogenesis and embryological studies covering Polyneoptera will surely lead to a well-founded and detailed evolutionary scenario of enigmatic Polyneoptera and the final settlement of “Zoraptera problem”.

ACKNOWLEDGMENTS

I wish to express my hearty thanks to Prof. Dr. Ryuichiro Machida of the Sugadaira Montane Research Center, University of Tsukuba (SMRC) for his constant guidance as well as invaluable suggestions and advices given to me throughout this study.

For the valuable advice and critical reading of the manuscript, I wish to express my sincerest thanks to Prof. Dr. Osamu Numata, Prof. Dr. Hiroshi Wada and Prof. Dr. Jun-Ichi Hayashi of University of Tsukuba. I am also grateful to Prof. Dr. Rolf G. Beutel of Institut für Spezielle Zoologie und Evolutionsbiologie mit Phyletischem Museum, Friedrich-Schiller-Universität Jena, Prof. Dr. Romano Dallai of University of Siena, Prof. Dr. Bernhard Misof of Zoologisches Forschungsmuseum Alexander König, Rheinische Friedrich-Wilhelms-Universität Bonn, Prof. Dr. Yukimasa Kobayashi of Tokyo Metropolitan University, Prof. Dr. Chow-Yang Lee of Universiti Sains Malaysia, and Prof. Dr. Idris Abd. Ghani of Universiti Kebangsaan Malaysia for critical reading of the manuscript and their valuable discussion and advices.

Finally, I deeply thank Dr. Toshiki Uchifune of Yokosuka City Museum, Dr. Yoshie Uchifune-Jintsu of Japan Agency for Marine-Earth Science and Technology, Dr. Makiko Fukui of Ehime University, Dr. Kaoru Sekiya, Dr. Shota Shimizu of SMRC, Mr. Yasutaka Nakagaki, Mr. Shigekazu Tomizuka, Ms. Mari Fujita, Ms. Michiyo Matsushima of SMRC, Mr. Daichi Kato of Hirosaki

University, Mr. Kim Hong Yap, Mr. Shahrul Nazly B. Mahmud and Mr. Norazli Nordin for their kind help in collecting materials.

The present study was partly supported by a Sasakawa Scientific Research Grant (22-504) from The Japan Science Society and by University of Tsukuba Research Infrastructure Support Program.

LETERATURE CITED

Anderson, D.T. (1972) The development of apterygote Insects. *In*: S.J. Counce and C.H. Waddington (eds.), *Developmental systems: insects, Vol. 1*, pp. 95–163. Academic Press, New York.

Ando, H. (1962) *The comparative embryology of Odonata with special reference to a relic dragonfly,* Epiophlebia superstes *Selys*. Japan Society for the Promotion of Science, Tokyo.

Ando, H. (1971) Studies on the pleuropodia of an ovoviviparous cockroach, *Opisthoplatia orientalis* Burmeister (Blattaria: Epilampridae). *Bulletin of the Sugadaira Biological Laboratory*, **4**, 59–71.

Bedford, G.O. (1970) The development of the egg of *Didymuria violescens* (Phasmatodea: Phasmatidae: Podacanthinae) –Embryology and determination of the stage at which first diapause occurs. *Australian Journal of Zoology*, **18**, 155–169.

Bellés, X., P. Cassier, X. Cerdá, N. Pascual, M. André, Y. Rósso and M.D. Piulachs (1994) Induction of choriogenesis by 20-hydroxyecdysone in the german cockroach. *Tissue & Cell*, **25**, 195–204.

Bentley, D., H. Keshishian, M. Shankland, and A. Toroian-Raymond (1979) Quantitative staging of embryonic development of the grasshopper, *Schistocerca nitens*. *Journal of Embryology and Experimental Morphology*, **54**, 47–74.

Beutel, R.G. (1997) Über Phylogenese und Evolution der Coleoptera (Insecta), insbesondere der Adephaga. *Verhandlungen des Naturwissenschaftlichen Vereins in Hamburg. N.F.*, **31**, 1–164.

Beutel, R.G. and S.N. Gorb (2001) Ultrastructure of attachment specializations of hexapods (Arthropoda): Evolutionary patterns inferred from a revised ordinal phylogeny. *Journal of Zoological Systematics and Evolutionary Research* **39**, 177–207.

Beutel, R.G. and S.N. Gorb (2006) A revised interpretation of the evolution of attachment structures in Hexapoda with special emphasis on Mantophasmatodea. *Arthropod Systematics & Phylogeny*, **64**, 3–25.

Beutel, R.G. and D. Weide (2005) Cephalic anatomy of *Zorotypus hubbardi* (Hexapoda: Zoraptera): New evidence for a relationship with Acercaria. *Zoomorphology*, **124**, 121–136.

Blanke, A.B. Wipfler, H. Letsch, M. Koch, F. Beckmann, R. Beutel and B. Misof (2012) Revival of Palaeoptera –head characters support a monophyletic origin of Odonata and Ephemeroptera (Insecta). *Cladistics*, **28**, 560–581.

Boudreaux, H.B. (1979) *Arthropod Phylogeny with Special Reference to Insects*. John Wiley & Sons, New York.

Bradler, S. (2009) Die Phylogenie der Stab- und Gespenstschrecken (Insecta: Phasmatodea). *Species, Phylogeny & Evolution*, **2**, 3–139.

Butt, F.H. (1949) Embryology of the milkweed bug, *Oncopeltus fasciatus* (Hemiptera). *Cornell University Agricultural*

Experiment Station Memoir, **283**:1–43.

Carpenter, J.M. and W.C. Wheeler (1999) Cladística numérica, análisis simultáneo y filogenia de hexápodos. *Boletín de la Sociedad Entomológica Aragonesa*, **26**, 333–346.

Caudell, A.N. (1918) *Zorotypus hubbardi*, a new species of the order Zoraptera from the United States. *Canadian Entomologist*, **50**, 375–381.

Caudell, A.N. (1920) Zoraptera not an apterous order. *Proceedings of the Entomological Society of Washington*, **22**, 84–97.

Chauvin, G., C. Hamon, M. Vancassel and G. Yannier (1991) The egg of *Forficula auricularia* L. (Dermaptera, Forficulidae): Ultrastructure and resistance to low and high temperatures. *Canadian Journal of Zoology*, **69**, 2873–2878.

Choe, J.C. (1989) *Zorotypus gurneyi*, new species, from Panama and redescription of *Z. barberi* Gurney (Zoraptera: Zorotypidae). *Annals of the Entomological Society of America*, **82**, 149–155.

Choe, J.C. (1994a) Sexual selection and mating system in *Zorotypus gurneyi* Choe (Insecta: Zoraptera). I. Dominance hierarchy and mating success. *Behavioral Ecology and Sociology*, **34**, 87–93.

Choe, J.C. (1994b) Sexual selection and mating system in *Zorotypus gurneyi* Choe (Insecta: Zoraptera). II. Determinants and dynamics of dominance. *Behavioral Ecology and Sociobiology*, **34**, 233–237.

Choe, J.C. (1995) Courtship feeding and repeated mating in *Zorotypus barberi* (Insecta: Zoraptera). *Animal Behaviour*, **49**, 1511–1520.

Choe, J.C. (1997) The evolution of mating systems in the Zoraptera: Mating variations and sexual conflicts. *In*: J.C. Choe and B.J. Crespi (eds.), *The Evolution of Mating Systems in Insects and Arachnids*, pp. 130–145. Cambridge University Press, Cambridge.

Cobben, R.H. (1968) *Evolutionary Trends in Heteroptera. Part I. Eggs, Architecture of the Shell, Gross Embryology and Eclosion*. Centre for Agriculture Publishing and Documentation, Wageningen.

Crampton, G.C. (1920) Some anatomical details of the remarkable winged zorapteron *Zorotypus hubbardis* [sic] Caudelli, with notes on its relationships. *Proceedings of the Entomological Society of Washington*, **22**, 98–106.

Crampton, G.C. (1926) Comparison of the neck and the prothoracic sclerites throughout the orders of insects from the standpoint of phylogeny. *Transactions of the American Entomological Society*, **52**, 199–248, 8 pls.

Dallai, R., D. Mercati, M. Gottardo, R. Machida, Y. Mashimo and R.G. Beutel (2011) The male reproductive system of *Zorotypus caudelli* Karny (Zoraptera): Sperm structure and spermiogenesis. *Arthropod Structure & Development*, **40**, 531–547.

Dallai, R., D. Mercati, M. Gottardo, R. Machida, Y. Mashimo and R.G. Beutel (2012a) The fine structure of the female reproductive system of *Zorotypus caudelli* Karny (Zoraptera). *Arthropod Structure & Development*, **41**, 51–63.

Dallai, R., D. Mercati, M. Gottardo, A.T. Dossey, R. Machida, Y.

Mashimo and R.G. Beutel (2012b) The male and female reproductive systems of *Zorotypus hubbardi* Caudell, 1918 (Zoraptera). *Arthropod Structure & Development*, **41**, 337–359.

Dallai, R., M. Gottardo, D. Mercati, R. Machida, Y. Mashimo, Y. Matsumura and R.G. Beutel (2013a) Divergent mating patterns and a unique mode of external sperm transfer in Zoraptera - an enigmatic group of pterygote insects. *Naturwissenschaften*, **100**, 581–594.

Dallai, R., M. Gottardo, D. Mercati, R. Machida, Y. Mashimo, Y. Matsumura and R.G. Beutel (2013b) Giant spermatozoa and a huge spermatheca: A case of coevolution of male and female reproductive organs in the ground louse *Zorotypus impolitus* (Insecta, Zoraptera). *Arthropod Structure & Development*, in press, http://dx.doi.org/10.1016/j.asd.2013.10.002

Davis, R.G. (1966) The postembryonic development of *Hemimerus vicinus* Rehn & Rehn (Dermaptera: Hemimeridae). *Proceedings of the Royal Entomological Society of London. Series A, General Entomology*, **41**, 67–77.

Delamare-Deboutteville, C. (1947) Sur la morphologie des adultes apteres et ailés de Zorapteres. *Annales des Sciences Naturelles - Zoologie et Biologie Animale*, **11**, 145–154.

Engel, M.S. (2009) A new apterous *Zorotypus* in Miocene amber from the Dominican Republic (Zoraptera: Zorotypidae). *Acta Entomologica Slovenica*, **16**, 127–136.

Engel, M.S. and D.A. Grimaldi (2000) A winged *Zorotypus* in

Miocene amber from the Dominican Republic (Zoraptera: Zorotypidae) with discussion on relationships of and within the order. *Acta Geologia Hispanica*, **35**, 149–164.

Engel, M.S. and D.A. Grimaldi (2002) The first Mesozoic Zoraptera (Insecta). *American Museum Novitates*, **3362**, 1–20.

Friedemann, K., B. Wipfler, S. Bradler and R.G. Beutel (2012) On the head morphology of *Phyllium* and the phylogenetic relationships of Phasmatodea (Insecta). *Acta Zoologica*, **93**, 184–199.

Friedrich, F. and R.G. Beutel (2008) The thorax of *Zorotypus* (Hexapoda, Zoraptera) and a new nomenclature for the musculature of Neoptera. *Arthropod Structure & Development*, **37**, 29–54.

Fujita, M. and R. Machida (2014) Preliminary Note on the Embryonic Development of *Eucorydia yasumatsui* Asahina (Insecta: Blattaria, Polyphagidae). *Proceedings of the Arthropodan Embryological Society of Japan*, **48** (in press).

Fuller, C. (1920) Studies on the post-embryonic development of the antennae of termites. *Annals of the Natal Museum*, **4**, 235–295.

Godeke, J. and L.P. Pijnacker (1984) Structure of the micropyle in the eggs of the parthenogenetic stick insect *Carausius morosus* Br. (Phasmatodea, Phasmatidea). *Netherlands Journal of Zoology*, **34**, 407–413.

Goss, R.J. (1952) The early embryology of the book louse, *Liposcelis divergens* Badonnel (Psocoptera; Liposcelidae). *Journal of Morphology*, **91**, 135–167.

Goss R.J. (1953) The advanced embryology of the book louse, *Liposcelis divergens* Badonnel (Psocoptera; Liposcelidae). *Journal of Morphology*, **92**, 157–205.

Grandi, G. (1990) Oogenesis in *Kalotermes flavicollis* (Fabr.) (Isoptera, Kalotermitidae) III. Choriogenesis and corpus luteum formation in female supplementary reproductive. *Bolletino di Zoologia*, **57**, 97–107.

Grandi, G. and M. Chicca (1999) Oogenesis in supplementary reproductives of *Reticulitermes lucifugus* Rossi (Isoptera Rhinotermitidae): An ultrastructural study. *Invertebrate Reproduction & Development*, **35**, 65–79.

Grimaldi, D. and M.S. Engel (2005) Evolution of the Insects. Cambridge University Press, New York.

Gurney, A.B. (1938) A synopsis of the order Zoraptera, with notes on the biology of *Zorotypus hubbardi* Caudell. *Proceedings of the Entomological Society of Washington*, **40**, 57–87.

Haga, K. (1985) Oogenesis and embryogenesis of the idolothripine thrips, *Bactrothrips brevitubus* (Thysanoptera, Phlaeothripidae). *In*: H. Ando and K. Miya (eds.), *Recent advances in insect embryology in Japan*, pp 45–106. Isebu, Tsukuba.

Hagan, H.R. (1917) Observations on the embryonic development of the mantid *Paratenodera sinensis*. *Journal of Morphology*, **30**, 223–243.

Heming, B.S. (1979) Origin and fate of germ cells in male and female embryos of *Haplothrips verbasci* (Osborn) (Insecta, Thysanoptera,

Phlaeothripidae). *Journal of Morphology*, **160**, 323–344.

Heming, B.S. (2003) *Insect development and evolution*. Cornell University Press, Ithaca.

Heming, B.S. and E. Huebner (1994) Development of the germ cells and reproductive primordial in male and female embryos of *Rhodnius prolixus* Stål (Hemiptera: Reduviidae). *Canadian Journal of Zoology*, **72**, 1100–1119.

Hennig, W. (1969) *Die Stammesgeschichte der Insekten*. Waldemar Kramer, Frankfurt am Main.

Heymons, R. (1895) *Die Embryonalentwicklung von Dermapteren und Orthopteren unter Besonderer Berücksichtigung der Keimblätterbildung*. Gustav Fischer, Jena.

Hinton, H.E. (1981) *Biology of Insect Eggs. Vol. 2*. Pergamon Press, Oxford.

Hockman, H., M.D. Picker, K.-D. Klass and L. Pretorius (2009) Postembryonic development of the unique antenna of Mantophasmatodea (Insecta). *Arthropod Structure & Development*, **38**, 125–133.

Hu, X.P. and Y. Xu (2005) Morphological embryonic development of the eastern subterranean termite, *Reticulitermes flavipes* (Isoptera: Rhinotermitidae). *Sociobiology*, **45**, 573–586.

Hünefeld, F. (2007) The genital morphology of *Zorotypus hubbardi* Caudell, 1918 (Insecta: Zoraptera: Zorotypidae). *Zoomorphology*, **126**, 135–151.

Ishiwata, K., G. Sasaki, J. Ogawa, T. Miyata and Z.-H. Su (2011)

Phylogenetic relationships among insect orders based on three nuclear protein-coding gene sequences. *Molecular Phylogenetics and Evolution*, **58**, 169–180.

Iwaikawa, Y. and K. Ogi (1982) Chorionic structures of the egg shells of mantis, *Tenodera aridifolia* (Dictyoptera: Mantidae). Mantidae). *Research Bulletin (Natural Science and Psychology), The College of General Education, Nagoya University*, **26**, 69–83 (in Japanese with English summary).

Jacob, C.G.C., G.L. Rezende, G.E.M. Lamers and M. van der Zee (2013) The extraembryonic serosa protects the insect egg against desiccation. *Proceedings of the Royal Society B*, **280**, 20131082.

Jarvis, K.J., F. Haas and M.F. Whiting (2005) Phylogeny of earwigs (Insecta: Dermaptera) based on molecular and morphological evidence: Reconsidering the classification of Dermaptera. *Systematic Entomology*, **30**, 442–453.

Jintsu, Y. (2010) *Embryological studies on* Aposthonia japonica *(Okajima) (Insecta: Embioptera)*. Doctoral dissertation. University of Tsukuba, Tsukuba.

Jintsu, Y. and R. Machida (2009) TEM observations of the egg membranes of a web-spinner, *Aposthonia japonica* (Okajima) (Insecta: Embioptera). *Proceedings of the Arthropodan Embryological Society of Japan*, **44**, 19–24.

Jintsu, Y., T. Uchifune and R. Machida (2007) Egg membranes of a web-spinner, *Aposthonia japonica* (Okajima) (Insecta: Embioptera). *Proceedings of the Arthropodan Embryological*

Society of Japan, **42**, 1–5.

Jintsu, Y., T. Uchifune and R. Machida (2010) Structural features of eggs of the basal phasmatodean *Timema monikensis* Vickery & Sandoval, 1998 (Insecta: Phasmatodea: Timematidae). *Arthropod Systematics & Phylogeny*, **68**, 71–78.

Johannsen, O.A. and F.G. Butt (1941) *Embryology of Insects and Myriapods*. McGraw-Hill, New York.

Kawanishi, C.Y. (1975) Embryonic development of the drywood termite, *Cryptotermes brevis*. *Hawaii Agricultural Experiment Station*, **95**, 1–36.

Kershaw, J.C. (1914) Development of an embiid. *Journal of the Royal Microscopical Society*, **34**, 24–27.

Kishimoto, T. and H. Ando (1985) External features of the developing embryo of the stonefly, *Kamimuria tibialis* (Pictét) (Plecoptera, Perlidae). *Journal of Morphology*, **183**, 311–326.

Kjer, K.M. (2004) Aligned 18S and insect phylogeny. *Systematic Biology*, **53**, 506–514.

Kjer, K.M., F.L. Carl, J. Litman and J. Ware (2006) A molecular phylogeny of Hexapoda. *Arthropod Systematics & Phylogeny*, **64**, 35–44.

Kjer, K.M., J.J. Gillespie and K.A. Ober (2007) Opinions on multiple sequence alignment, and an empirical comparison of repeatability and accuracy between POY and structural alignments. *Systematic Biology*, **56**, 133–146.

Klass, K.-D. (2009) A critical review of current data and hypotheses

on hexapod phylogeny. *Proceedings of the Arthropodan Embryological Society of Japan*, **43**, 3–22.

Knower, H.M. (1900) The embryology of a termite. *Journal of Morphology*, **16**, 505–568, 2 pls.

Konopová, B. and J. Zrzavý (2005) Ultrastructure, development, and homology of insect embryonic cuticles. *Journal of Morphology*, **264**, 339–362.

Krause, G. (1939) Die Eitypen der Insecten. *Biologisches Zentralblatt*, **59**, 495–536.

Kristensen, N.P. (1975) The phylogeny of hexapod "orders". A critical review of recent accounts. *Journal of Zoological Systematics and Evolutionary Research*, **13**, 1–44.

Kristensen, N.P. (1981) Phylogeny of insect orders. *Annual Review of Entomology*, **26**, 135–157.

Kristensen, N.P. (1991) Phylogeny of extant hexapods. *In*: CSIRO (ed.), *The insects of Australia. 2nd ed. Vol. 1*, pp 125–140. Melbourne University Press, Carlton.

Kristensen, N.P. (1995) Forty years' insect phylogenetic systematics: Hennig's "Kritische Bemerkungen…", and subsequent developments. *Zoologische Beiträge, Neue Folge*, **36**, 83–124.

Kukalová-Peck, J. and S.B. Peck (1993) Zoraptera wing structures: Evidence for new genera and relationship with the blattoid orders (Insecta: Blattoneoptera). *Systematic Entomology*, **18**, 333–350.

Lenoir-Rousseaux, J.J. and T. Lender (1970) Table de développement embryonnaire de *Periplaneta america* (L.) Insecte, Dictyoptère.

Bulletin de la Société zoologique de France, **95**, 737–751.

Letsch, H. and S. Simon (2013) Insect phylogenomics: New insights on the relationships of lower neopteran orders (Polyneoptera). *Systematic Entomology*, **38**, 783–793.

Letsch, H.O., K. Meusemann, B. Wipfler, K. Schütte, R. Beutel and B. Misof (2012) Insect phylogenomics: Results, problems and the impact of matrix composition. *Proceedings of the Royal Society B*, **279**, 3282–3290.

Machida, R. (2000a) Serial homology of the mandible and maxilla in the jumping bristletail *Pedetontus unimaculatus* Machida, based on external embryology (Hexapoda: Archaeognatha, Machilidae). *Journal of Morphology*, **245**, 19–28.

Machida, R. (2000b) Usefulness of low-vacuum scanning electron microscopy in descriptive insect embryology. *Proceedings of Arthropodan Embryological Society of Japan*, **35**, 17–19.

Machida, R., T. Nagashima and H. Ando (1990) The early embryonic development of the jumping bristletail *Pedetontus unimaculatus* Machida (Hexapoda: Microcoryphia, Machilidae). *Journal of Morphology*, **206**, 181–195.

Machida, R., T. Nagashima and H. Ando (1994a) Embryonic development of the jumping bristletail *Pedetontus unimaculatus* Machida, with special reference to embryonic membranes (Hexapoda: Microcoryphia: Machilidae). *Journal of Morphology*, **220**, 147–165.

Machida, R., T. Nagashima and T. Yokoyama (1994b) Mesoderm

segregation of a jumping bristletail, *Pedetontus unimaculatus* Machida (Hexapoda, Microcoryphia), with a note on an automatic vacuum infiltrator. *Proceedings of Arthropodan Embryological Society of Japan*, **29**, 23–24 (in Japanese with English figure legend).

Machida, R., K. Tojo, T. Tsutsumi, T. Uchifune, K.-D. Klass, M.D. Picker and L. Pretorius (2004) Embryonic development of heel-walkers: Reference to some prerevolutionary stages (Insecta: Mantophasmatodea). *Proceedings of Arthropodan Embryological Society of Japan*, **39**, 31–39.

Masumoto, M. (2006) *Studies on the egg membranes and embryonic membranes of Zygentoma (Insecta): Innovation of the egg membrane and embryonic membrane systems under the invasion and adaptation to terrestrial habitats in insects*. Doctoral dissertation. University of Tsukuba, Tsukuba.

Masumoto, M. and R. Machida (2006) Development of embryonic membranes in the silverfish *Lepisma saccharina* Linnaeus (Insecta: Zygentoma, Lepismatidae). *Tissue & Cell*, **38**, 159–169.

Matsuda, R. (1970) Morphology and evolution of the insect thorax. *Memoirs of the Entomological Society of Canada*, **76**, 1–431.

Melander, A.L. (1903) Notes on the structure and development of *Embia texana*. *The Biological Bulletin*, **4**, 99–118.

Mellanby, H. (1935) The early embryonic development of *Rhodnius prolixus* (Hemiptera, Heteroptera). *Quarterly Journal of Microscopical Science*, **78**, 71–90, 1 pl.

Mellanby, H. (1936) The later embryology of *Rhodnius prolixus*. *Quarterly Journal of Microscopical Science*, **79**, 1–42.

Miller, A. (1939) The egg and early development of the stonefly, *Pteronarcys proteus* Newman (Plecoptera). *Journal of Morphology*, **64**, 555–609.

Miller, A. (1940) Embryonic membranes, yolk cells, and morphogenesis of the stonefly *Pteronarcys proteus* Newman (Plecoptera: Pteronarcidae). *Annals of the Entomological Society of America*, **33**, 437–477.

Minet, J. and T. Bourgoin (1986) Phylogenie et classification des Hexapodes (Arthropoda). *Cahiers Liaison OPIE*, **20**, 23–28.

Misof, B., O. Niehuis, I. Bischoff, A. Rickert, D. Erpenbeck and A. Staniczek (2007) Towards an 18S phylogeny of hexapods: Accounting for group-specific character covariance in optimized mixed nucleotide/doublet models. *Zoology*, **110**, 409–429.

Morgan, J.M. and S.A. Kelchner (2010) Inference of molecular homology and sequence alignment by direct optimization. *Molecular Phylogenetics and Evolution*, **56**, 305–311.

Moritz, G. (1988) Die Ontogenese der Thysanoptera (Insecta) unter besonderer Berücksichtigung des Fransenflüglers *Hercinothrips femoralis* (O.M. Reuter, 1891) (Thysanoptera, Thripidae, Panchaetothripinae) I. Embryonalentwicklung. *Zoologische Jahrbucher. Abteilung für Anatomie und Ontogenie der Tiere*, **117**, 1–64.

Mukerji, D. (1970) Embryology of termites. *In*: K. Krishma and F.M.

Weesner (eds.), *Biology of Termites, vol. 2*, pp. 37–72. Academic Press, New York/London.

Mukerji, D. and R. Chowdhuri (1962) Developmental stages of *Odontotermes redemanni* (Wasmann). *Proceedings of the New Delhi Symposium, UNESCO Paris*, 77–95, 17 pls.

Nagashima, T. (1991) Postembryonic development and homology of external genitalia in *Galloisiana nipponensis* (Caudell et King) (Notoptera: Grylloblattidae). *International Journal of Insect Morphology and Embryology*, **20**, 157–168.

Niehuis, O., G. Hartig, S. Grath, H. Pohl, J. Lehmann, H. Tafer, A. Donath, V. Krauss, C. Eisenhardt, J. Hertel, M. Peterson, C. Mayer, K. Meusemann, R.S. Peters, P.F. Stadler, R.G. Beutel, E. Bornberg-Bauer, D.D. McKenna and B. Misof. (2012) Genomic and morphological evidence converge to resolve the enigma of Strepsiptera. *Current Biology*, **22**, 1309–1313.

Ogden, T.H. and M.S. Rosenberg (2007) Alignment and topological accuracy of the direct optimization approach via POY and traditional phylogenetics via ClustalW + PAUP*. *Systematic Biology*, **56**, 182–193.

Panfilio, K.A. (2008) Extraembryonic development in insects and the acrobatics of blastokinesis. *Developmental Biology*, **313**, 471–491.

Panfilio, K.A. (2009) Late extraembryonic morphogenesis and its *zen*^{RNAi}-induced failure in the milkweed bug *Oncopeltus fasciatus*. *Developmental Biology*, **333**, 297–311.

Panfilio, K.A. and S. Roth (2010) Epithelial reorganization events during late extraembryonic development in a hemimetabolous insect. *Developmental Biology*, **340**, 100–115.

Panfilio, K.A., P.Z. Liu, M. Akam and T.C. Kaufman (2006) *Oncopeltus fasciatus zen* is essential for serosal tissue function in katatrepsis. *Developmental Biology*, **292**, 226–243.

Panfilio K.A., G. Oberhofer and S. Roth (2013) High plasticity in epithelial morphogenesis during insect dorsal closure. *Biology Open*, **2**, 1108–1118.

Pétavy, G. (1985) Origin and development of the vitellophags during embryogenesis of the migratory locust, *Locusta migratoria* L. (Orthoptera: Acrididae). *International Journal of Insect Morphology and Embryology*, **14**, 361–379.

Pohl, H. and R.G. Beutel, R.G. (2013) The Strepsiptera-Odyssey - the history of the systematic placement of an enigmatic parasitic insect order. *Entomologia*, **1**, e4.

Qadri, M.A.H. (1938) The Life-history and growth of the cockroach *Blatta orientalis*, Linn. *Bulletin of Entomological Research*, **29**, 263–276.

Qadri, M.A.H. (1940) On the development of the genitalia and their ducts of orthopteroid insects. *Transactions of the Royal Entomological Society of London*, **90**, 121–175, 7 pls.

Rafael, J.A. and M.S. Engel (2006) A new species of *Zorotypus* from Central Amazonia, Brazil (Zoraptera: Zorotypidae). *American Museum Novitates*, **3528**, 1–11.

Rähle, W. (1970) Untersuchungen an Kopf und Prothorax von *Embia ramburi* Rimsky-Korsakow 1906 (Embioptera, Embiidae). *Zoologische Jahrbucher. Abteilung für Anatomie und Ontogenie der Tiere*, **87**, 248–330.

Rakshpal, R. (1962) Morphogenesis and embryonic membranes of *Gryllus assimilis* (Fabricius) (Orthoptera: Gryllidae). *Proceedings of the Royal Entomological Society of London. Series A*, **37**, 1–12.

Rasnitsyn, A.P. (1998) On the taxonomic position of the insect order Zorotypida = Zoraptera. *Zoologischer Anzeiger*, **237**, 185–194.

Riegel, G.T. (1987) Order Zoraptera. *In*: F.W. Stehr (ed.), *Immature Insects. vol. 1*, pp. 184–185. Kendall/Hunt Publishing Co., Dubuque, Iowa.

Riegel, G.T. and S.J. Eytalis (1974) Life history studies on Zoraptera. *Proceedings North Central Branch, Entomological Society of America*, **29**, 106–107.

Roonwal, M.L. (1936) Studies on the embryology of the African migratory locust, *Locusta migratoria migratorioides* Reiche and Frm. (Orthoptera, Acrididae). I. The early development, with a new theory of multi-phased gastrulation among insects. *Philosophical Transactions of the Royal Society B*, **226**, 391–421, 3 pls.

Roonwal, M.L. (1937) Studies on the embryology of the African migratory locust, *Locusta migratoria migratorioides* Reiche and Frm. (Orthoptera, Acrididae). II. Organogeny. *Philosophical Transactions of the Royal Society B*, **227**, 175–244, 7 pls.

Ross, D.A. (1986) The evolution of wing dimorphism in insects. *Evolution*, **40**, 1009–1020.

Sander, K. (1984) Extrakaryotic determinants, a link between oogenesis and embryonic pattern formation in insect. *Proceedings of Arthropodan Embryological Society of Japan*, **19**, 1–12.

Schölzel, G. (1937) Die Embryologie der Anopluren und Mallophagen. *Zeitschrift für Parasitenkunde*, **9**, 730–770.

Seeger, W. (1979) Spezialmerkmale an eihüllen und embronen von Psocoptera im vergleich zu anderen Paraneoptera (Insecta); Psocpotera als monophyletische gruppe. *Stuttgarter Beiträge zu Naturkunde, Series A*, **329**, 1–57.

Sharma, R., A. Beermann and R. Schröder (2013) The dynamic expression of extraembryonic marker genes in the beetle *Tribolium castaneum* reveals the complexity of serosa and amnion formation in a short germ insect. *Gene Expression Patterns*, **13**, 362–371.

Shetlar, D.J. (1974) *The biology, morphology, and taxonomy of* Zorotypus hubbardi *Caudell (Insecta: Zoraptera)*. Master's thesis. The University of Oklahoma, Norman.

Shetlar, D.J. (1978) Biological observations on *Zorotypus hubbardi* Caudell (Zoraptera). *Entomological News*, **89**, 217–223.

Shimizu, S. (2013) *Comparative Embryology of Dermaptera (Insecta)*. Doctoral dissertation. University of Tsukuba, Tsukuba.

Shimizu, S. and R. Machida (2011) Reproductive biology and postembryonic development in the basal earwig *Diplatys*

flavicollis (Shiraki) (Insect: Dermaptera: Diplatyidae). *Arthropod Systematics & Phylogeny*, **69**, 83–97.

Sikes, E.K. and V.B. Wigglesworth (1931) The hatching of insects from the egg and appearance of air in the tracheal system. *Quarterly Journal of Microscopical Science*, **74**, 165-192.

Silvestri, F. (1913) Descrizione di un nuovo ordine di insetti. *Bollettino del Laboratorio di Zoologia Generale e Agraria*, **7**, 193–209.

Silvestri, F. (1946) Descrizione di due specie neotropicali di *Zorotypus* (Insecta, Zoraptera). *Bollettino del Laboratorio di Entomologia Agraria*, **7**, 1–12.

Simmons, M.P. (2004) Independence of alignment and tree search. *Molecular Phylogenetics and Evolution*, **31**, 874–879.

Simmons, M.P., K.F. Müller and C.T. Webb (2011) The deterministic effects of alignment bias in phylogenetic inference. *Cladistics*, **27**, 402–416.

Simon, S., A. Narechania, R. DeSalle and H. Hadrys (2012) Insect phylogenomics: Exploring the source of incongruence using new transcriptomic data. *Genome Biology and Evolution*, **4**, 1295–1309.

Simpson, S.J., G.A. Sword and N. Lo (2011) Polyphenism in insects. *Current Biology*, **21**, R738–R749.

Snodgrass, R.E. (1935) *Principles of Insect Morphology*. McGraw-Hill, New York.

Striebel, H. (1960) Zur Embryonalentwicklung der Termiten. *Acta*

Tropica, **17**, 193–260.

Tanaka, A. (1976) Stages in the embryonic development of the German cockroach, *Blattella germanica* Linné (Blattaria, Blattellidae). *Kontyû*, **44**, 512–525.

Terry, M.D. and M.F. Whiting (2005) Mantophasmatodea and phylogeny of the lower neopterous insects. *Cladistics*, **21**, 240–257.

Terry, M.D. and M.F. Whiting (2012) *Zorotypus novobritannicus*, the first species of the order Zoraptera (Zorotypidae) from the Australasian Ecozone. *Zootaxa*, **3260**, 52–61.

Thomas, A.J. (1936) The embryonic development of the stick insect, *Carausius morosus*. *Quarterly Journal of Microscopical Science*, **78**, 487–511, 2 pls.

Tilgner, E.H. (2002) *Systematics of Phasmida*. Doctoral dissertation, University of Georgia, Georgia.

Tojo, K. and R. Machida (1997) Embryogenesis of the mayfly *Ephemera japonica* McLachlan (Insecta: Ephemeroptera, Ephemeridae), with special reference to abdominal formation. *Journal of Morphology*, **234**, 97–107.

Tojo, K. and R. Machida (1998) Early embryonic development of the mayfly *Ephemera japonica* McLachlan (Insecta: Ephemeroptera, Ephemeridae). *Journal of Morphology*, **238**, 327–335.

Trautwein, M.D., B.M. Wiegmann, R. Beutel, K.M. Kjer and D.K. Yeates (2012) Advances in insect phylogeny at the dawn of the postgenomic era. *Annual Review of Entomology*, **57**, 449–468.

Uchifune, T. and R. Machida (2002) Note on the early germ band stage in *Galloisiana yuasai* Asahina (Insecta: Notoptera). *Proceedings of Arthropodan Embryological Society of Japan*, **37**, 45–48.

Uchifune, T. and R. Machida (2005) Embryonic development of *Galloisiana yuasai* Asahina, with special reference to external morphology (Insecta: Grylloblattodea). *Journal of Morphology*, **266**, 182–207.

Valentine, B.D. (1986) Grooming behavior in Embioptera and Zoraptera (Insecta). *The Ohio Journal of Science*, **86**, 150–152.

Wang, Y., M.S. Engel, J.A. Rafael, K. Dang, H. Wu, Y. Wang, Q. Xie and W. Bu (2013) A unique box in 28S rRNA is shared by the enigmatic insect order Zoraptera and Dictyoptera. *PLOS ONE*, **8**, e53679.

Warne, A.C. (1972) Embryonic development and the systematics of the Tettigoniidae (Orthoptera: Saltatoria). *International Journal of Insect Morphology and Embryology*, **1**, 267–287.

Weidner, H. (1969) Die Ordnung Zoraptera oder Bodenläuse. *Entomologische Zeitschrift*, **79**, 29–51.

Weidner, H. (1970) Zoraptera (Bodenläuse). *In*: J.G. Helmcke, D. Starck and H. Wermuth (eds.), *Handbuch der Zoologie. Vol. 4*, pp. 1–12. Walter de Gruyter, Berlin.

Wheeler, W.M. (1889) The embryology of *Blatta germanica* and *Doryphora decemlineata*. *Journal of Morphology*, **3**, 290–387.

Wheeler, W.M. (1893) A contribution to insect embryology. *Journal*

of Morphology, **8**, 1–160. 6 pls.

Wheeler, W.C., M. Whiting, Q.D. Wheeler and J.M. Carpenter (2001) The phylogeny of the extant hexapod orders. *Cladistics*, **17**, 113–169.

Wipfler, B., R. Machida, B. Müller and R.G. Beutel (2011) On the head morphology of Grylloblattodea (Insecta) and the systematic position of the order, with a new nomenclature for the head muscles of Dicondylia. *Systematic Entomology*, **36**, 241–266.

Yoshizawa, K. (2007) The Zoraptera problem: Evidence for Zoraptera + Embiodea from the wing base. *Systematic Entomology*, **32**, 197–204.

Yoshizawa, K. (2010) Direct optimization overly optimizes data. *Systematic Entomology*, **35**, 199–206.

Yoshizawa, K. (2011) Monophyletic Polyneoptera recovered by wing base structure. *Systematic Entomology*, **36**, 377–394.

Yoshizawa, K. and D.P. Johnson (2005) Aligned 18S for Zoraptera (Insecta): Phylogenetic position and molecular evolution. *Molecular Phylogenetics and Evolution*, **37**, 572–580.

Zeh, D.W., J.A. Zeh and R.L. Smith (1989) Ovipositors, amnions and eggshell architecture in the diversification of terrestrial arthropods. *The Quarterly Review of Biology*, **64**, 147-168.

TABLES

Table 1. Major developmental events in each stage in *Zorotypus caudelli*.

Stage 1 (12–15% DT)	Formation of embryo
Stage 2 (15–20% DT)	Differentiation of protocephalon and protocorm, formation of amnioserosal fold (anatrepsis)
Stage 3 (20–22% DT)	Commencement of segmentation, differentiation of cephalic and thoracic segments
Stage 4 (22–25% DT)	Formation of appendages in the differentiated segments, formation of stomodaeum, commencement of caudal flexure
Stage 5 (25–28% DT)	Differentiation of clypeolabrum, segmentation of abdomen
Stage 6 (28–30% DT)	Elongation and articulation of cephalic and thoracic appendages, immersion of embryo in the yolk
Stage 7 (30–40% DT)	Completion of segmentation, formation of abdominal appendages and proctodaeum
Stage 8 (40–50% DT)	Differentiation of clypeus and labrum, formations of spiracles and sternal apophyses.
Stage 9 (50–60% DT)	Development of egg tooth, completion of appendicular articulation
Stage 10 (60–65% DT)	Regression of amnioserosal fold (katatrepsis), progressive provisional dorsal closure
Stage 11 (65–80% DT)	Formation of head capsule, secretion of embryonic cuticle
Stage 12 (80–100% DT)	Completion of definitive dorsal closure, acquisition of definitive form by embryo, secretion of larval cuticle

Table 2. Duration of nymphal instars of *Zorotypus caudelli*.

Instar	I	II	III	Apterous IV	Winged IV	Apterous V	Winged V
Specimens examined	46	21	33	12	35	18	32
Average duration [days]	14.98 ± 2.82	13.48 ± 5.74	12.12 ± 3.07	14.58 ± 3.66	17.51 ± 5.33	16.44 ± 3.10	24.88 ± 4.64
Maximum duration [days]	20	25	19	24	30	24	34
Minimum duration [days]	11	8	8	10	11	11	17

Table 3. Measurements of *Zorotypus caudelli* nymphs of each instar.

Instar	Larva					Adult
	I	II	III	IV	V	VI
Specimens examined	5	5	5	5	5	9
Antennal length [mm]	0.64±0.02	0.77±0.02	0.82±0.03	0.93±0.06	1.16±0.01	1.35±0.08
Head width [μm]	260±8	318±7	336±4	388±19	436±23	455±32
Pronotum length [μm]	170±8	198±10	244±10	294±19	320±13	355±15
Pronotum width [μm]	216±10	252±7	274±14	318±25	376±27	405±40
Profemur length [μm]	209±9	242±11	270±8	321±11	372±22	441±23
Profemur width [μm]	88±6	109±9	120±8	136±8	161±16	181±12
Protibia length [μm]	190±6	233±11	253±2	298±6	357±14	404±30
Mesofemur length [μm]	180±10	233±14	264±8	308±10	368±35	428±23
Mesofemur width [μm]	69±3	92±6	98±4	112±7	140±12	143±4
Mesotibia length [μm]	182±11	218±6	253±16	302±11	339±15	396±13
Metatibia length [μm]	227±10	292±10	327±14	395±16	485±15	566±37
Metafemur width [μm]	83±5	113±8	129±8	158±9	208±12	214±12
Metatibia length [μm]	257±6	315±10	341±14	425±12	509±18	575±21

FIGURES

Fig. 1. Adults and mating of *Zorotypus caudelli*. A: Female. B: Male. C: Mating.

Scale bars = 500 μm.

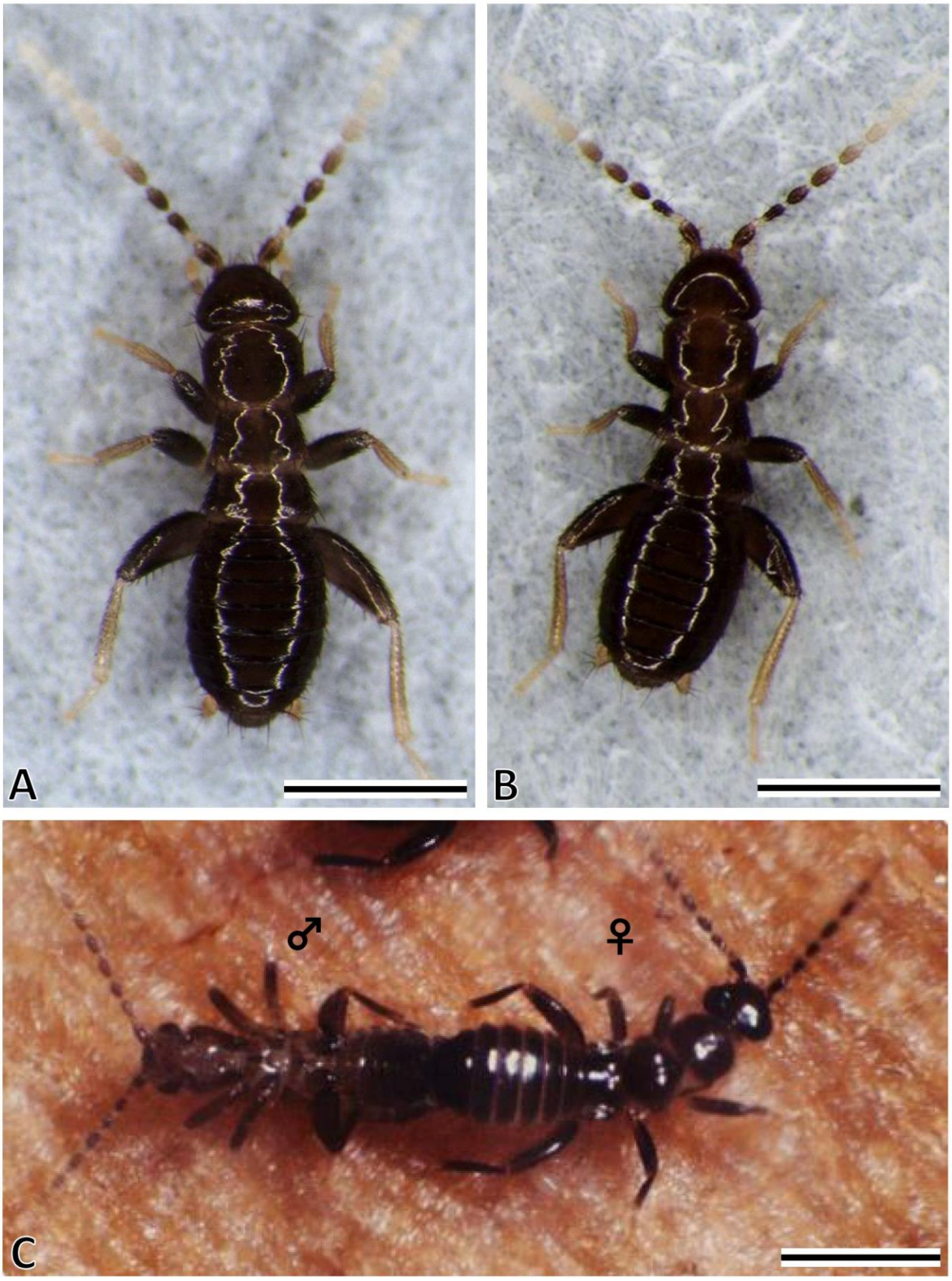
A
B
♂
♀
C

Fig. 2. Eggs of *Zorotypus caudelli*. A, B: An egg, ventral (A) and lateral (B) views, anterior to the top. Arrowheads show micropyles. C: An enlargement of the surface around micropyle. A micropyle is visible in the small polygon, and from it a micropylar canal is found to run.

ap, aeropyle; mp, micropyle; mpc, micropylar canal.

Scale bars = A, B: 100 µm; C: 50 µm.

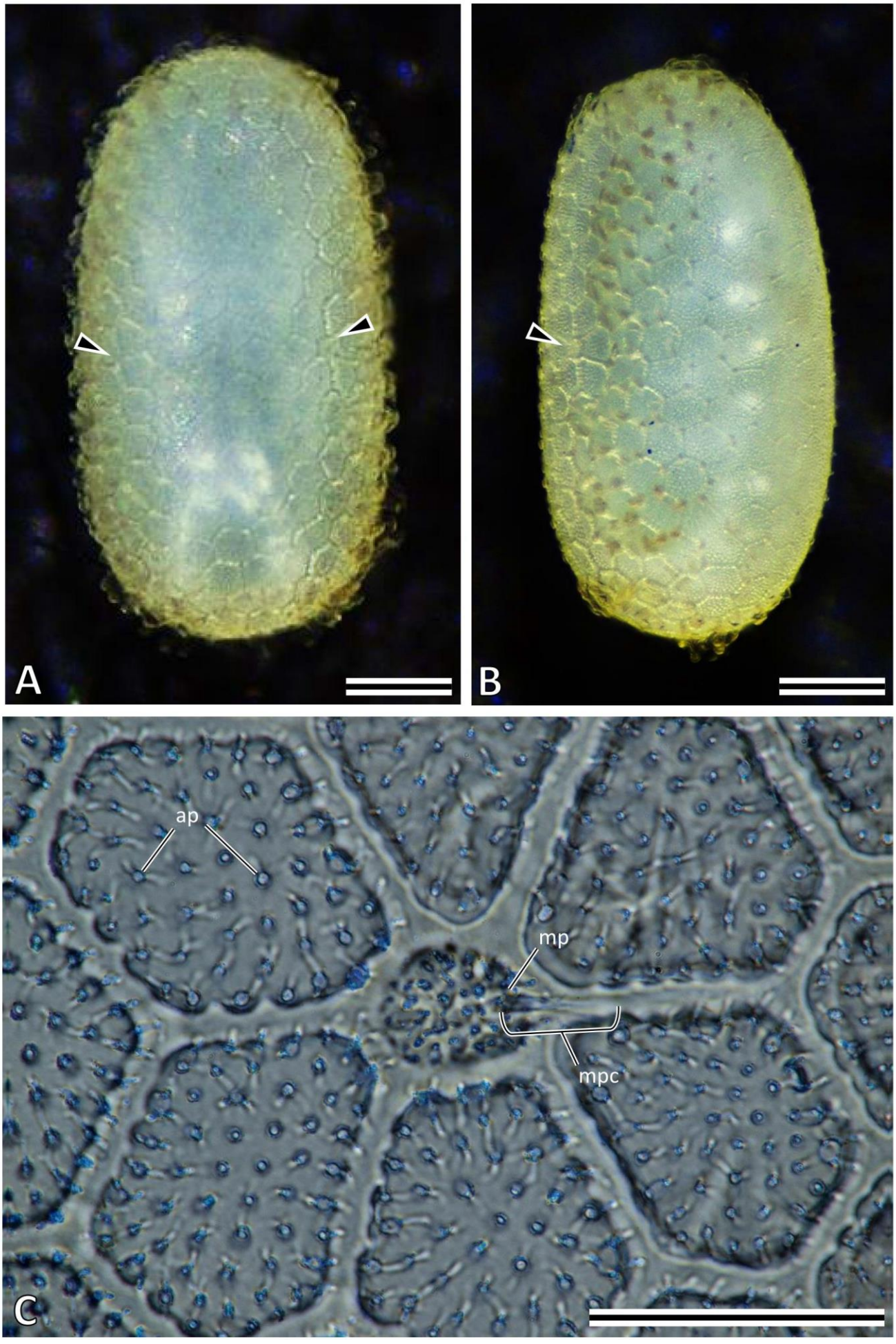
A
B
ap
mp
mpc
C

Fig. 3. Eggs of *Zorotypus caudelli*, SEM. A, B: An egg, ventral (A) and lateral (B) views. Arrowheads and arrows show micropyles and a fringe, respectively. C: An enlargement of the dorsal surface of the egg. D: An enlargement of the ventral surface of the egg. E: An enlargement of a small polygon with a micropyle. F, G: An egg, posterior (F) and anterior (G) views.

ap, aeropyle; fr, fringe made of a fibrillar substance; mp, micropyle.

Scale bars = A, B, F, G: 100 µm; C, D: 50 µm; E: 10µm.

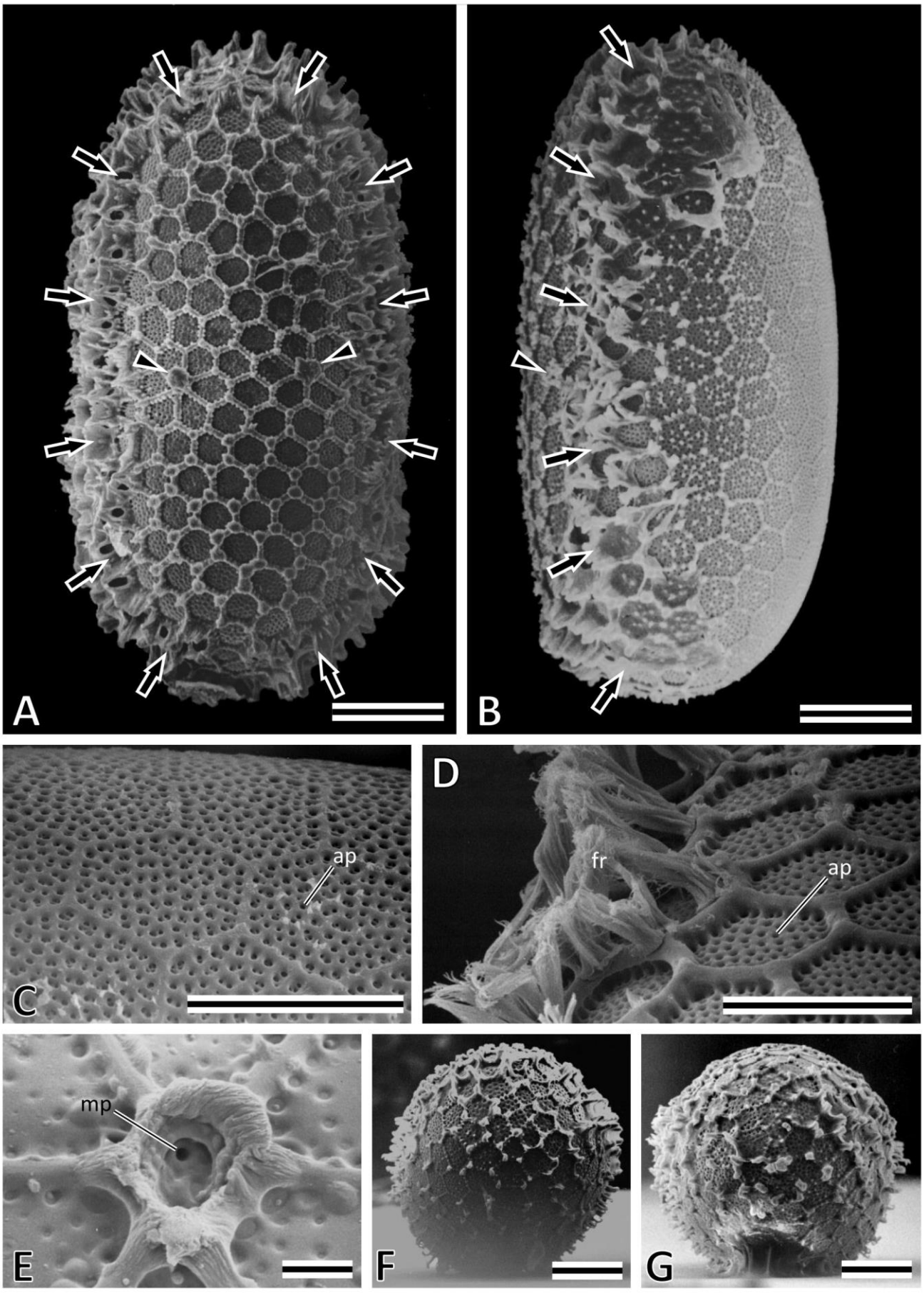
A
B
C
ap
D
fr
ap
E
mp
F
G

Fig. 4. Eggs and micropylar structures of *Zorotypus caudelli*. A: An egg, ventral view. Arrowheads show a pair of micropyles and an additional one, SEM. B: Enlargement, SEM. C: A longitudinal section of the micropylar canal. An asterisk shows the basophilic substance filling the micropylar canal. D: A flap covering the inner opening of the micropylar canal, SEM. E: A section of the micropylar canal, TEM. An asterisk shows the electron-denser substance filling the micropylar canal.

ap, aeropyle; cs, columnar structure; ench, endochorion; exch, exochorion; f, flap covering the inner opening of the micropylar canal; fexen, fusion of the exochorion and endochorion; mpc, micropylar canal.

Scale bars = A: 100 µm; B: 50 µm; C, D: 5 µm; E: 2 µm.

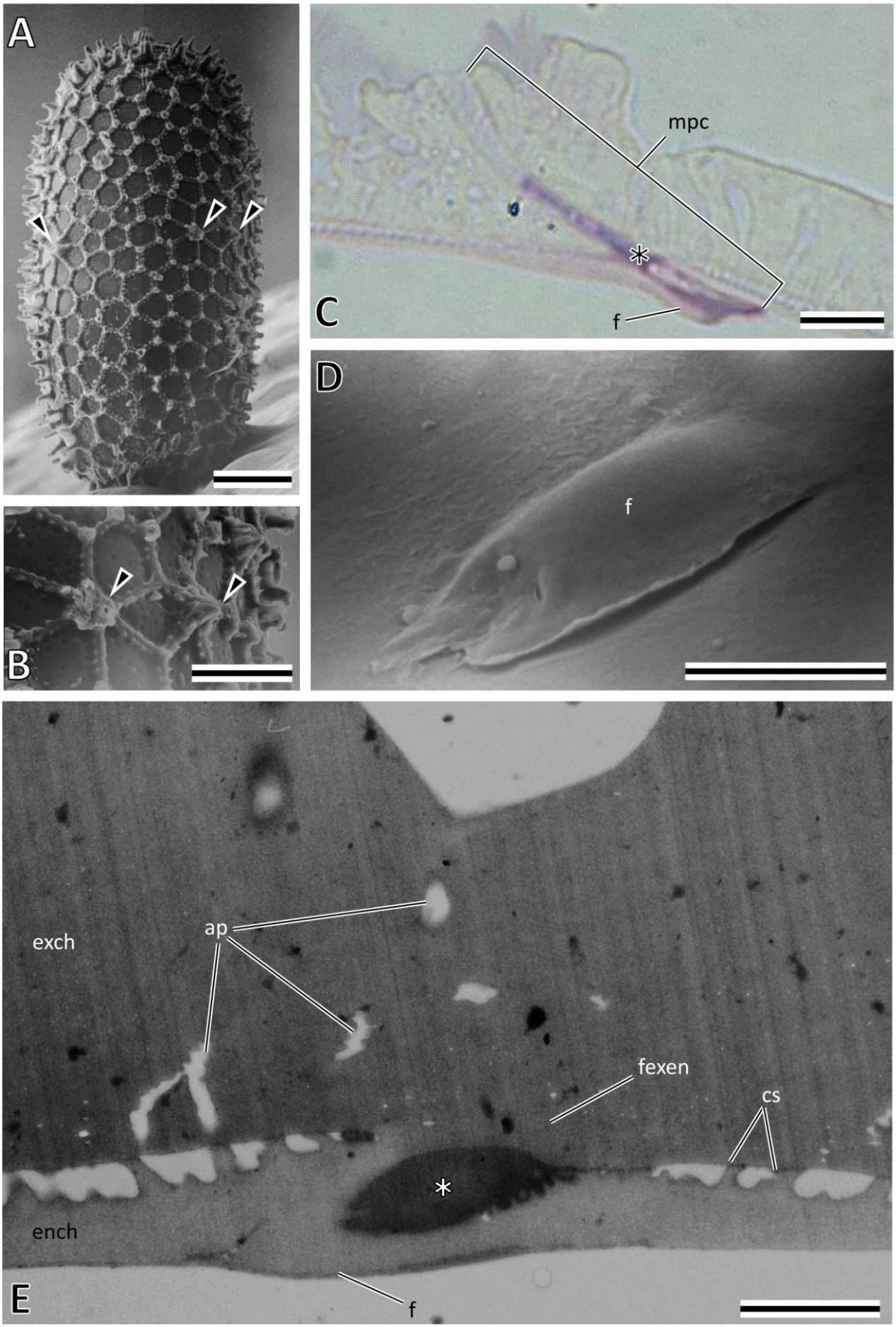
A
B
C
mpc
f
D
f
E
exch
ap
fexen
cs
ench
f

Fig. 5. Egg membranes of *Zorotypus caudelli*. A: Cross section of egg membrane of the ventral side, TEM. B, C: Cross sections of fringe structures, TEM (B) and LM (C).

ap, aeropyle; cs, columnar structure; ench, endochorion; exch, exochorion; fr, fringe made of fibrillar substance; vm, vitelline membrane.

Scale bars = 5 µm.

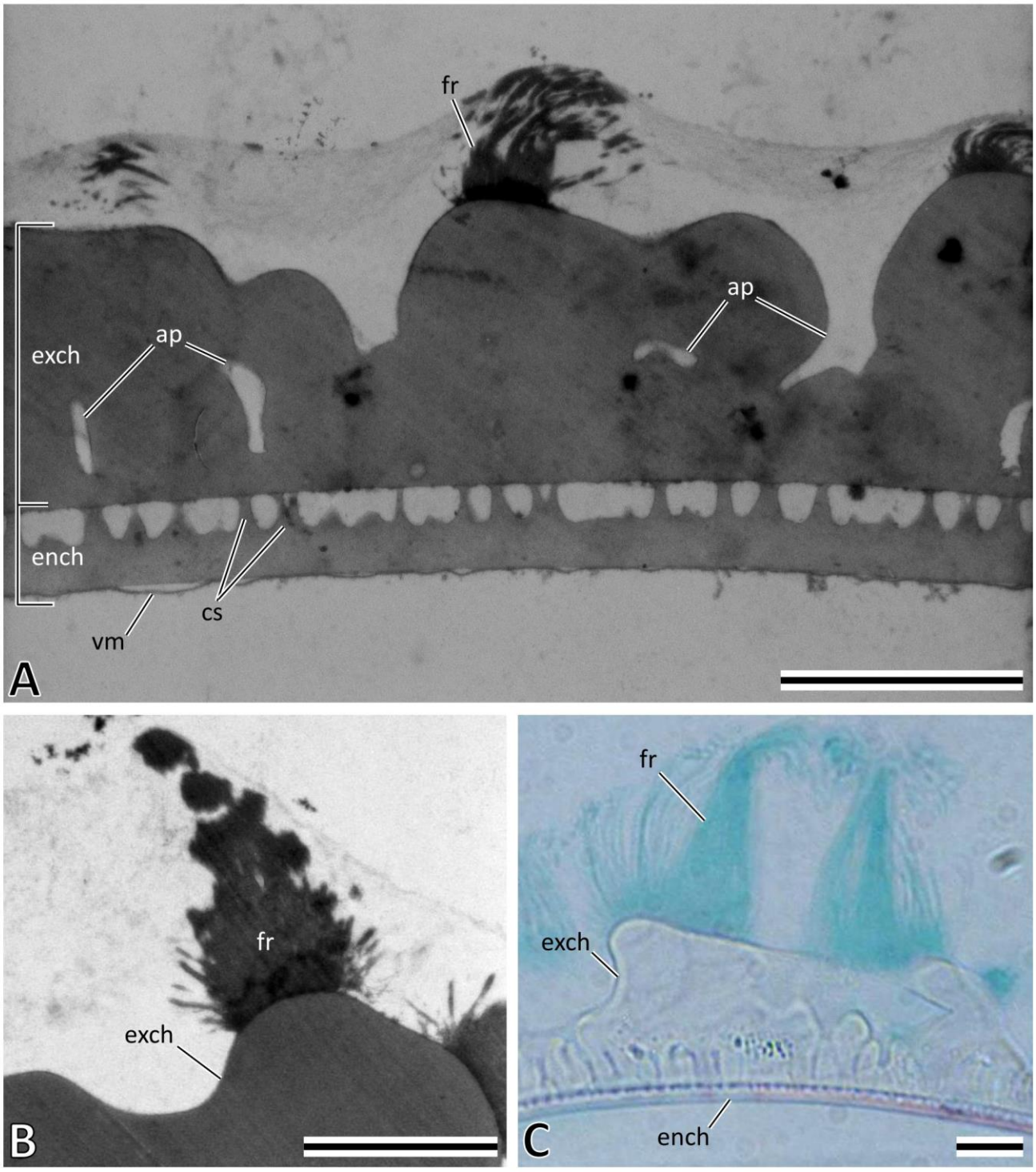
fr
ap
exch
ap
ench
cs
vm
A
fr
exch
B
fr
exch
ench
C

Fig. 6. Embryonic development of *Zorotypus caudelli*, lateral view of eggs, anterior to the top, ventral to the left, fluorescence microscopy with DAPI staining other than L. A: 12-15% DT. The serosal cells and secondary yolk cells which were segregated from the formers are clearly distinguished in size of nuclei: the nuclei of the secondary yolk cells are more compact than those of serosal cells. B: 15-20% DT. C: 20-22% DT. D: 22-25% DT. E: 25-28% DT. F: 28-30% DT. G: 30-40% DT. H: 40-50% DT. I: 50-60% DT. J: 60-65% DT. K: 65-80% DT. L: 80-100% DT.

am, amnion; an, antenna; em, embryo; et, egg tooth; hc, head capsule; hl, head lobe; l1-3, pro-, meso- and metathoracic legs; mxp, maxillary palp; pce, protocephalon; pco, protocorm; sdo, secondary dorsal organ; se, serosa; sec, serosal cell; syc, secondary yolk cell; y, yolk. White and black arrowheads show cephalic and caudal ends of the embryo, respectively. Asterisks show the position of micropyles.

Scale bar = 200 μm.

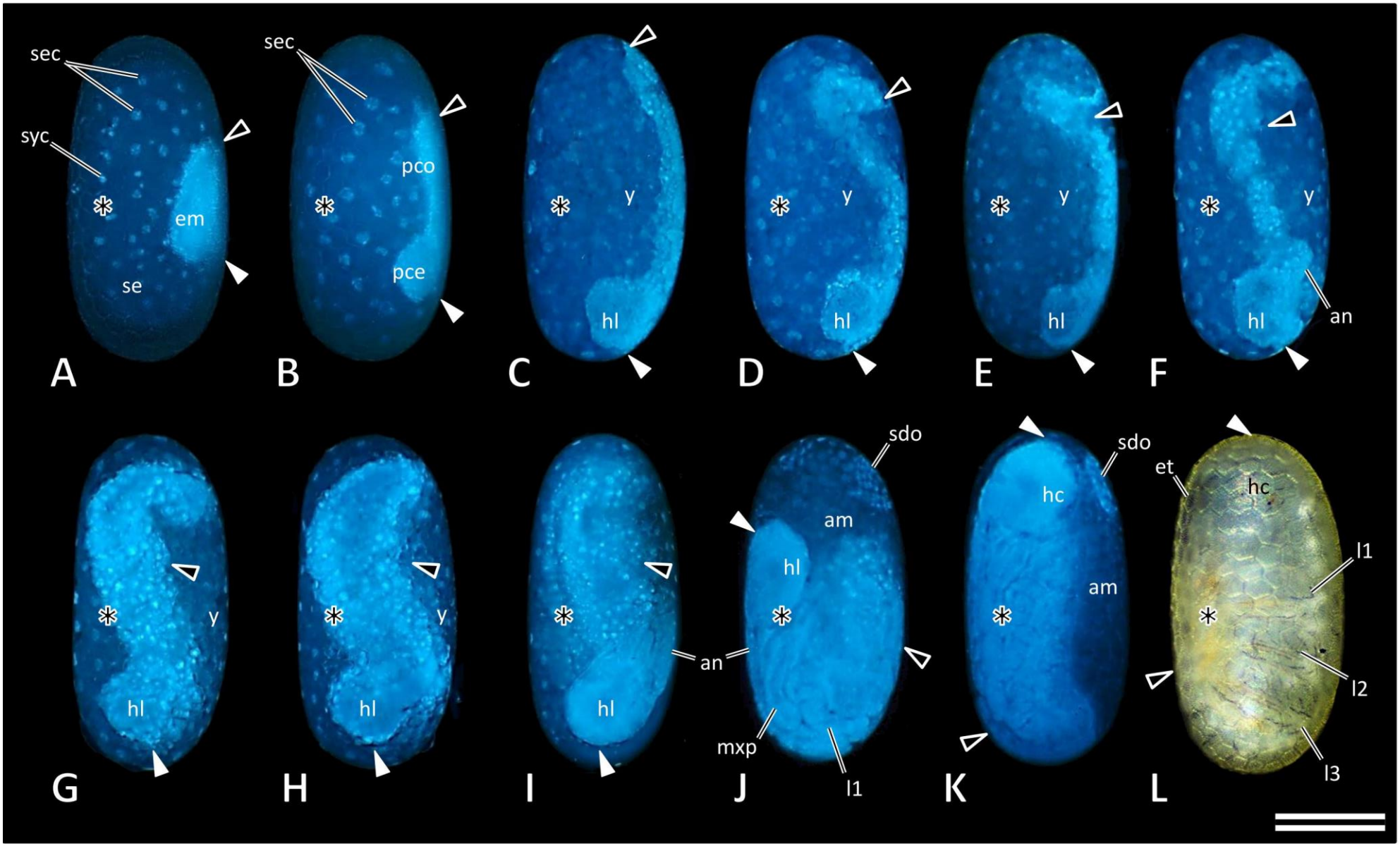
sec
syc
em
se
A
sec
pco
pce
B
y
hl
C
y
hl
D
y
hl
E
y
hl
an
F
y
hl
G
y
hl
H
hl
I
sdo
am
hl
an
mxp
l1
J
sdo
et
hc
am
K
hc
l1
l2
l3
L

Fig. 7. Embryonic development of *Zorotypus caudelli*, anterior to the top, ventral view to the embryo: A-I, dorsal view to the egg; J-L, ventral view to the egg, fluorescence microscopy with DAPI staining other than L. A: 12-15% DT. B: 15-20% DT. C: 20-22% DT. D: 22-25% DT. E: 25-28% DT. F: 28-30% DT. G: 30-40% DT. H: 40-50% DT. I: 50-60% DT. J: 60-65% DT. K: 65-80% DT. L: 80-100% DT.

am, amnion; an, antenna; ans, antennal segment; ce, cercus; cllr, clypeolabrum; em, embryo; et, egg tooth; hc, head capsule; hl, head lobe; ics, intercalary segment; lb, labium; lbs, labial segment; lr, labrum; l1-3, pro-, meso- and metathoracic legs; md, mandible; mds, mandibular segment; mx, maxilla; mxp, maxillary palp; mxs, maxillary segment; pce, protocephalon; pco, protocorm; sdo, secondary dorsal organ; se, serosa; sec, serosal cell; th1-3, pro-, meso- and metathoracic segments; y, yolk. Asterisks show the position of micropyles.

Scale bar = 200 μm.

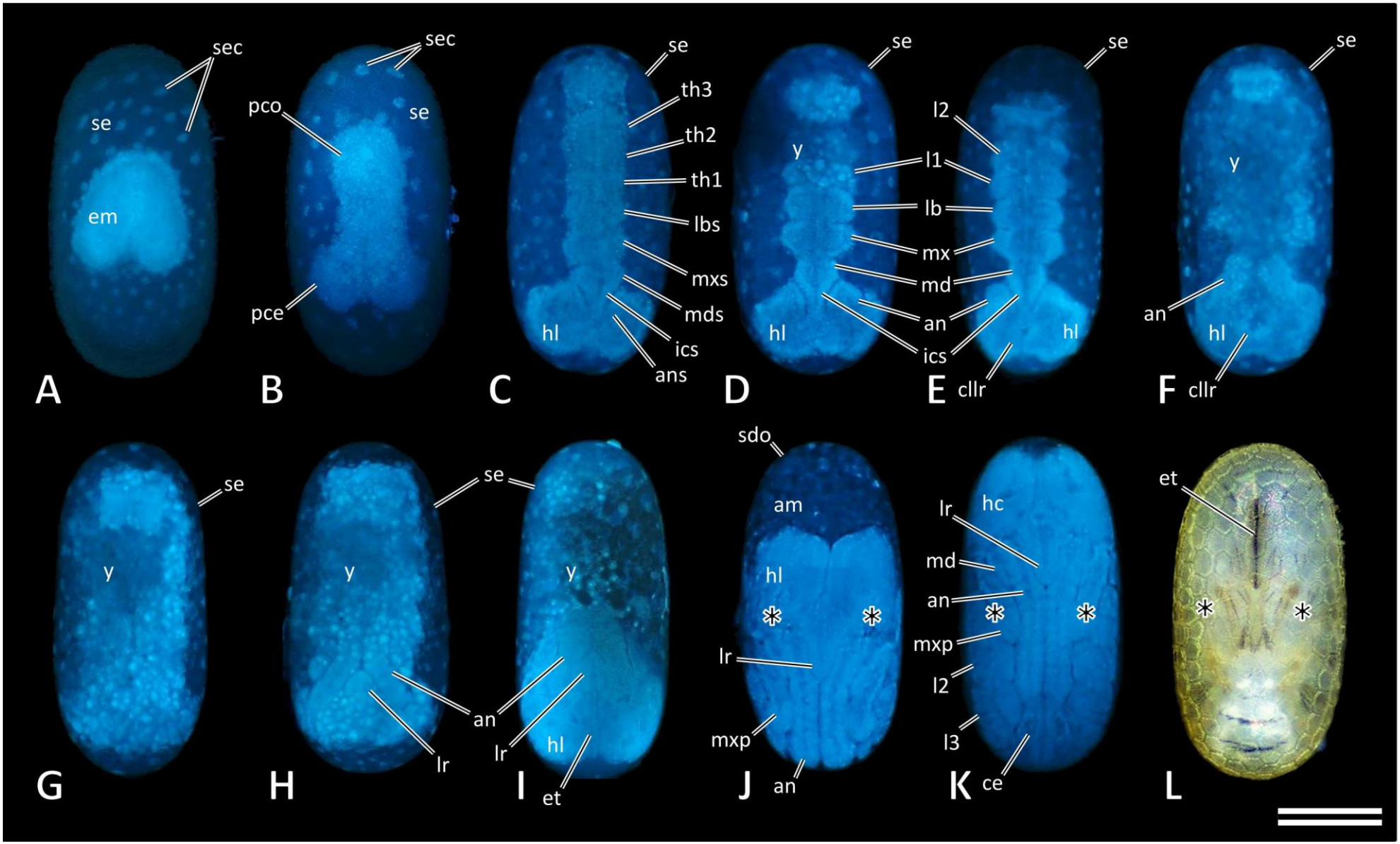
A
sec
se
em
B
sec
pco
se
pce
C
se
th3
th2
th1
lbs
mxs
mds
ics
ans
hl
D
se
y
hl
E
se
l2
l1
lb
mx
md
an
ics
hl
cllr
F
se
y
an
hl
cllr
G
y
se
H
y
an
lr
I
se
y
lr
hl
et
J
sdo
am
hl
lr
mxp
an
K
hc
lr
md
an
mxp
l2
l3
ce
L
et

Fig. 8. Eggs of *Zorotypus caudelli*. A: Cross section of an egg at 12-15% DT. A secondary yolk cell is observed to be just segregated. B-G: Eggs in early (B, C), middle (D, E), and late (F, G) Stage of 15-20% DT, dorsal (B, D, F) and lateral (C, E, G) views to the egg, anterior to the top, fluorescence microscopy with DAPI staining. H, I: An egg in early stage of 15-18% DT, dorsal (H) and lateral (I) views, anterior to the top, fluorescence microscopy with DAPI staining. Black and white arrowheads show margin of embryonic area and that of amnioserosal fold, respectively. Asterisks show paired regions with higher cellular density.

ch, chorion; em, embryo; pce, protocephalon; pco, protocorm; se, serosa; sec, serosal cell; syc, secondary yolk cell; y, yolk.

Scale bar = A: 100 μm; B-I: 200 μm.

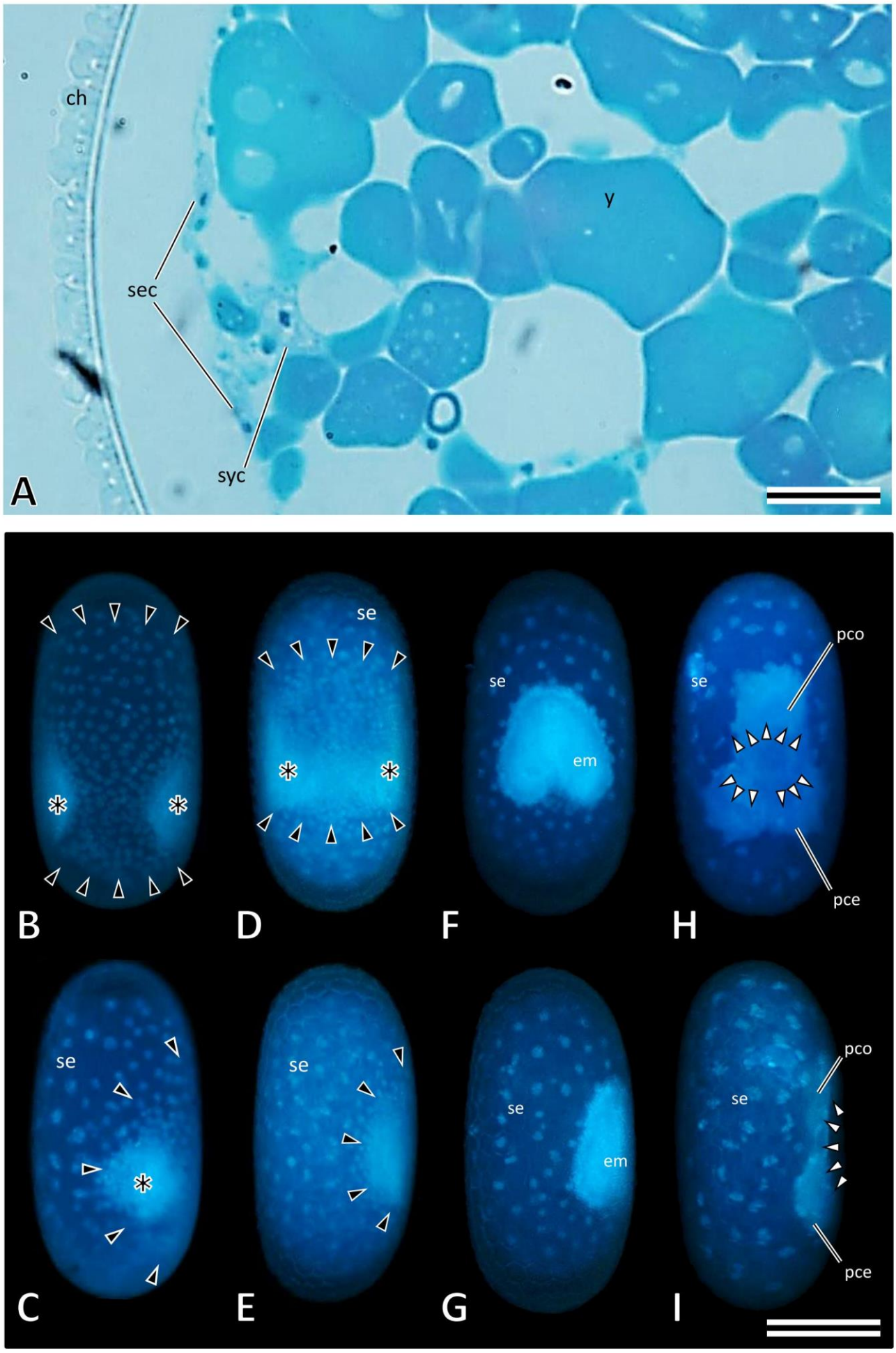
ch
y
sec
syc
A
se
pco
em
pce
B
D
F
H
C
E
G
I

Fig. 9. External features of the embryos of *Zorotypus caudelli*, ventral view. A: 12-15% DT. B, C, D: Early (B), middle (C), and late (D) stage in 15-20% DT. E: 20-22% DT.

ans, antennal segment; asf, amnioserosal fold; hl, head lobe; ics, intercalary segment; lbs, labial segment; mds, mandibular segment; mxs; maxillary segment; ng, neural groove; pce, protocephalon; pco, protocorm; th1-3, pro-, meso- and metathoracic segments.

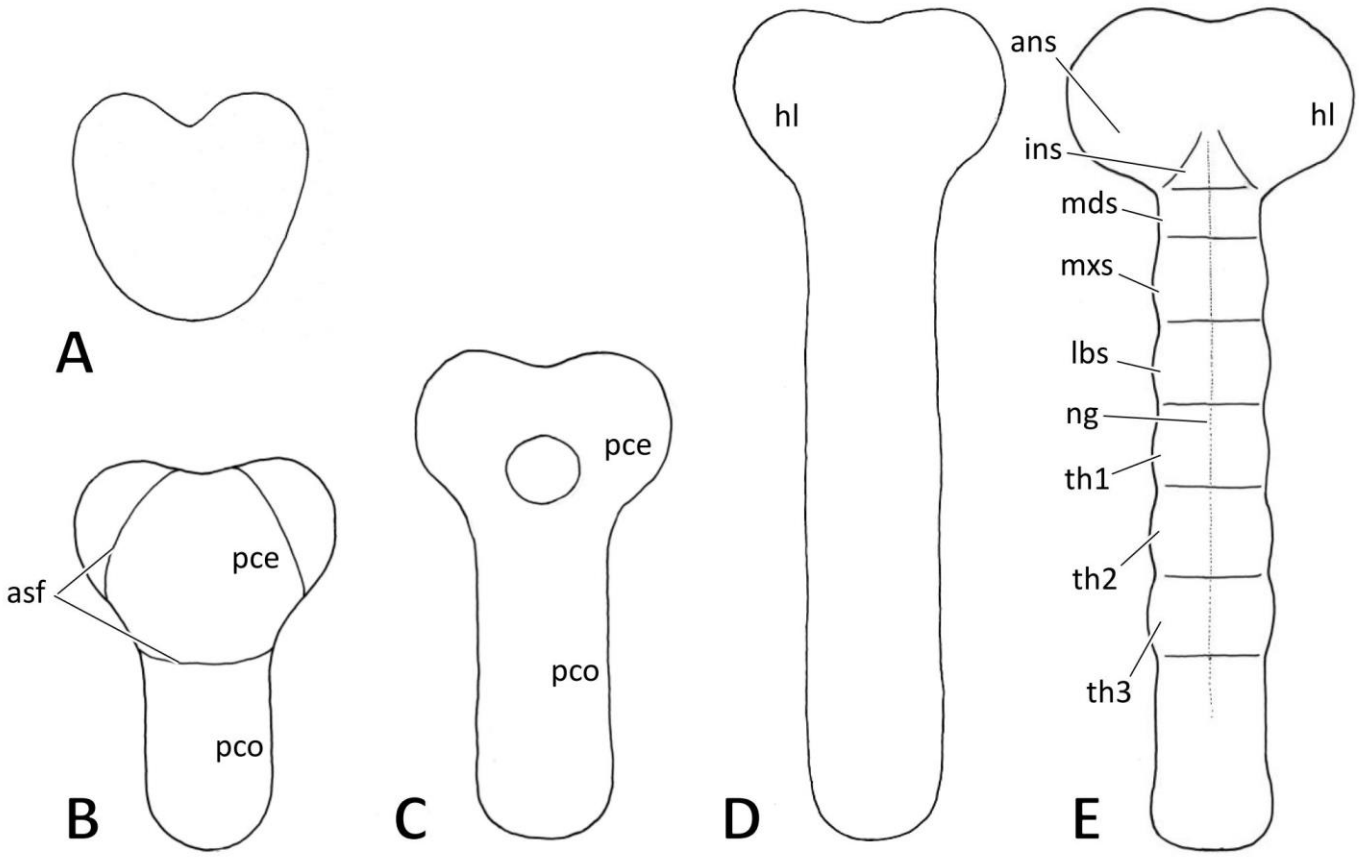
A
B
asf
pce
pco
C
pce
pco
D
hl
E
ans
hl
ins
mds
mxs
lbs
ng
th1
th2
th3

Fig. 10. Eggs and embryos at 22-25% DT of *Zorotypus caudelli*, anterior to the top. A, B: An egg, dorsal (A) and lateral (B) views, fluorescence microscopy with DAPI staining. C, D: External features of the embryo, ventral (C) and lateral (D) views.

an, antenna; hl, head lobe; ics, intercalary segment; lb, labium; l1-3, pro-, meso- and metathoracic legs; md, mandible; mx, maxilla; ng, neural groove; sd, stomodaeum; I, first abdominal segment.

Scales = 100 µm

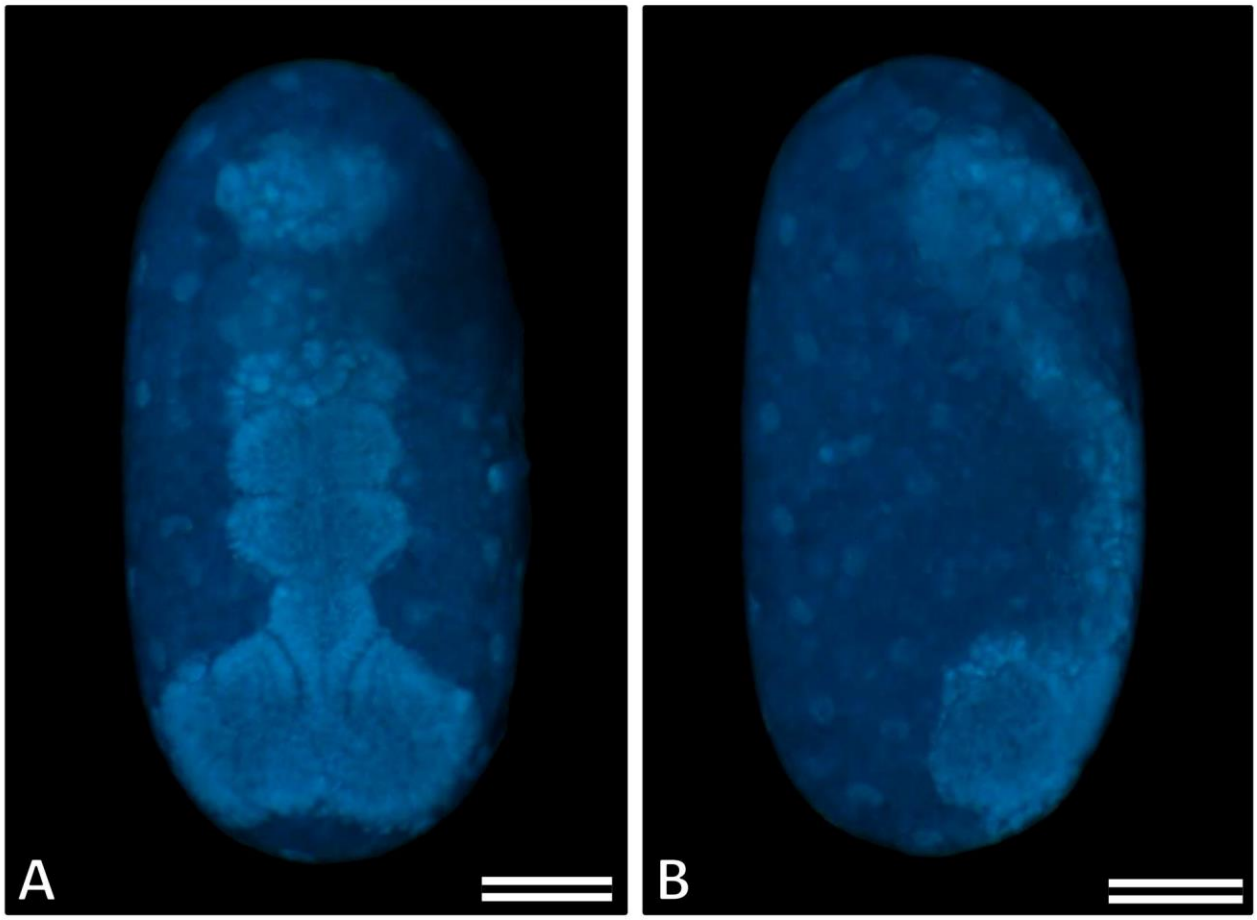
A
B

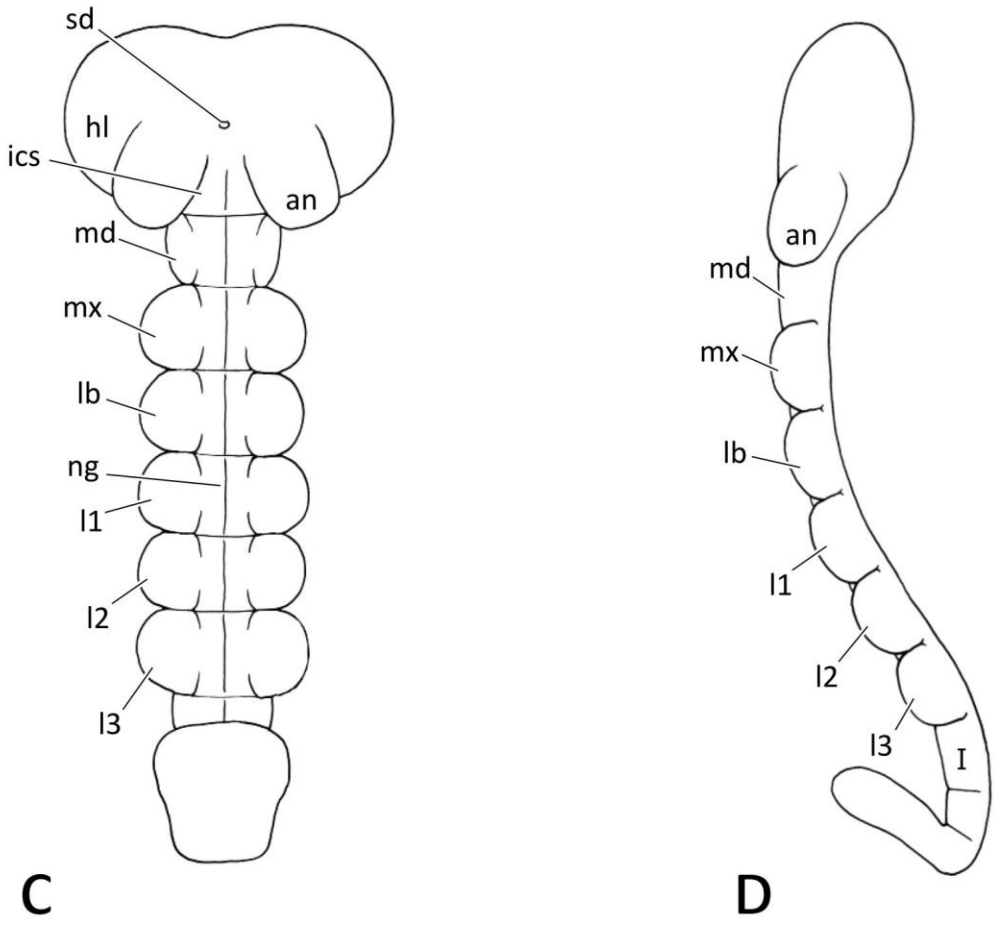
sd
hl
ics
an
md
mx
lb
ng
l1
l2
l3
C
an
md
mx
lb
l1
l2
l3
I
D

Fig. 11. Eggs and embryos at 25-28% DT of *Zorotypus caudelli*, anterior to the top. A, B: An egg, dorsal (A) and lateral (B) views, fluorescence microscopy with DAPI staining. C, D: External features of the embryo, ventral (C) and lateral (D) views.

an, antenna; cllr, clypeolabrum; hl, head lobe; ics, intercalary segment; lb, labium; l1-3, pro-, meso- and metathoracic legs; md, mandible; mx, maxilla; sd, stomodaeum; I, III, first and third abdominal segments.

Scales = 100 µm

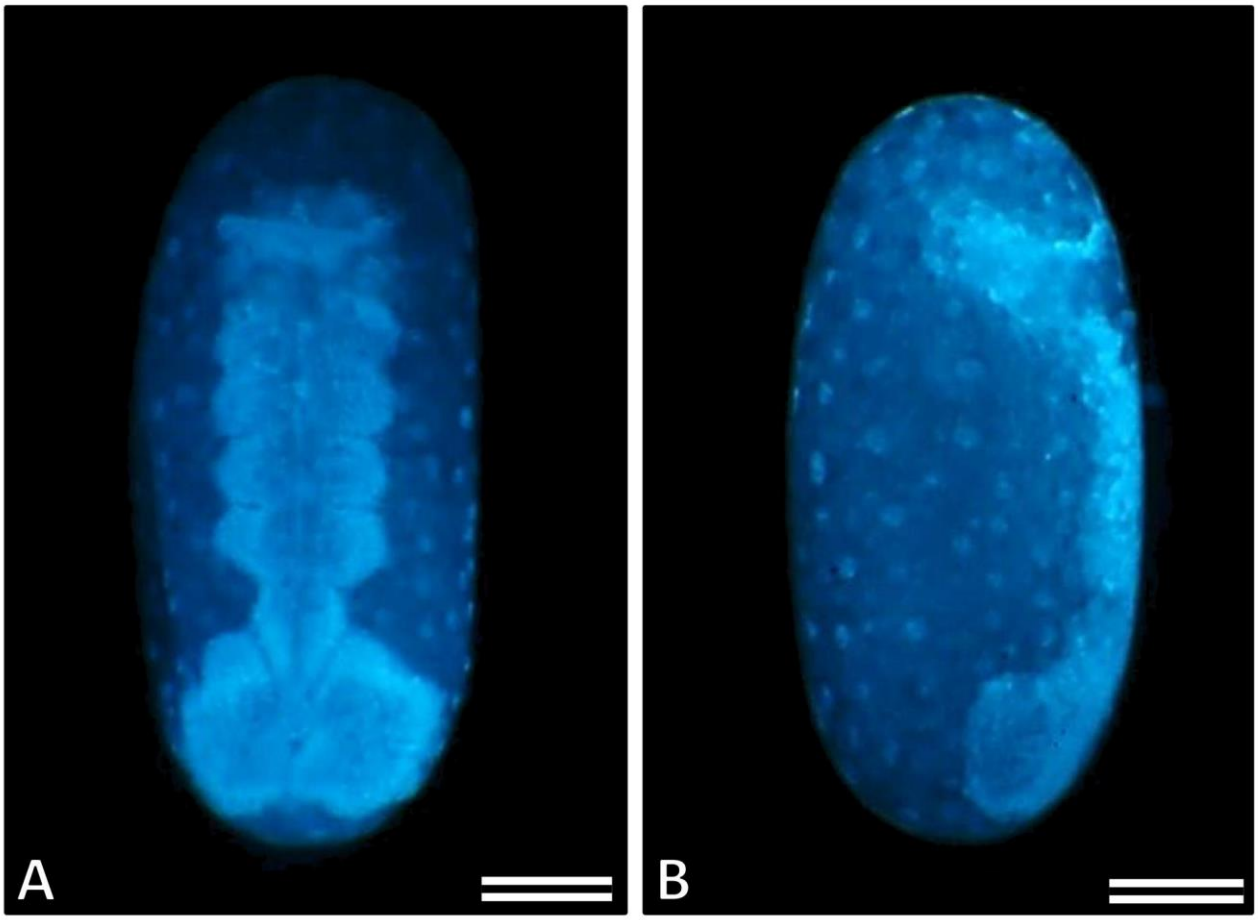
A
B

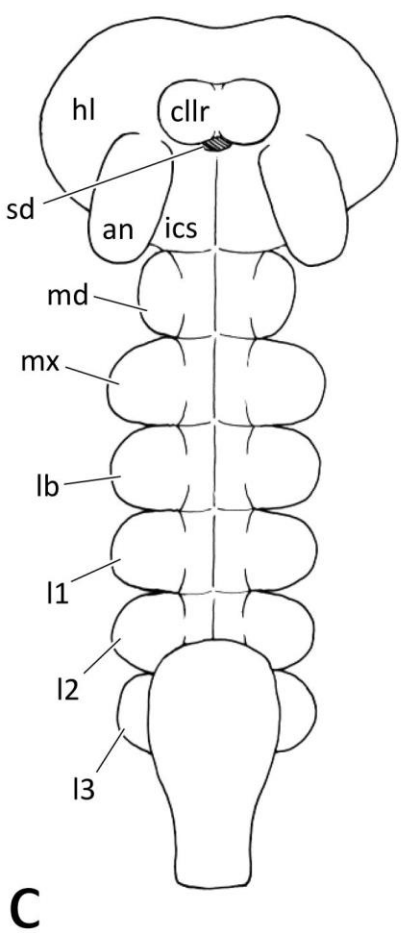
hl
cllr
sd
an
ics
md
mx
lb
l1
l2
l3
C

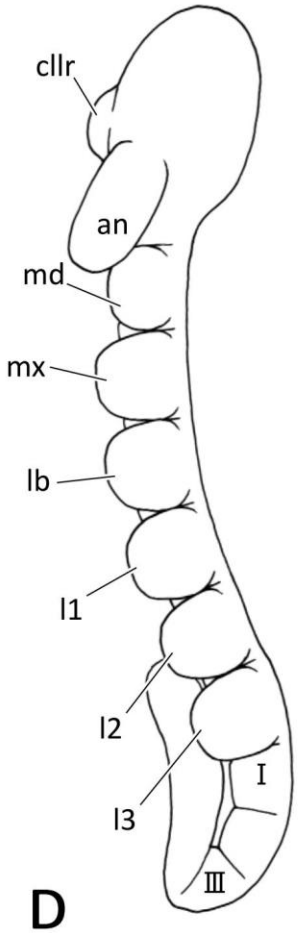
cllr
an
md
mx
lb
l1
l2
l3
I
III
D

Fig. 12. Eggs and embryos at 28-30% DT of *Zorotypus caudelli*, anterior to the top. A, B: An egg, dorsal (A) and lateral (B) views, fluorescence microscopy with DAPI staining. C, D: External features of the embryo, ventral (C) and lateral (D) views.

an, antenna; cllr, clypeolabrum; cp, coxopodite; fl, flagellum; hl, head lobe; ics, intercalary segment; lb, labium; lbe, labial endite; l1-3, pro-, meso- and metathoracic legs; md, mandible; mx, maxilla; mxe, maxillary endite; pe, pedicellus; sc, scapus; tp, telopodite; I, VI, first and sixth abdominal segments.

Scales = 100 µm

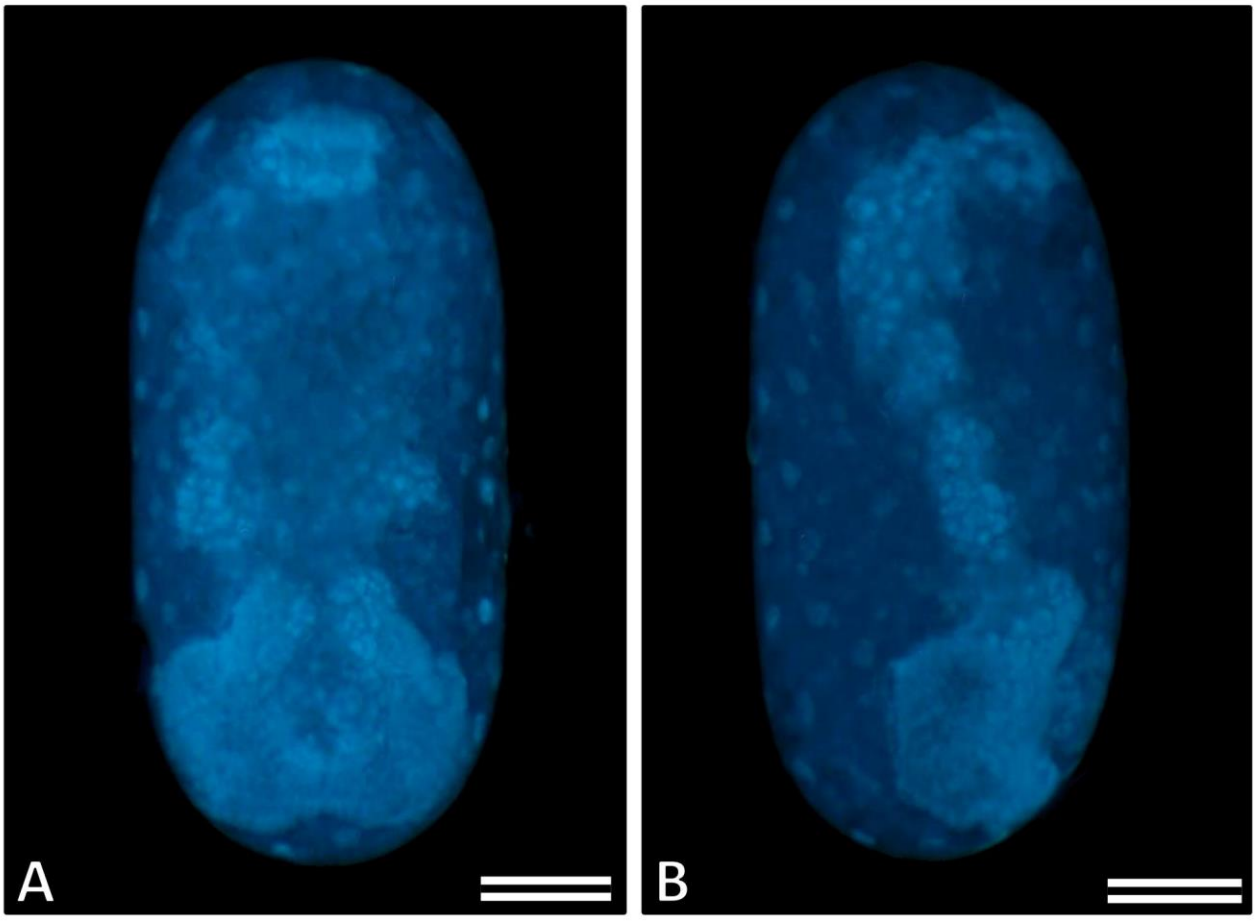
A
B

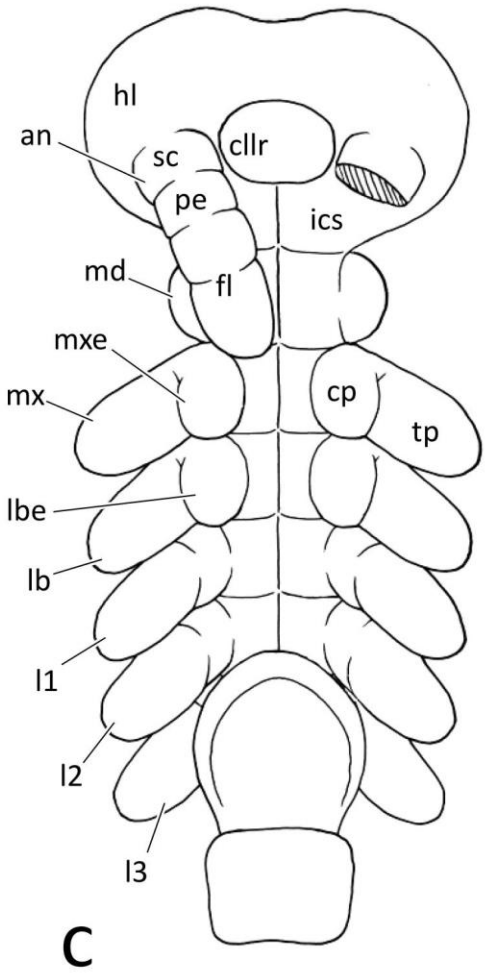
hl
an
sc
cllr
pe
ics
md
fl
mxe
mx
cp
tp
lbe
lb
l1
l2
l3
C

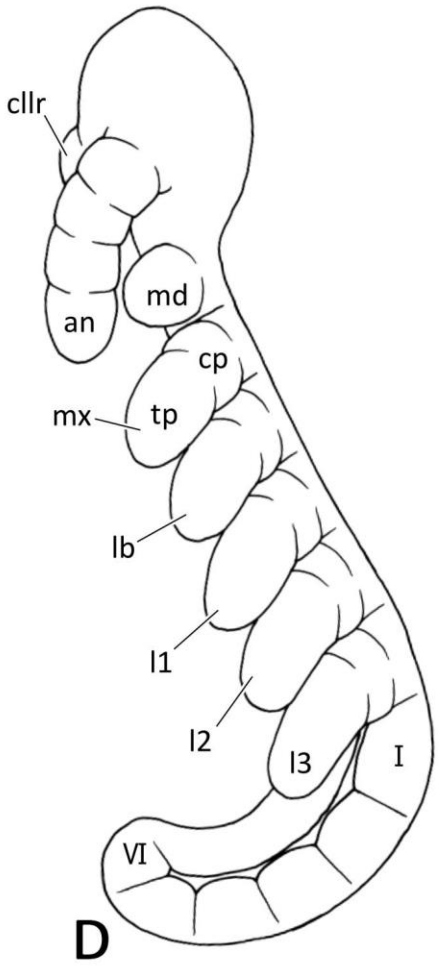
cllr
md
an
cp
mx
tp
lb
l1
l2
l3
I
VI
D

Fig. 13. Eggs and embryos at 30-40% DT of *Zorotypus caudelli*. A, B: An egg, dorsal (A) and lateral (B) views, anterior to the top, fluorescence microscopy with DAPI staining. C, D: External features of the embryo, ventral (C) and lateral (D) views, anterior to the top. E, F, G: External features of the abdomen, ventral (E), lateral (F) and caudal (G) views, anterior to the top.

an, antenna; ce, cercus; cllr, clypeolabrum; cp, coxopodite; fe, femur; hl, head lobe; lbe, labial endite; lbp, labial palp; l1-3, pro-, meso- and metathoracic legs; md, mandible; mxe, maxillary endite; mxp, maxillary palp; pd, proctodaeum; pp, pleuropodium; pta, pretarsus; ta, tarsus; tht, thoracic tergum; ti, tibia; tp, telopodite; tr, trochanter; I, V-XI, first and fifth to 11th abdominal segments.

Scales = 100 µm

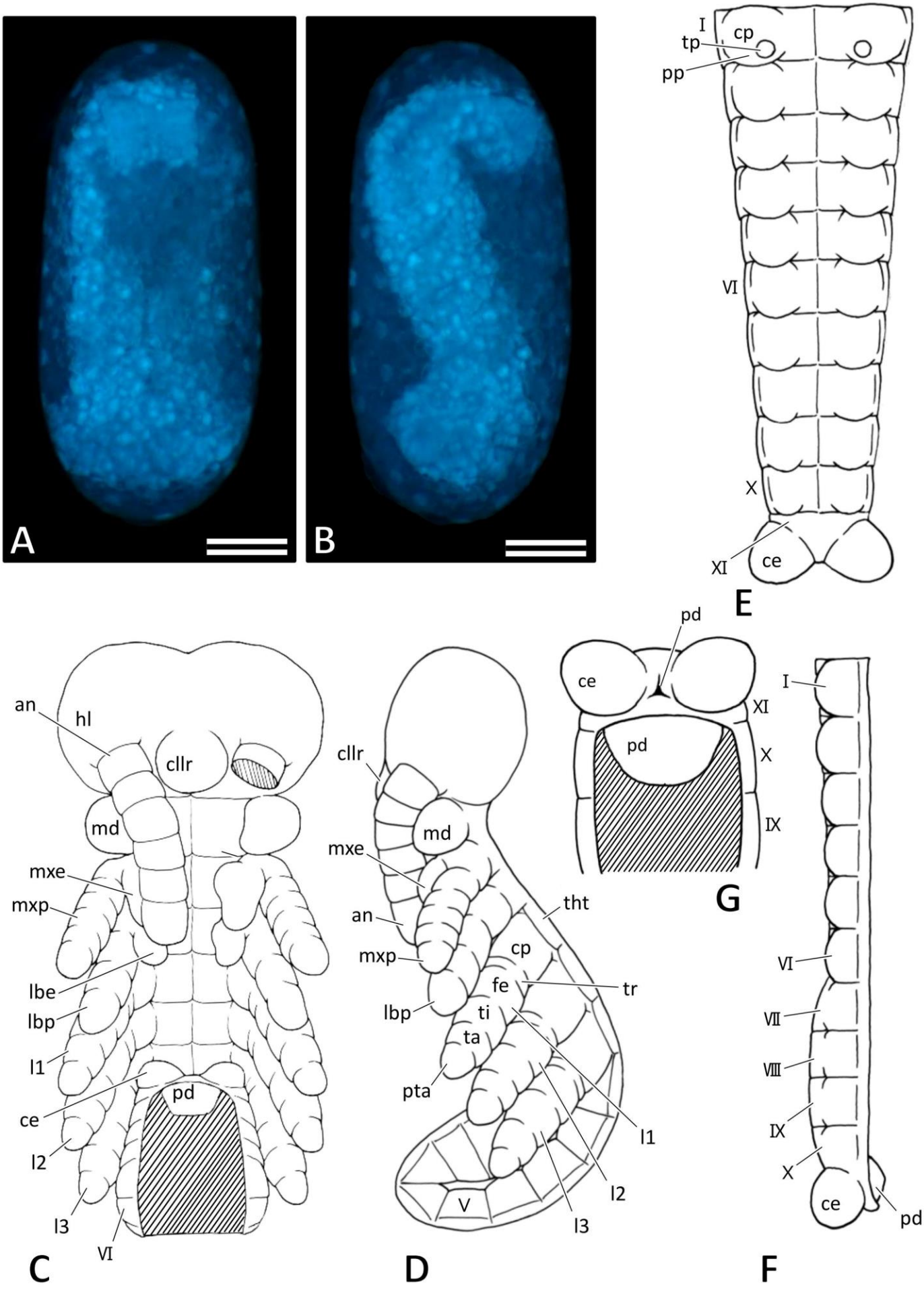
A
B
I
cp
tp
pp
VI
X
XI
ce
E
an
hl
cllr
md
mxe
mxp
lbe
lbp
l1
ce
pd
l2
l3
VI
C
cllr
md
mxe
an
mxp
lbp
tht
cp
fe
tr
ti
ta
pta
l1
l2
V
l3
D
pd
ce
XI
pd
X
IX
G
I
VI
VII
VIII
IX
X
ce
pd
F

Fig. 14. Eggs and embryos at 40-50% DT of *Zorotypus caudelli*. A, B: An egg, dorsal (A) and lateral (B) views, anterior to the top, fluorescence microscopy with DAPI staining. C, D: External features of the embryo, ventral (C) and lateral (D) views. E, F: External features of the abdomen, ventral (E) and lateral (F) views.

abt, abdominal tergum; acl, anteclypeus; an, antenna; ce, cercus; cp, coxopodite; cx, coxa; fe, femur; ga, galea; gl, glossa; hl, head lobe; la, lacinia; lbp, labial palp; lr, labrum; l1-3, pro-, meso- and metathoracic legs; md, mandible; mdcx, mandibular coxa; mxcx, maxillary coxa; mxp, maxillary palp; pcl, postclypeus; pd, proctodaeum; pgl, paraglossa; pp, pleuropodium; pta, pretarsus; scx, subcoxa; sd, stomodaeum; ta, tarsus; ti, tibia; tp, telopodite; tr, trochanter; I, VI-XI, first and fifth to 11th abdominal segments. Arrowheads show the spiracles.

Scales = 100 µm

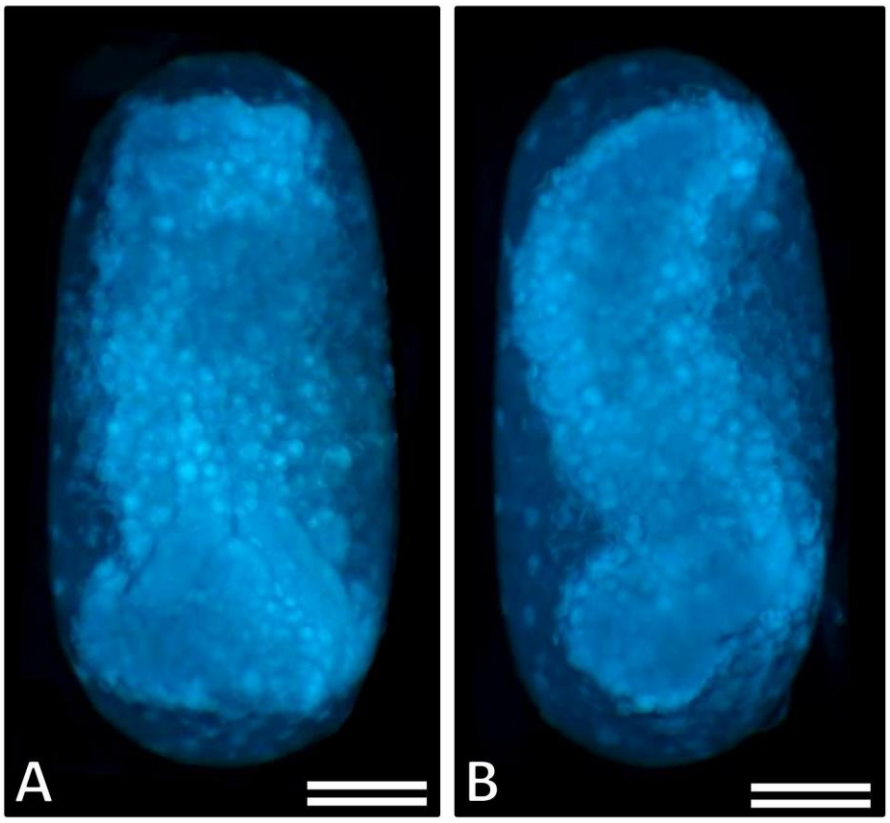
A
B

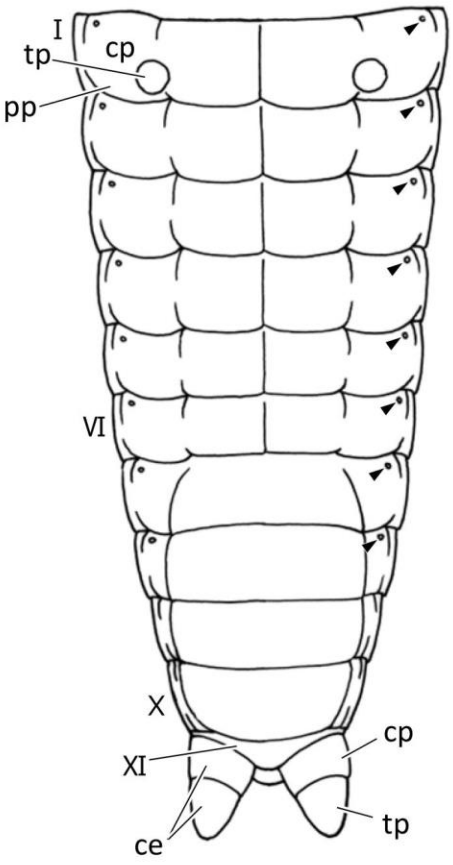
I
tp
cp
pp
VI
X
XI
cp
ce
tp
E

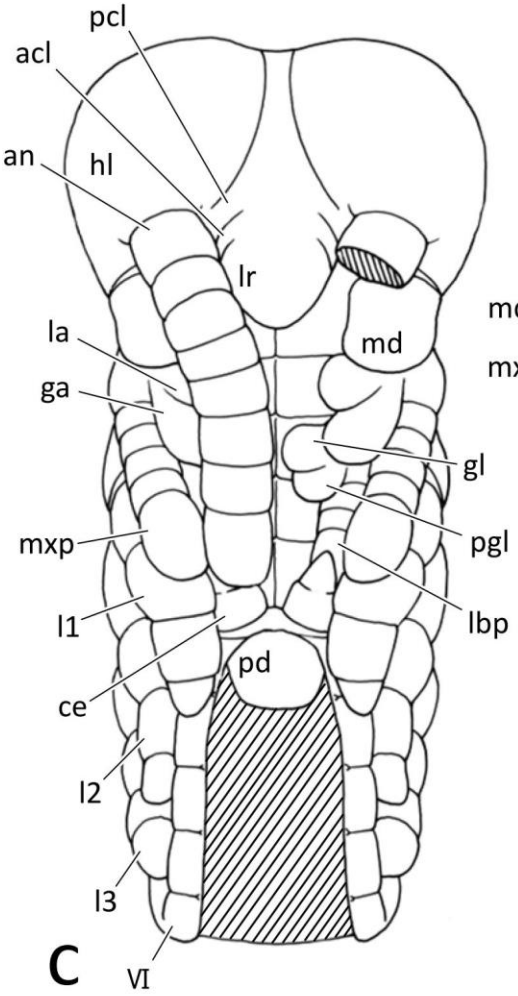
pcl
acl
an
hl
lr
la
md
ga
gl
mxp
pgl
l1
lbp
pd
ce
l2
l3
VI
C

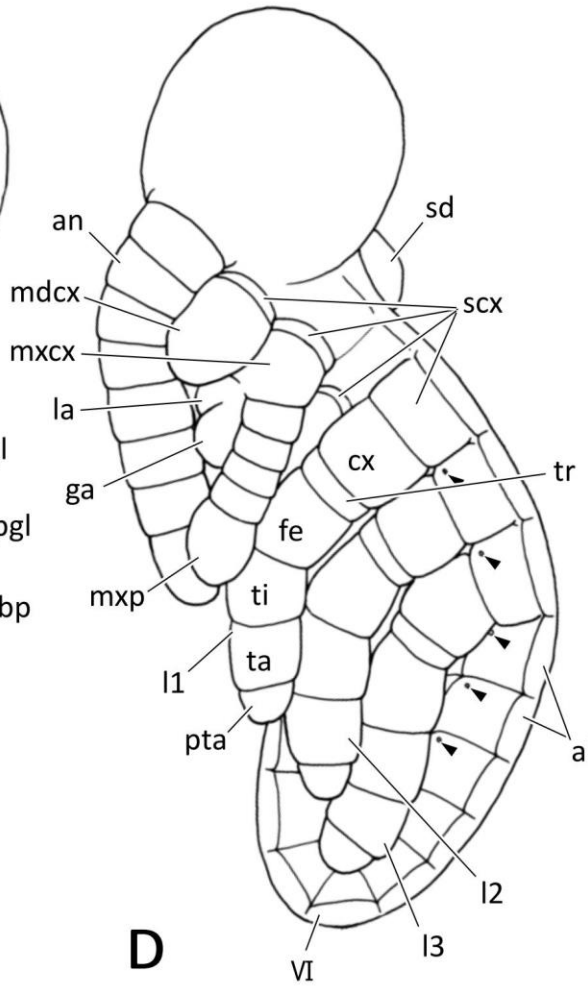
an
sd
mdcx
scx
mxcx
la
ga
cx
tr
fe
mxp
ti
ta
l1
pta
abt
l2
l3
VI
D

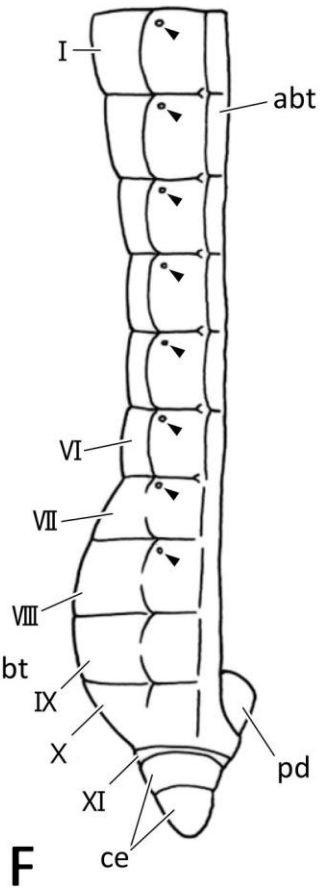
I
abt
VI
VII
VIII
IX
X
XI
pd
ce
F

Fig. 15. Eggs and embryos at 50-60% DT of *Zorotypus caudelli*. A, B: An egg, dorsal (A) and lateral (B) views, anterior to the top, fluorescence microscopy with DAPI staining. C, D: External features of the embryo, ventral (C) and lateral (D) views. For arrows, see the text. E, F: External features of the abdomen, ventral (E) and lateral (F) views.

acl, anteclypeus; an, antenna; ce, cercus; cp, coxopodite; et, egg tooth; fe, femur; ga, galea; gl, glossa; hl, head lobe; hp, hypopharynx; lbp, labial palp; lr, labrum; l1-3, pro-, meso- and metathoracic legs; md, mandible; mxp, maxillary palp; pcl, postclypeus; pd, proctodaeum; pgl, paraglossa; pp, pleuropodium; pta, pretarsus; sd, stomodaeum; ta1, 2, first and second tarsomere; ti, tibia; tp, telopodite; I, V-XI, first and fifth to 11th abdominal segments. Arrowheads and asterisk show the spiracles and mandibular teeth, respectively.

Scales = 100 µm

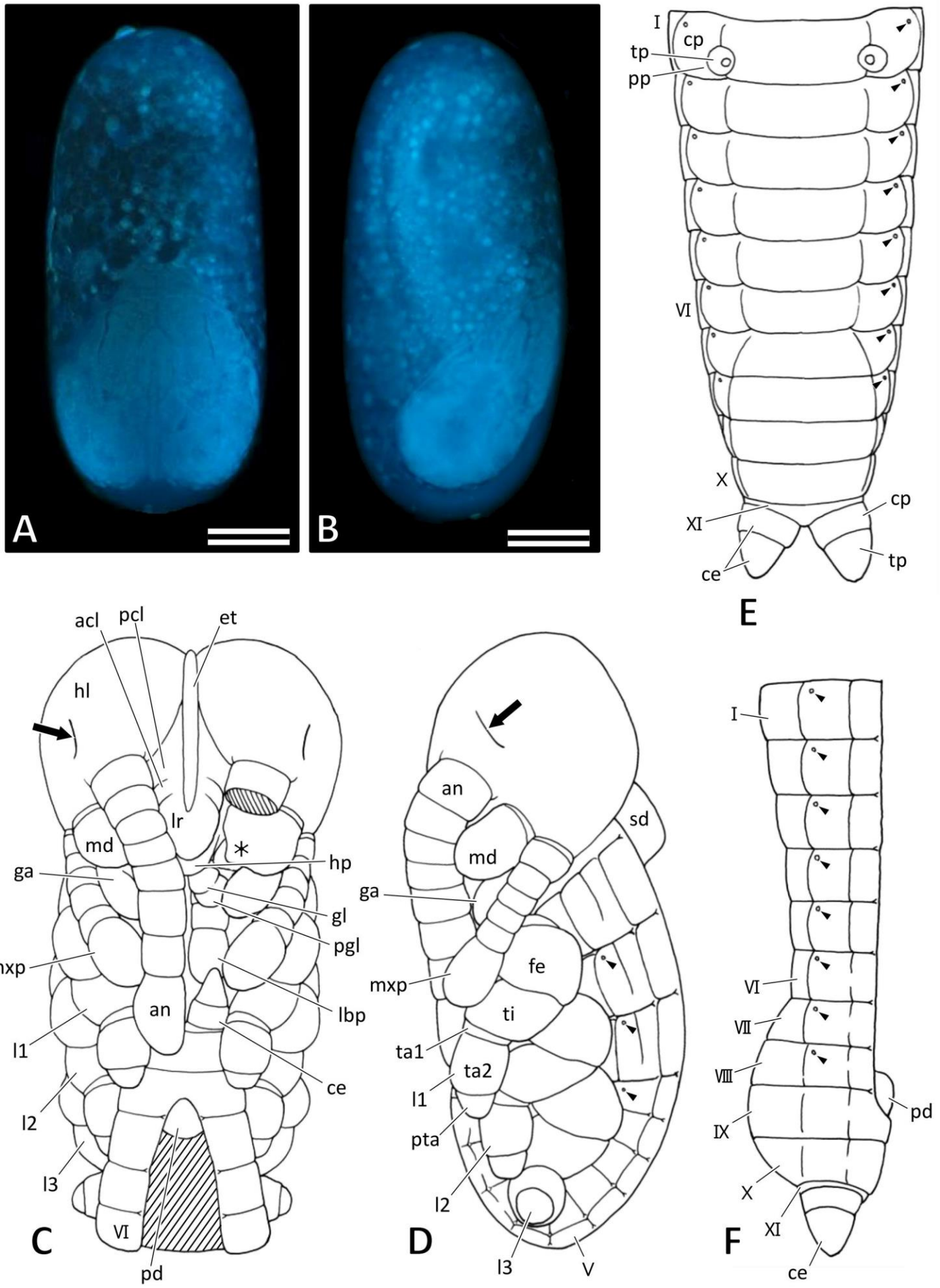
A
B
I
cp
tp
pp
VI
X
XI
cp
ce
tp
E
acl
pcl
et
hl
lr
md
*
hp
ga
gl
pgl
mxp
an
lbp
l1
ce
l2
l3
VI
pd
C
an
sd
md
ga
fe
mxp
ti
ta1
ta2
l1
pta
l2
l3
V
D
I
VI
VII
VIII
IX
X
XI
pd
ce
F

Fig. 16. Eggs and embryos at 60-65% DT of *Zorotypus caudelli*. A, B: An egg, dorsal (A) and lateral (B) views, anterior to the top, fluorescence microscopy with DAPI staining. C, D: External features of the embryo, ventral (C) and lateral (D) views.

acl, anteclypeus; am, amnion; an, antenna; ce, cercus; et, egg tooth; gl, glossa; hl, head lobe; lbp, labial palp; lr, labrum; l1-3, pro-, meso- and metathoracic legs; md, mandible; mxp, maxillary palp; pcl, postclypeus; pgl, paraglossa; sdo, secondary dorsal organ; tht1-3, pro-, meso- and metathoracic terga; VI, sixth abdominal segment.

Scales = 100 µm


A

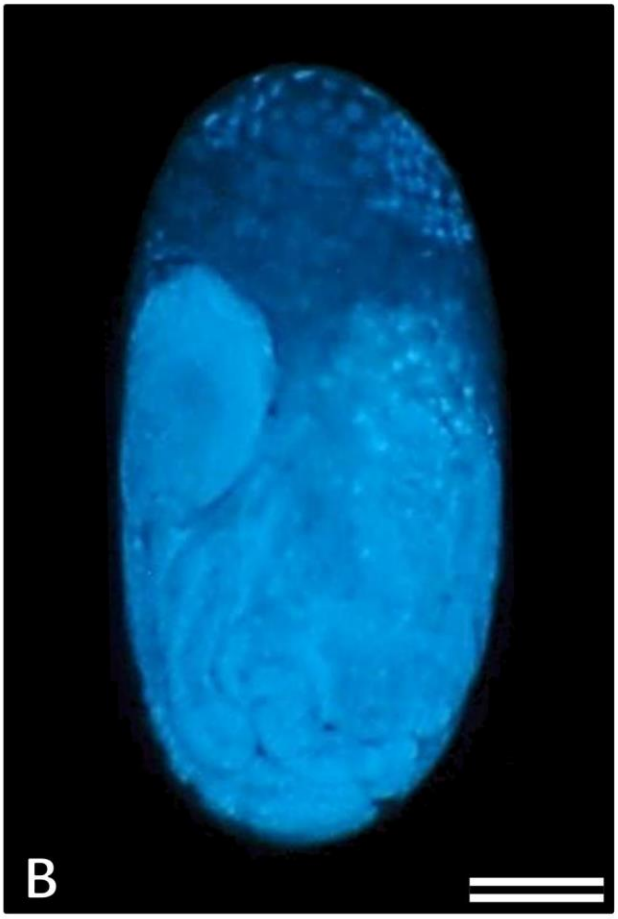
B

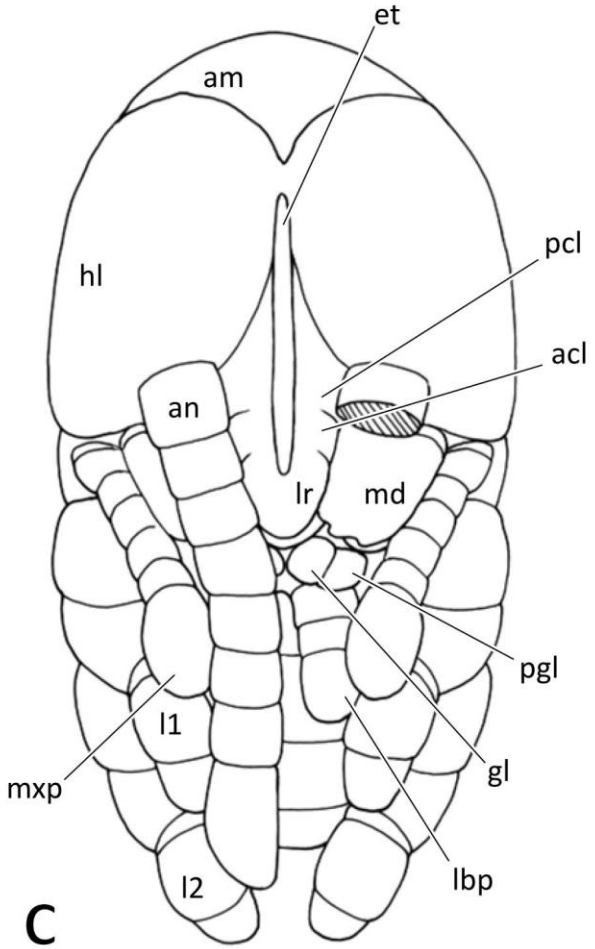
et
am
hl
pcl
acl
an
lr
md
pgl
gl
mxp
l1
l2
lbp
C

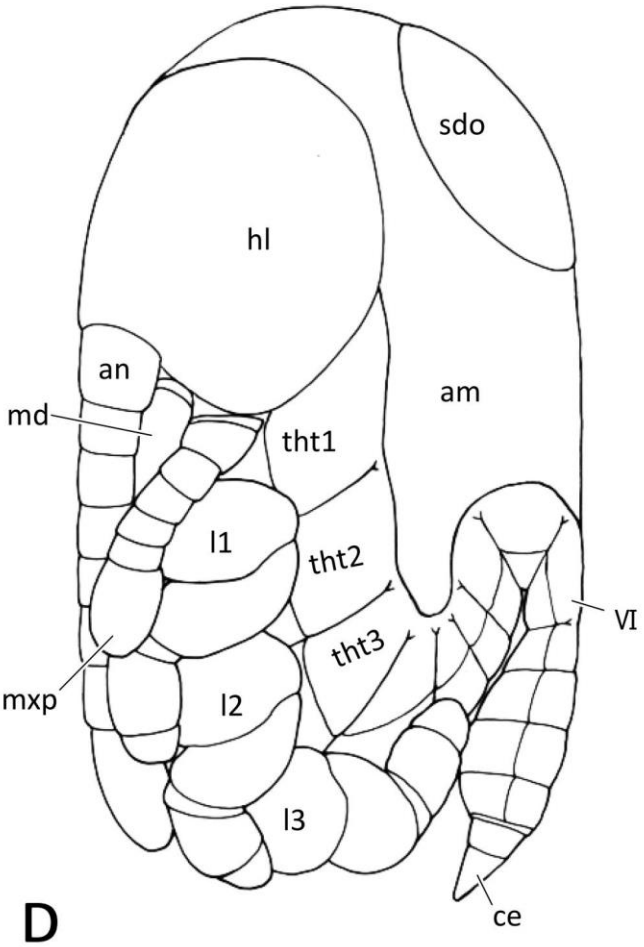
sdo
hl
an
am
md
tht1
l1
tht2
VI
tht3
mxp
l2
l3
ce
D

Fig. 17. Eggs and embryos at 65-80% DT of *Zorotypus caudelli*. A, B: An egg, dorsal (A) and lateral (B) views, anterior to the top, fluorescence microscopy with DAPI staining. C, D: External features of the embryo, ventral (C) and lateral (D) views. E, F: External features of the abdomen, ventral (E) and lateral (F) views.

acl, anteclypeus; am, amnion; an, antenna; ce, cercus; cp, coxopodite; et, egg tooth; gl, glossa; hc, head capsule; lbp, labial palp; lr, labrum; l1-3, pro-, meso- and metathoracic legs; md, mandible; mxp, maxillary palp; pcl, postclypeus; pgl, paraglossa; pp, pleuropodium; sdo, secondary dorsal organ; tht1-3, pro-, meso- and metathoracic terga; tp, telopodite; I, VI, X-XI, first, sixth and tenth to 11th abdominal segments. Arrowheads show the spiracles.

Scales = 100 μm

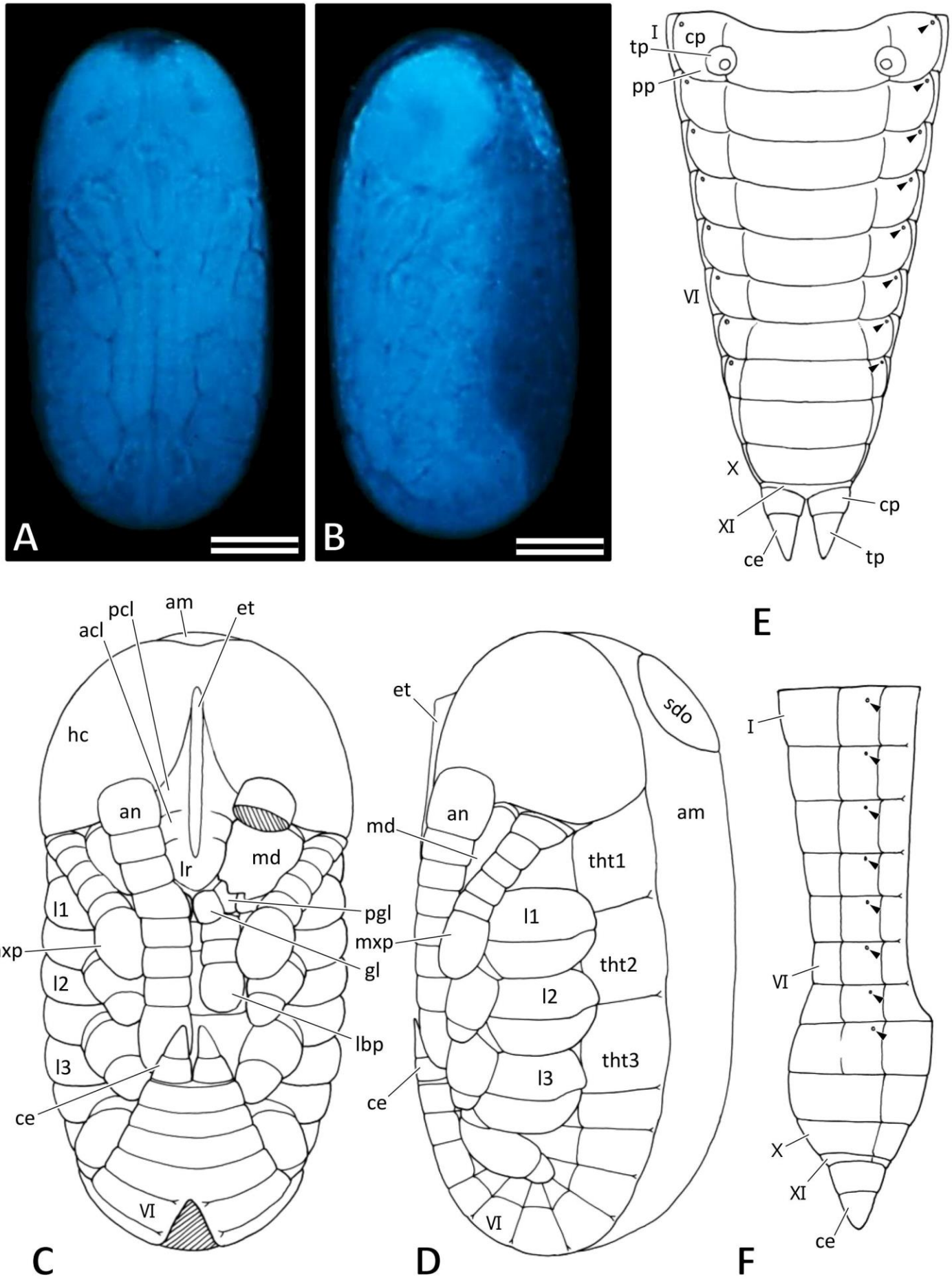
A
B
I
cp
tp
pp
VI
X
XI
cp
ce
tp
E
pcl
am
et
acl
hc
an
lr
md
l1
pgl
mxp
gl
l2
lbp
l3
ce
VI
C
et
sdo
an
am
md
tht1
l1
mxp
tht2
l2
tht3
l3
ce
VI
D
I
VI
X
XI
ce
F

Fig. 18. Eggs and embryos at 80-100% DT of *Zorotypus caudelli*. A, B: An egg, dorsal (A) and lateral (B) views, anterior to the top. C, D: External features of the embryo, ventral (C) and lateral (D) views. E, F: External features of the abdomen, ventral (E) and lateral (F) views.

acl, anteclypeus; an, antenna; ce, cercus; cp, coxopodite; et, egg tooth; fro, frons; gl, glossa; hc, head capsule; lbp, labial palp; lr, labrum; l1-3, pro-, meso- and metathoracic legs; md, mandible; mxp, maxillary palp; pcl, postclypeus; pgl, paraglossa; tht1-3, pro-, meso- and metathoracic terga; tp, telopodite; I, VI, IX-XI, first, sixth and ninth to 11th abdominal segments. Arrowheads show the spiracles.

Scales = 100 μm

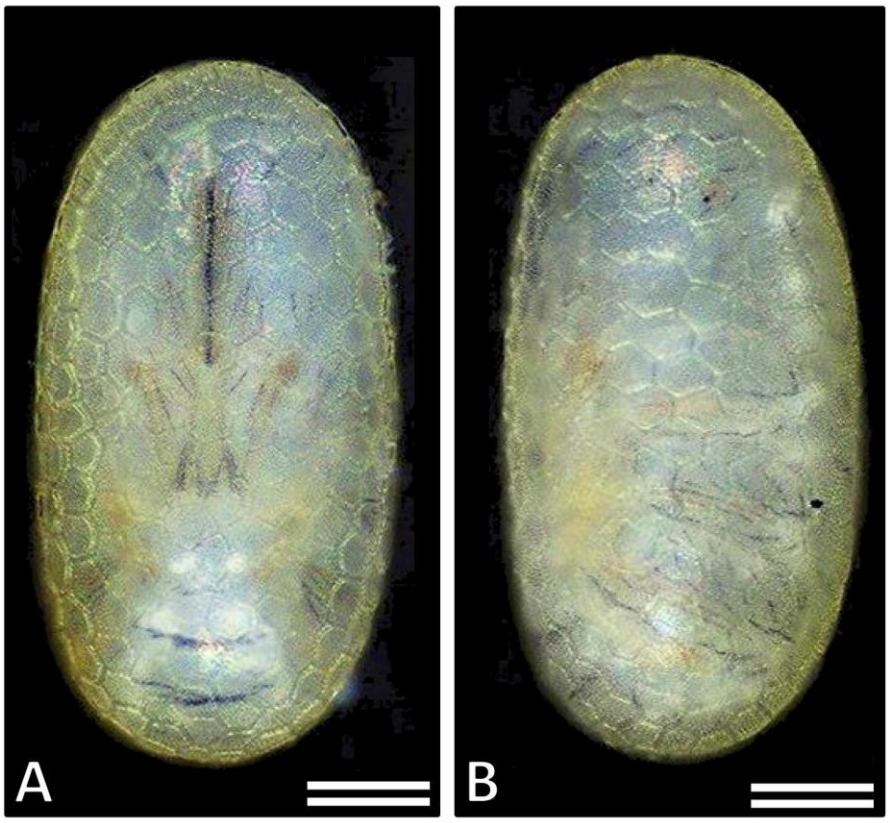
A
B

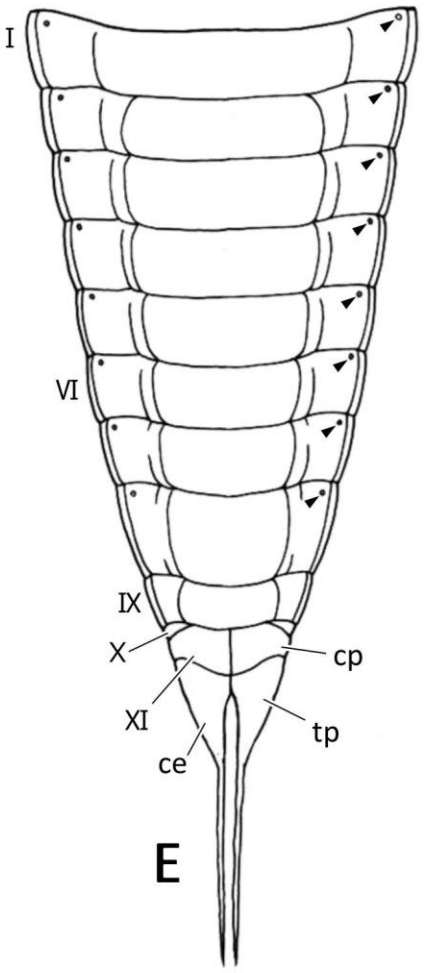
I
VI
IX
X
XI
ce
cp
tp
E

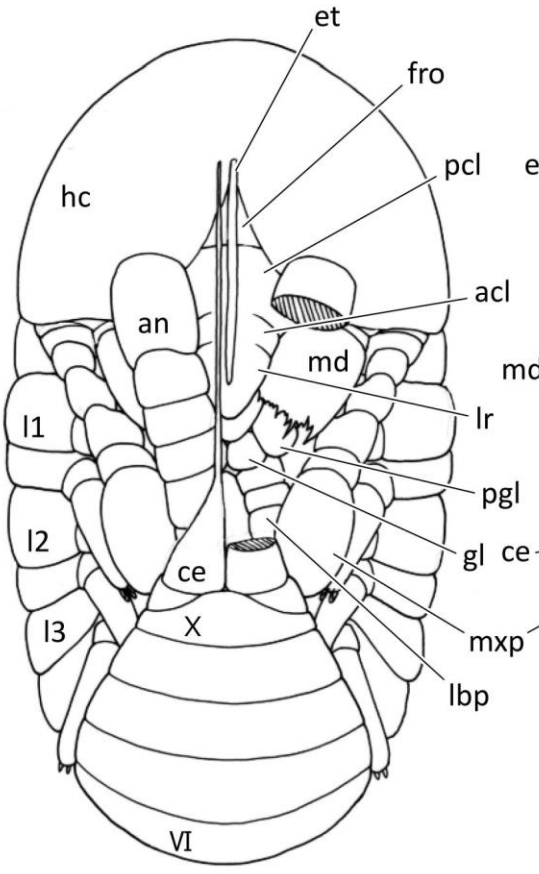
et
fro
pcl
hc
acl
an
md
lr
l1
pgl
l2
gl
ce
X
l3
mxp
lbp
VI
C

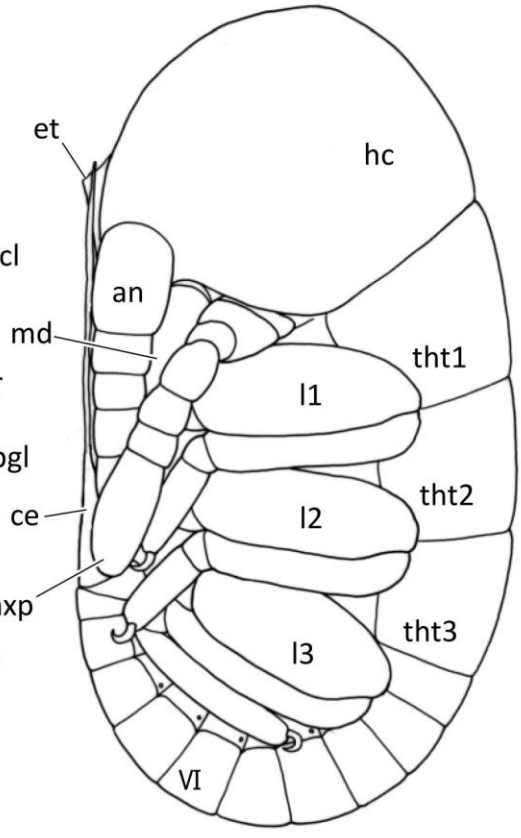
et
hc
an
md
tht1
l1
tht2
l2
ce
tht3
l3
VI
D

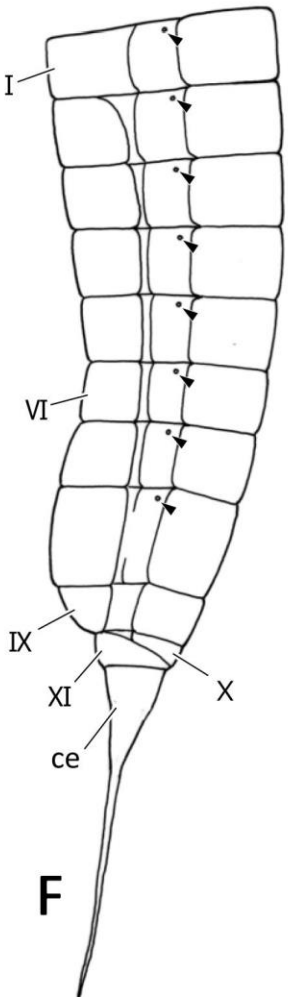
I
VI
IX
XI
X
ce
F

Fig. 19. Eggs and larva of *Zorotypus caudelli*. A, B: Hatching, posterior (A) and lateral (B) views, SEM. The egg was cleaned in advance with bleach to remove extrinsic material such as the fringe. C: Egg exuvia, lateroventral view. The egg was cleaned as in A and B. White and black arrowheads show a split line in the chorion for hatching and the position of micropyles, respectively.

ab, abdomen; an, antenna; eg, egg; emcu, embryonic cuticle; et, egg tooth; hc, head capsule; l1, prothoracic leg; mxp, maxillary palp;th1-3, pro-, meso- and metathoracic segments.

Scale bars = 100 μm.

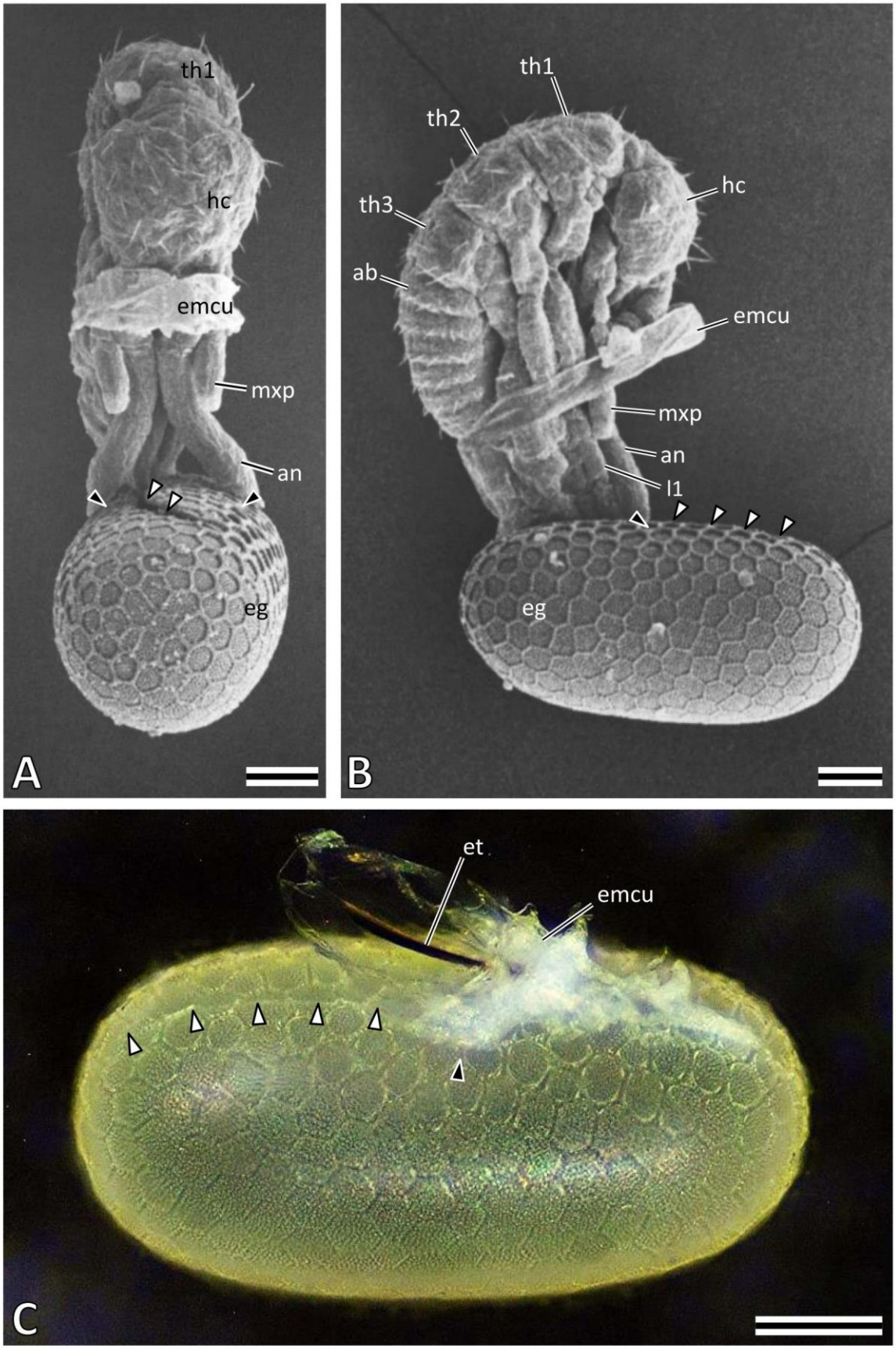
th1
hc
emcu
mxp
an
eg
A
th1
th2
th3
ab
hc
emcu
mxp
an
l1
eg
B
et
emcu
C

Fig. 20. Embryos of *Zorotypus caudelli*. A: Head at 80-100% DT, anterior view, SEM. B: An enlargement of head with embryonic cuticle removed at 80-100% DT, anterior view, SEM. White and black arrowheads show boundary between ante- and postclypeus and that between anteclypeus and labrum, respectively. C: Sagittal section of head at 80-100% DT. Black arrow shows protrusion of the egg tooth over the proximal part of labrum.

acl, anteclypeus; an, antenna; es, epistomal suture; et, egg tooth; fro, frons; hc, head capsule; hp, hypopharynx; lb, labium; lr, labrum; mxp, maxillary palp; pcl, postclypeus; sd, stomodaeum.

Scale bars = A: 100 μm; B, C: 50 μm.

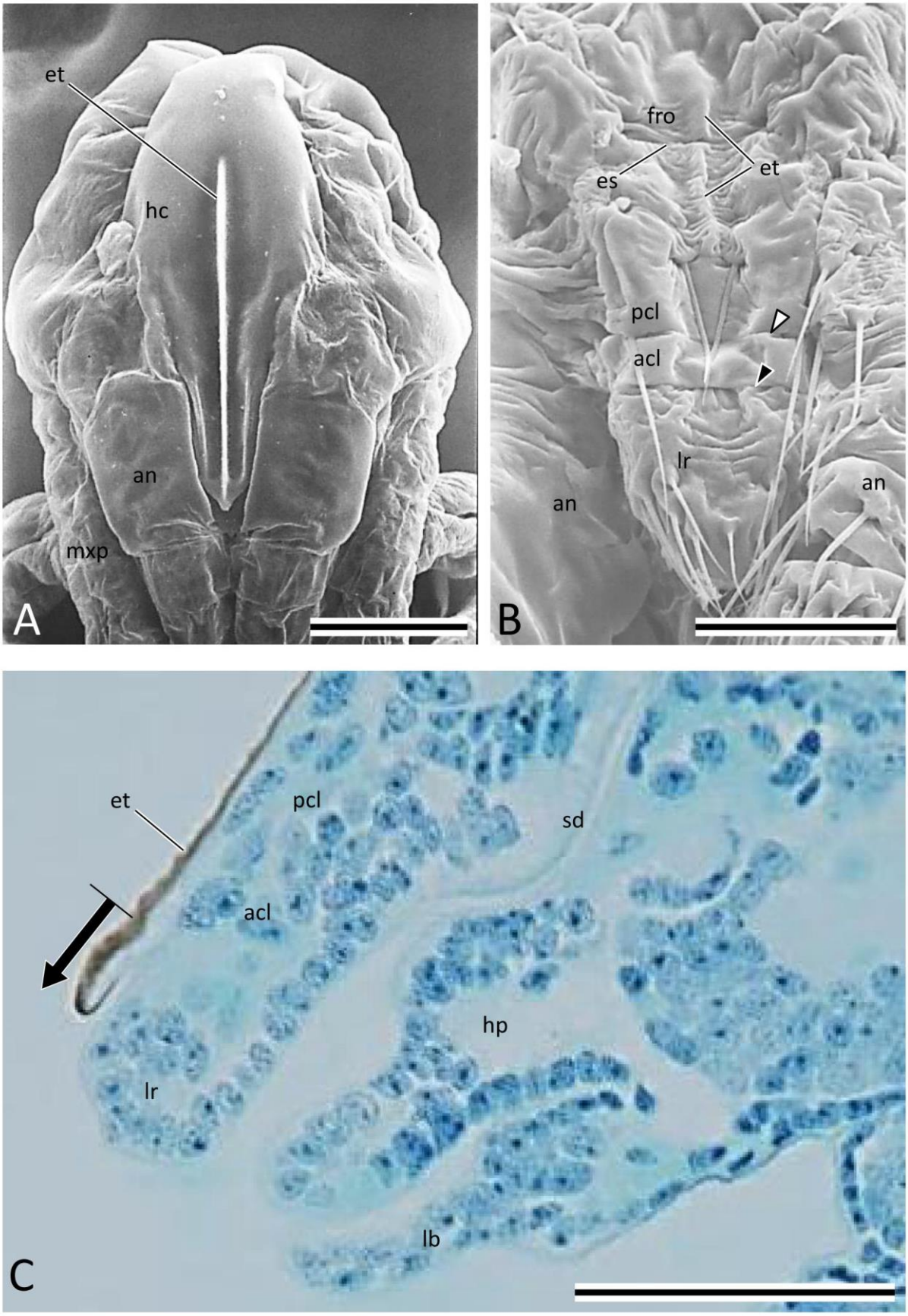
et
hc
an
mxp
A
fro
et
es
pcl
acl
lr
an
an
B
et
pcl
sd
acl
hp
lr
lb
C

Fig. 21. Eggs and embryos of *Zorotypus caudelli*. A: Cross section of an egg at 40-50% DT. B: Cross section of an egg with chorion and serosal cuticle removed at 80-100% DT. C: Abdomen at 80-100% DT, lateral view, SEM. D: Sagittal section of abdomen at 80-100% DT. White arrow shows the invagination of 10th abdominal sternum between ninth and 11th sterna.

ab, abdomen; an, antenna; ce, cercus; cx1-3, pro-, meso- and metacoxa; fe1, 2, pro- and mesofemur; fu, furca; ga, galea; gl, glossa; la, lacinia; lb, labium; mxp, maxillary palp; pd, proctodaeum; pgl, paraglossa; pp, pleuropodium; sa, sternal apophysis; sd, stomodaeum; secu, serosal cuticle; thg1, 2, pro- and mesothoracic ganglia; tht1, 2, pro- and mesothoracic terga; y, yolk; I -XI, first to 11th abdominal segments.

Scale bars = 100 μm.

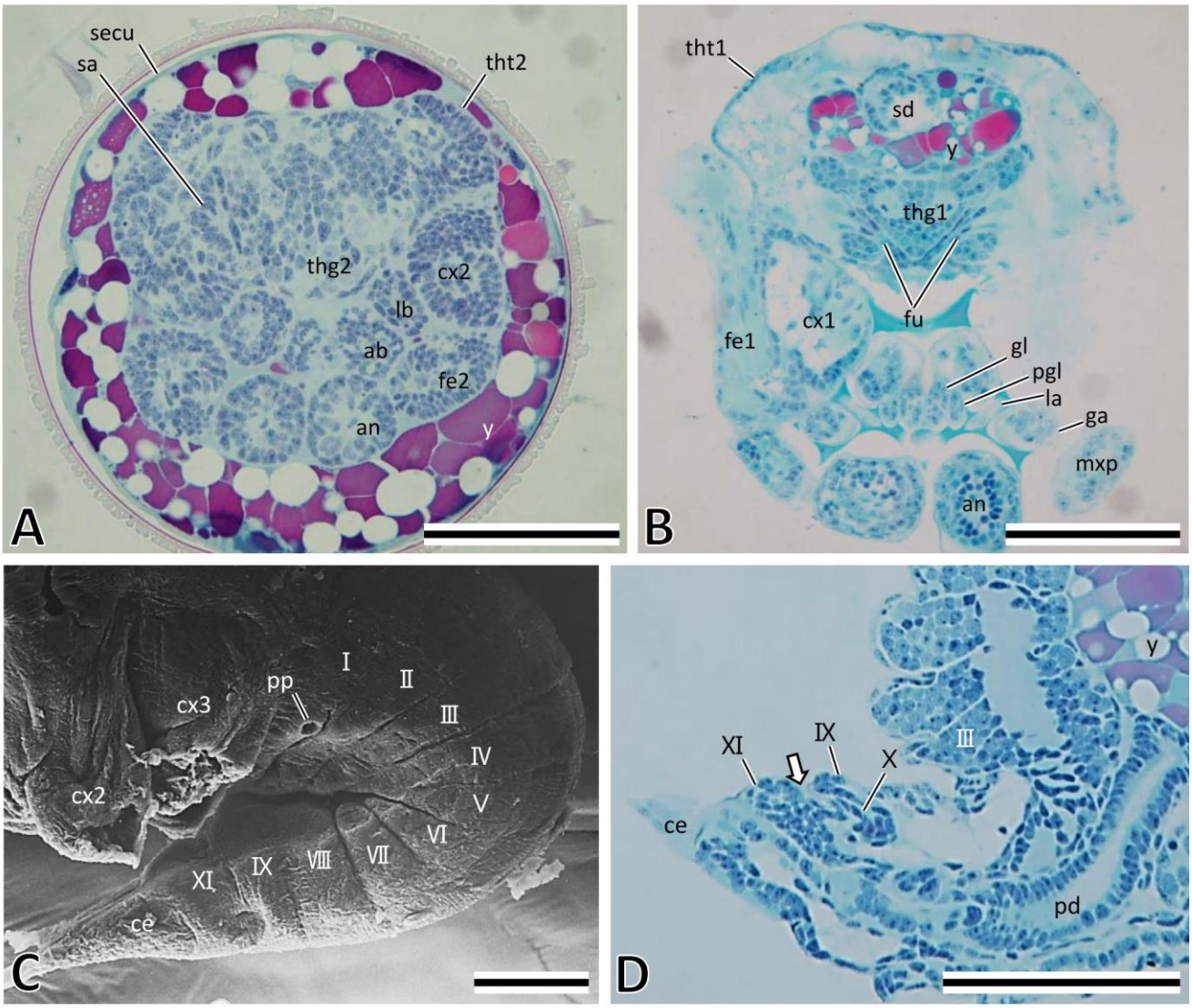
secu
sa
tht2
thg2
cx2
lb
ab
fe2
an
y
A
tht1
sd
y
thg1
fu
cx1
fe1
gl
pgl
la
ga
mxp
an
B
cx3
pp
I
II
III
IV
V
VI
VII
VIII
IX
XI
cx2
ce
C
y
III
XI
IX
X
ce
pd
D

Fig. 22. Larvae and adults of *Zorotypus caudelli*. A: First instar larva. B: Second instar larva. C: Third instar larva. D: Fourth instar larva of apterous form. E: Fifth instar larva of apterous form. F: Adult of apterous form, female. G: Fourth instar larva of winged form. H, H', H'': Early (H), middle (H') and late (H'') fifth instar larvae of winged form. I: Adult of winged form, male.

Scale bar = 1 mm.

A
B
C
D
E
F
G
H
H'
H''
I

Fig. 23. Fourth and fifth instar larvae of *Zorotypus caudelli*. A: Thorax and abdomen of the late fifth instar larva of winged form. Under the cuticle the chaetotaxy of the next instar or the adult can be seen: among the setae “seemingly bifurcated”, a little faintly seen is the seta for the next instar (arrows). B, C: Heads of fourth (B) and fifth (C) instar larvae of winged form. D: Wing pads of late fifth instar larva. E: Head and thorax of fifth instar larva. Arrowheads show posterolateral projections of the pterothoracic nota.

an, antenna; at1-3, first to third abdominal terga; ce, compound eye; hc, head capsule; l1, proleg; lbp, labial palp; nt1-3, pro-, meso- and metathoracic nota; oc, ocellus; wp, wing pad.

Scale bars = 200 μm.

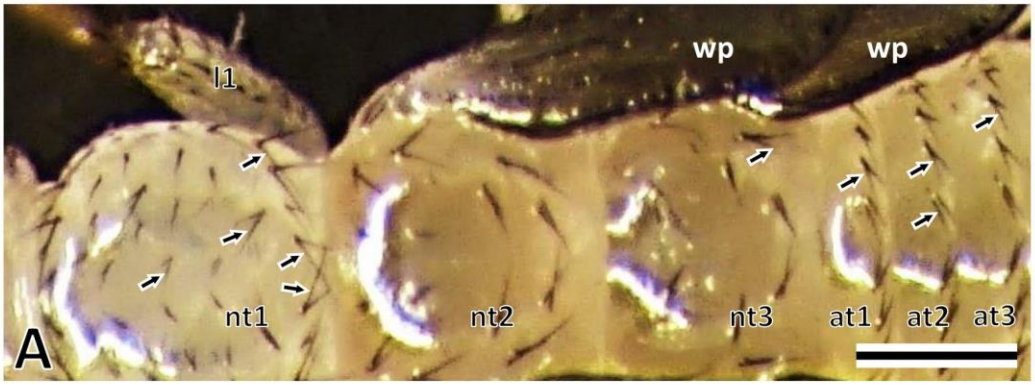
l1
wp
wp
nt1
nt2
nt3
at1
at2
at3
A

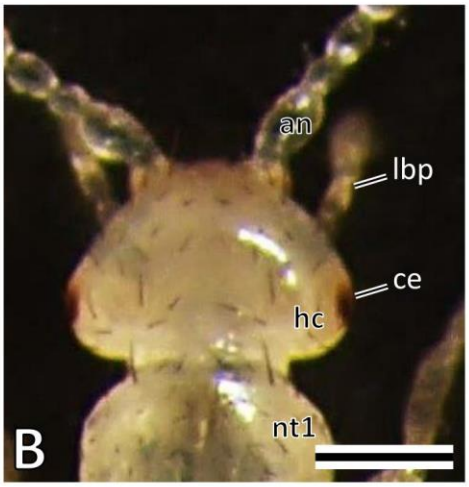
an
lbp
ce
hc
nt1
B

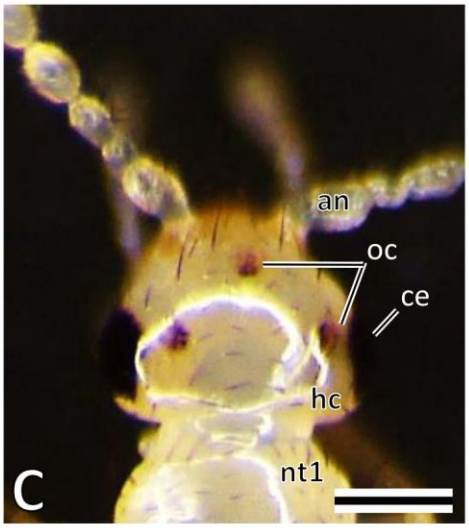
an
oc
ce
hc
nt1
C

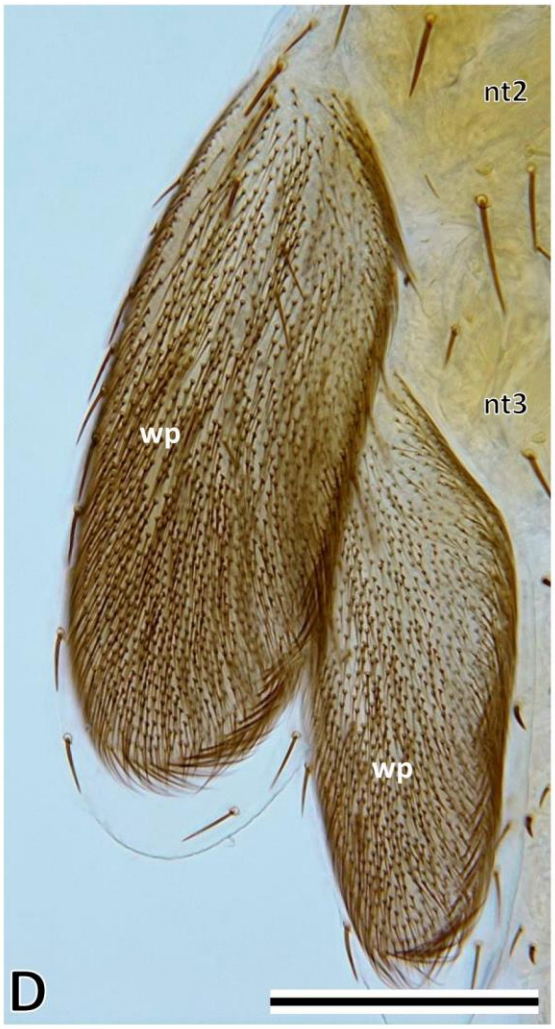
nt2
nt3
wp
wp
D

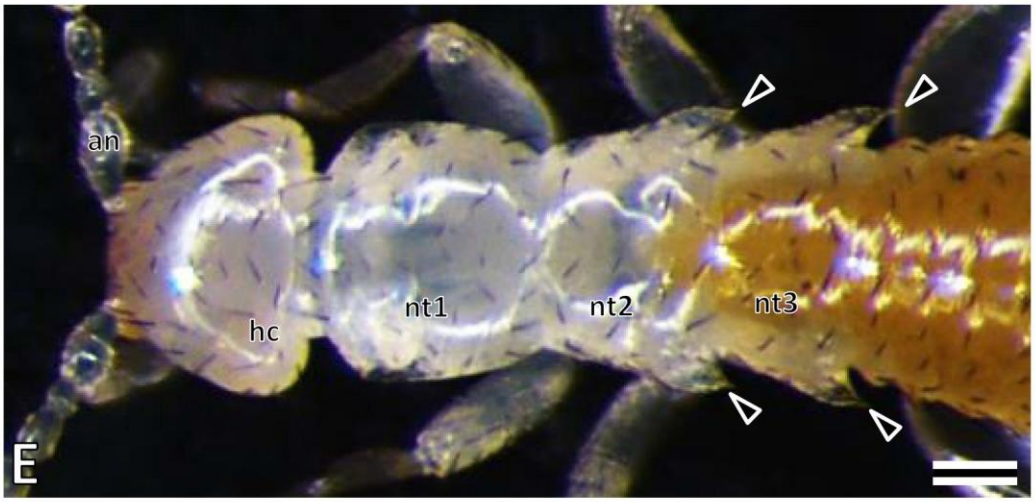
an
hc
nt1
nt2
nt3
E

Fig. 24. First instar larvae of *Zorotypus caudelli*, SEM. A: Body, lateral view. B, B': Left antenna (B) and its second to fourth antennomeres (B'). C: Prothorax, lateral view. D: Meso- and metathorax, lateral view. Black and white stars show small sclerites anterior to meso- and metathoracic anepisterna, respectively. E, F, G: Abdomen, lateral (E), caudal (F) and ventral (G) views. Asterisks and Arrows show coxopodites of 11th abdominal segment and lateral margin of each small sclerotized region of the third to seventh abdominal sterna, respectively. White and black arrowheads show lateral margins of abdominal terga and spiracles, respectively.

aeps2, 3, meso- and metathoracic anepisterna; an, antenna; apl, anterior propleurite; as1-10, 11, first to 10th and 11th abdominal sterna; at1-11, first to 11th abdominal terga; ce, cercus; cx1-3, pro-, meso- and metacoxa; ep, epiproct; epm2, 3, meso- and metathoracic epimera; hc, head capsule; lbp, labial palp; lr, labrum; md, mandible; mpl, middle propleurite; mx, maxilla; mxp, maxillary palp; nt1-3, pro-, meso- and metathoracic nota; pcj1-3, pro-, meso- and metathoracic pleuro-coxal joints; pls1-3, pro-, meso- and metathoracic pleural sutures; ppl, posterior propleurite; ti1-3, pro-, meso- and metatrochantines; 1-8, first to eighth antennomeres.

Scale bars = A, B, E, G: 100 μm; B', C, D, F: 50 μm.

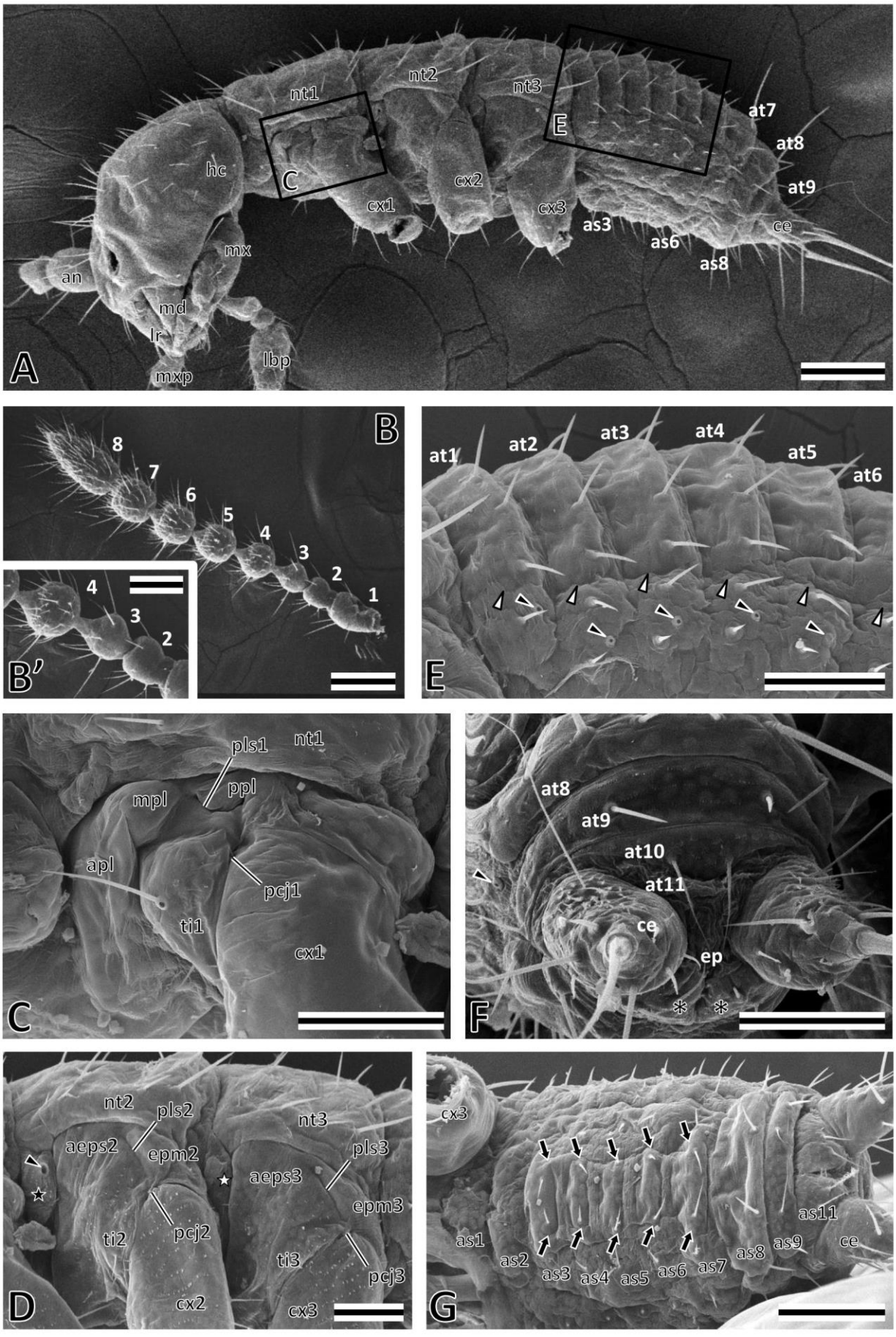
A
nt1
nt2
nt3
C
E
at7
at8
at9
hc
cx1
cx2
cx3
as3
as6
as8
ce
mx
an
md
lr
mxp
lbp
B
8
7
6
5
4
3
2
1
B′
4
3
2
E
at1
at2
at3
at4
at5
at6
C
pls1
nt1
ppl
mpl
apl
pcj1
ti1
cx1
F
at8
at9
at10
at11
ce
ep
D
nt2
pls2
aeps2
epm2
nt3
pls3
aeps3
epm3
pcj2
ti2
ti3
pcj3
cx2
cx3
G
cx3
as1
as2
as3
as4
as5
as6
as7
as8
as9
as11
ce

Fig. 25. Second instar larvae of *Zorotypus caudelli*, SEM. A: Body, lateral view. B, B’: Left antenna (B) and its second to fourth antennomeres (B’). C, D: Abdomen, lateral (C) and caudal (D) views. White and black arrowheads show lateral margins of each abdominal tergopleurite and spiracles, respectively. Asterisk shows unsclerotized area of the tergopleurite.

an, antenna; as4-8, 11, fourth to eighth and 11th abdominal sterna; at1-11, first to 11th abdominal terga; ce, cercus; cx1-3, pro-, meso- and metacoxa; ep, epiproct; hc, head capsule; lbp, labial palp; lr, labrum; md, mandible; mx, maxilla; mxp, maxillary palp; nt1-3, pro-, meso- and metathoracic nota; 1-8, first to eighth antennomeres.

Scale bars = A, B: 100 μm; B’, C, D: 50 μm.

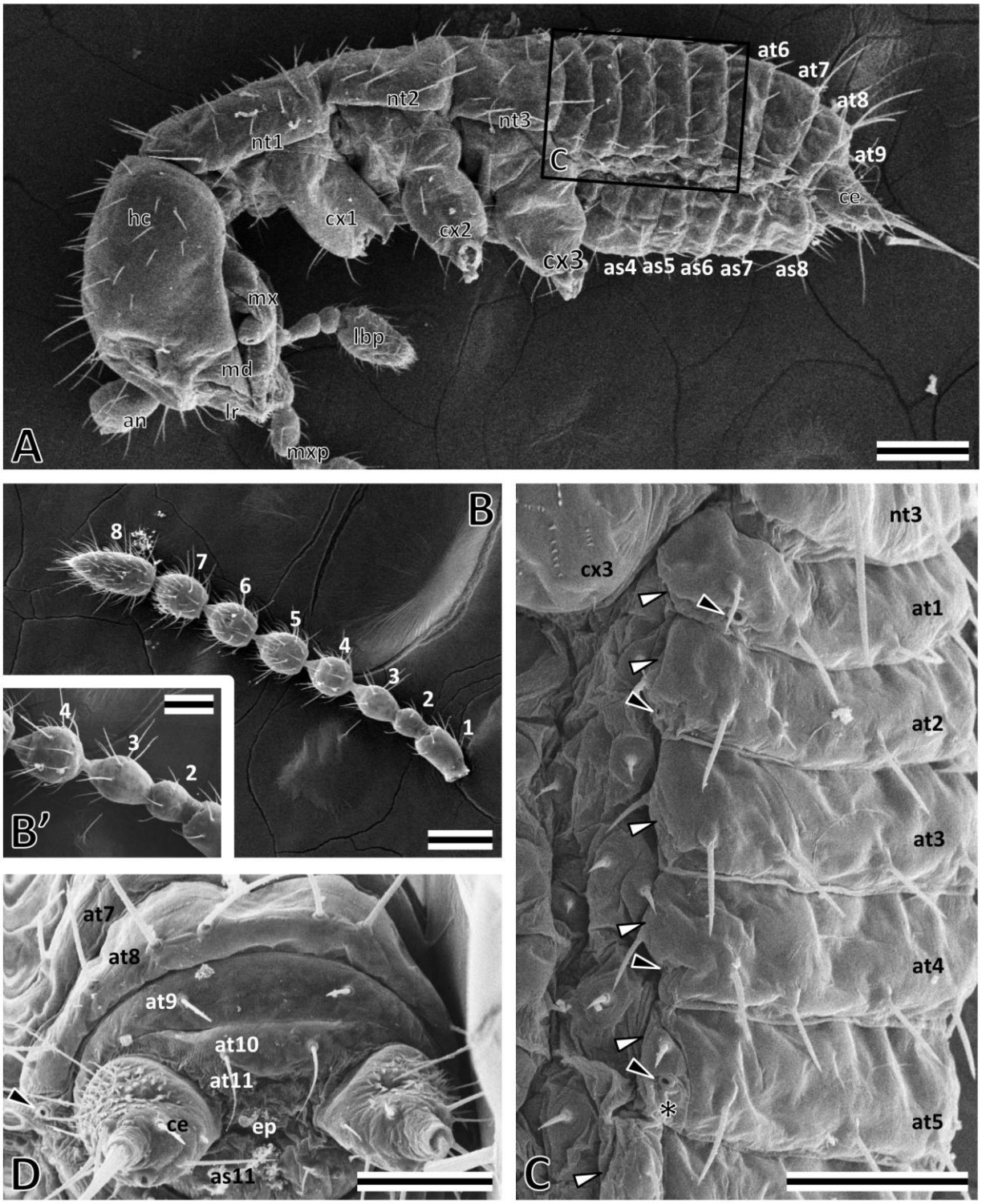
A
nt1
nt2
nt3
C
at6
at7
at8
at9
ce
hc
cx1
cx2
cx3
as4 as5 as6 as7
as8
mx
lbp
md
lr
an
mxp
B
8
7
6
5
4
3
2
1
B'
4
3
2
D
at7
at8
at9
at10
at11
ce
ep
as11
C
nt3
cx3
at1
at2
at3
at4
at5

Fig. 26. Third instar larvae of *Zorotypus caudelli*, SEM. A: Body, lateral view. B, B’: Left antenna (B) and its second to fourth antennomeres (B’). C: Mesothorax, lateral view. D, E: Abdomen, lateral (D) and caudal (E) views. White and black arrowheads show lateral margins of abdominal tergum and spiracles, respectively. An asterisk shows small sclerotized region anterior to mesothoracic anepisternum.

an, antenna; aeps2, mesothoracic anepisternum; as4-9, 11, fourth to ninth and 11th abdominal sterna; at2-11, second to 11th abdominal tergum; ce, cercus; cx1-3, pro-, meso- and metacoxa; ep, epiproct; epm2, mesothoracic epimeron; hc, head capsule; lbp, labial palp; lr, labrum; md, mandible; mx, maxilla; mxp, maxillary palp; nt1-3, pro-, meso- and metathoracic nota; pcj2, mesothoracic pleuro-coxal joint; peps2, mesothoracic preepisternum; pls2, mesothoracic pleural suture; ti2, mesotrochantin; 1-8, first to eighth antennomeres.

Scale bars = A: 200 μm; B, C, D: 100 μm; B’, E: 50 μm.

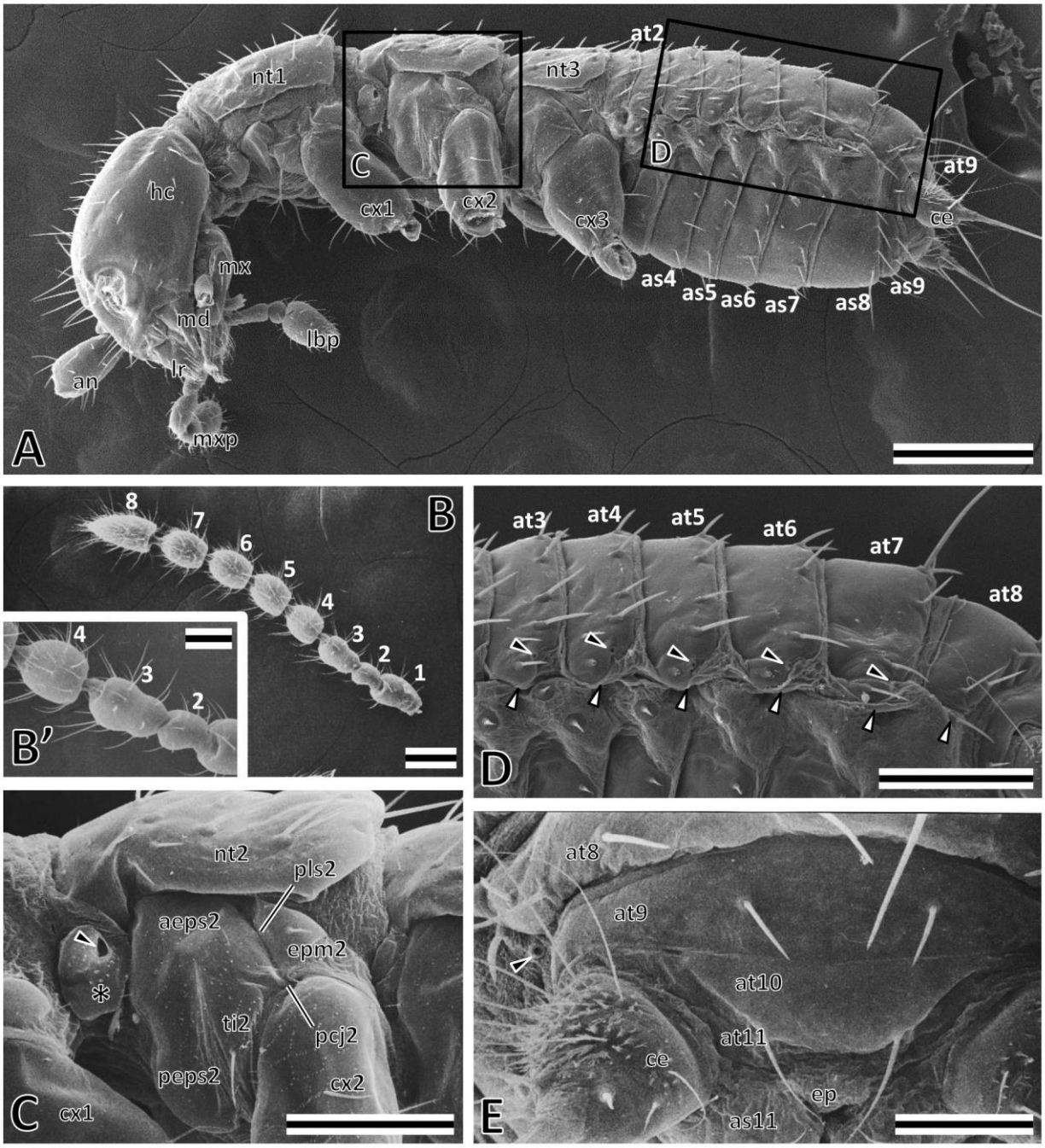
A
nt1
nt3
at2
C
D
at9
ce
hc
cx1
cx2
cx3
mx
md
lbp
lr
an
mxp
as4
as5
as6
as7
as8
as9
B
8
7
6
5
4
3
2
1
B'
4
3
2
D
at3
at4
at5
at6
at7
at8
C
nt2
pls2
aeps2
epm2
ti2
pcj2
peps2
cx2
cx1
E
at8
at9
at10
at11
ce
ep
as11

Fig. 27. Fourth instar larvae of *Zorotypus caudelli*, SEM. A: Body of apterous form, lateral view. B, B': Left antenna (B) and its second to fourth antennomeres (B'). C: Head of winged form, lateral view. A black ocular spot is seen under light microscopy (e.g., Fig. 2B), but the cuticular specialization on cuticle around it has not yet occurred (cf. C). D: Meso- and metathorax of winged form, lateral view. Arrowhead shows spiracle. E: Abdomen, caudal view.

aeps2, 3, meso- and metathoracic anepisterna; an, antenna; as4-9, 11, fourth to ninth and 11th abdominal sterna; at1-11, first to 11th abdominal terga; ce, cercus; cx1-3, pro-, meso- and metacoxa; ep, epiproct; epm2, 3, meso- and metathoracic epimera; hc, head capsule; lbp, labial palp; lr, labrum; md, mandible; mx, maxilla; mxp, maxillary palp; nt1-3, pro-, meso- and metathoracic nota; pcj2, 3, meso- and metathoracic pleuro-coxal joints; pls2, 3, meso- and metathoracic pleural sutures; ti2, 3, meso- and metatrochantines; wp, wing pad; 1-9, first to ninth antennomeres.

Scale bars = A: 200 μm; B, C, D, E: 100 μm; B': 50 μm .

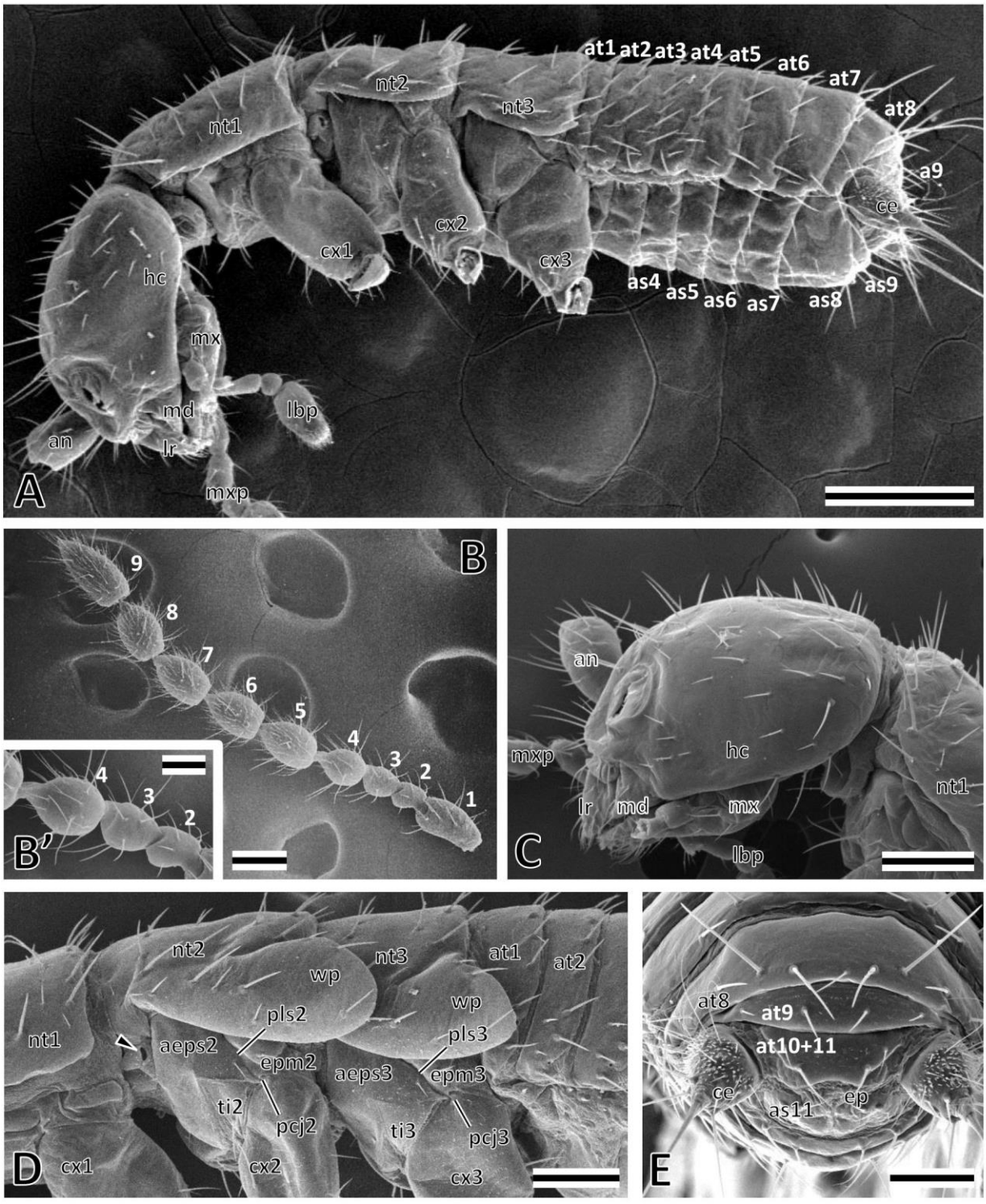
A
at1 at2 at3 at4 at5 at6 at7 at8
a9
ce
nt1
nt2
nt3
cx1
cx2
cx3
hc
mx
md
lbp
an
lr
mxp
as4 as5 as6 as7 as8 as9
B
9 8 7 6 5 4 3 2 1
B′
4 3 2
C
an
mxp
hc
nt1
lr
md
mx
lbp
D
nt1
nt2
nt3
wp
wp
pls2
pls3
aeps2
epm2
aeps3
epm3
ti2
pcj2
ti3
pcj3
cx1
cx2
cx3
at1
at2
E
at8
at9
at10+11
ce
as11
ep

Fig. 28. Fifth instar larvae and adults of *Zorotypus caudelli*, SEM. A: Body of apterous form of fifth instar larva, lateral view. B, B’: Left antenna (B) and its second to fourth antennomeres (B’) of fifth instar larva. C: Head of fifth instar larva of winged form, lateral view. D: Mesothorax of fifth instar larva of apterous form, lateral view. E: Mesothorax of fifth instar larva of winged form with wing pad removed, lateral view. F: Meso- and metathorax of fifth instar larva of winged form, lateral view. G-J: Abdomen, caudal views. Prospective male (G) and female (H) of fifth instar larva, male (I) and female (J) of adults. White and black arrows show postmedian swelling and mating hook on the 10th + 11th abdominal tergum, respectively. Arrowheads show spiracles. Asterisks show small sclerites anterior to mesothoracic anepisternum, respectively.

aeps2, 3, meso- and metathoracic anepisterna; an, antenna; as3-9, 11, third to ninth and 11th abdominal sterna; at1-11, first to 11th abdominal terga; ce, cercus; cx1-3, pro-, meso- and metacoxa; ep, epiproct; epm2, 3, meso- and metathoracic epimera; hc, head capsule; lbp, labial palp; lr, labrum; md, mandible; mx, maxilla; nt1-3, pro-, meso- and metathoracic nota; pcj2, mesothoracic pleuro-coxal joint; peps2, mesothoracic preepisternum; pls2, mesothoracic pleural suture; ti2, mesotrochantin; wp, wing pad; 1-9, first to ninth antennomeres.

Scale bars = A, F: 200 μm; B, C, G, H, I, J: 100 μm; B’, D, E: 50 μm.

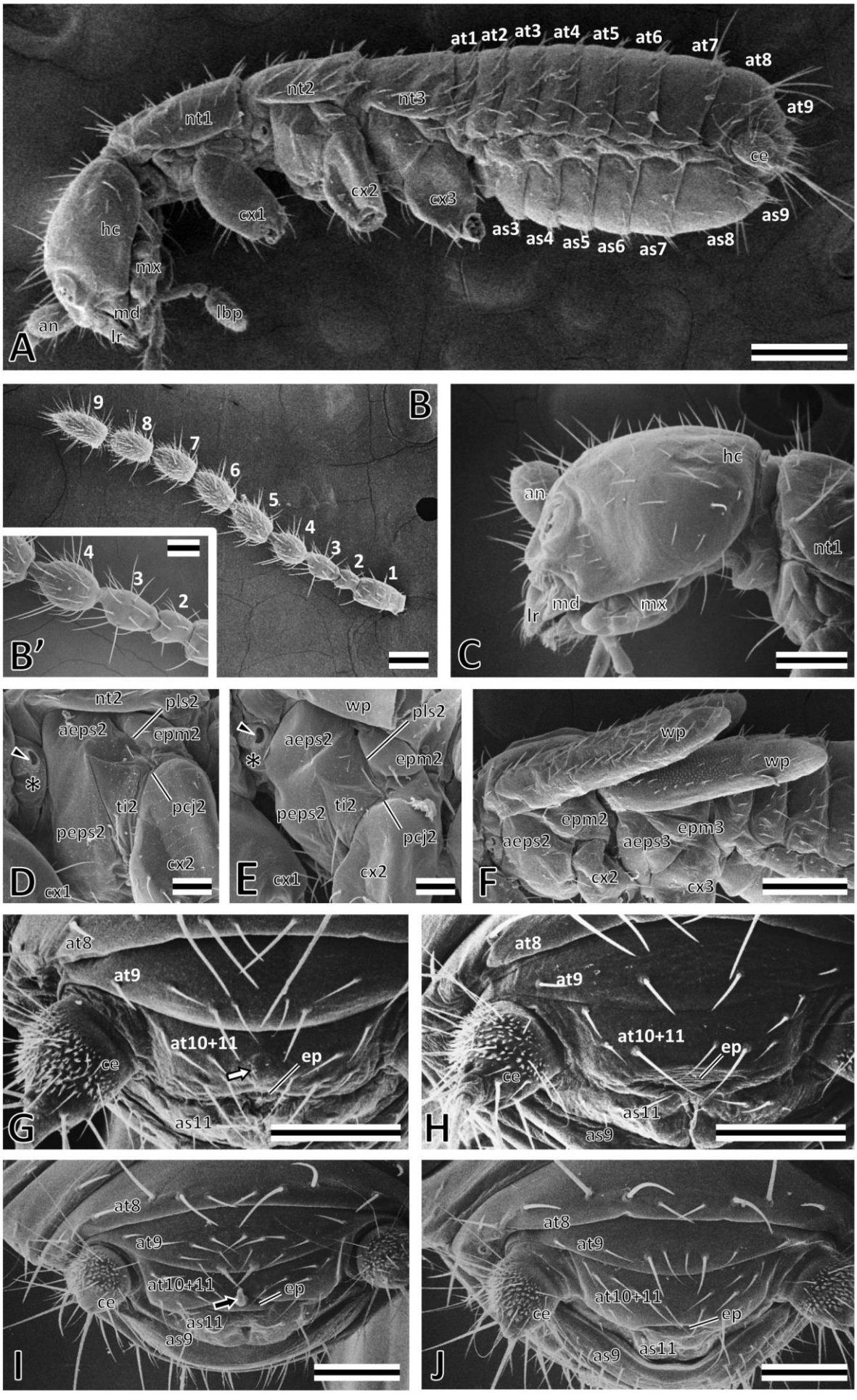
A
at1 at2 at3 at4 at5 at6 at7 at8 at9
nt1 nt2 nt3
ce
cx1 cx2 cx3
as3 as4 as5 as6 as7 as8 as9
hc
mx
md
lr
lbp
an
B
9 8 7 6 5 4 3 2 1
B′
4 3 2
C
hc
an
nt1
lr md mx
D
nt2 pls2 aeps2 epm2 ti2 pcj2 peps2 cx2 cx1
E
wp pls2 aeps2 epm2 peps2 ti2 pcj2 cx1 cx2
F
wp wp epm2 epm3 aeps2 aeps3 cx2 cx3
G
at8 at9 at10+11 ep ce as11
H
at8 at9 at10+11 ep ce as11 as9
I
at8 at9 at10+11 ep ce as11 as9
J
at8 at9 at10+11 ep ce as9 as11

Fig. 29. Left metafemora of *Zorotypus caudelli*, anterior view, SEM. A: First instar larva. B: Second instar larva. C: Third instar larva. D: Forth instar larva. E: Fifth instar larva. F: Adult.

Scale bars = 100 μm.

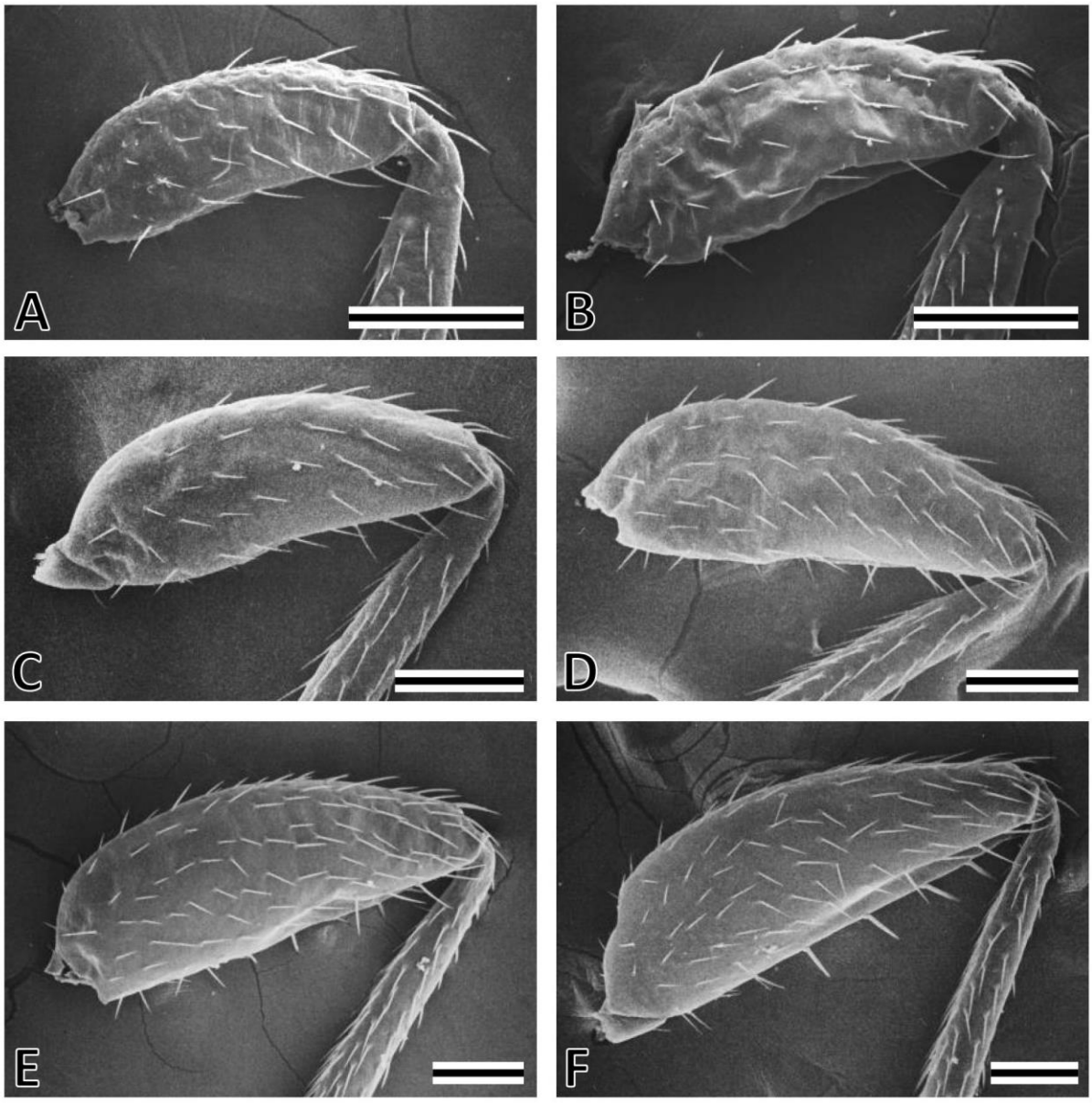
A
B
C
D
E
F

Fig. 30. Abdomen of *Zorotypus caudelli*, ventral view, SEM. A: Second instar larva. Black arrowheads show spiracles. Asterisk show a part of sclerotized region of the second abdominal sternum. B: Third instar larva. C: Fourth instar larva. D: Fifth instar larva.

as2-9, 11, second to ninth and11th abdominal sterna; ce, cercus; cx3, metacoxa.

Scale bars = 100 μm.

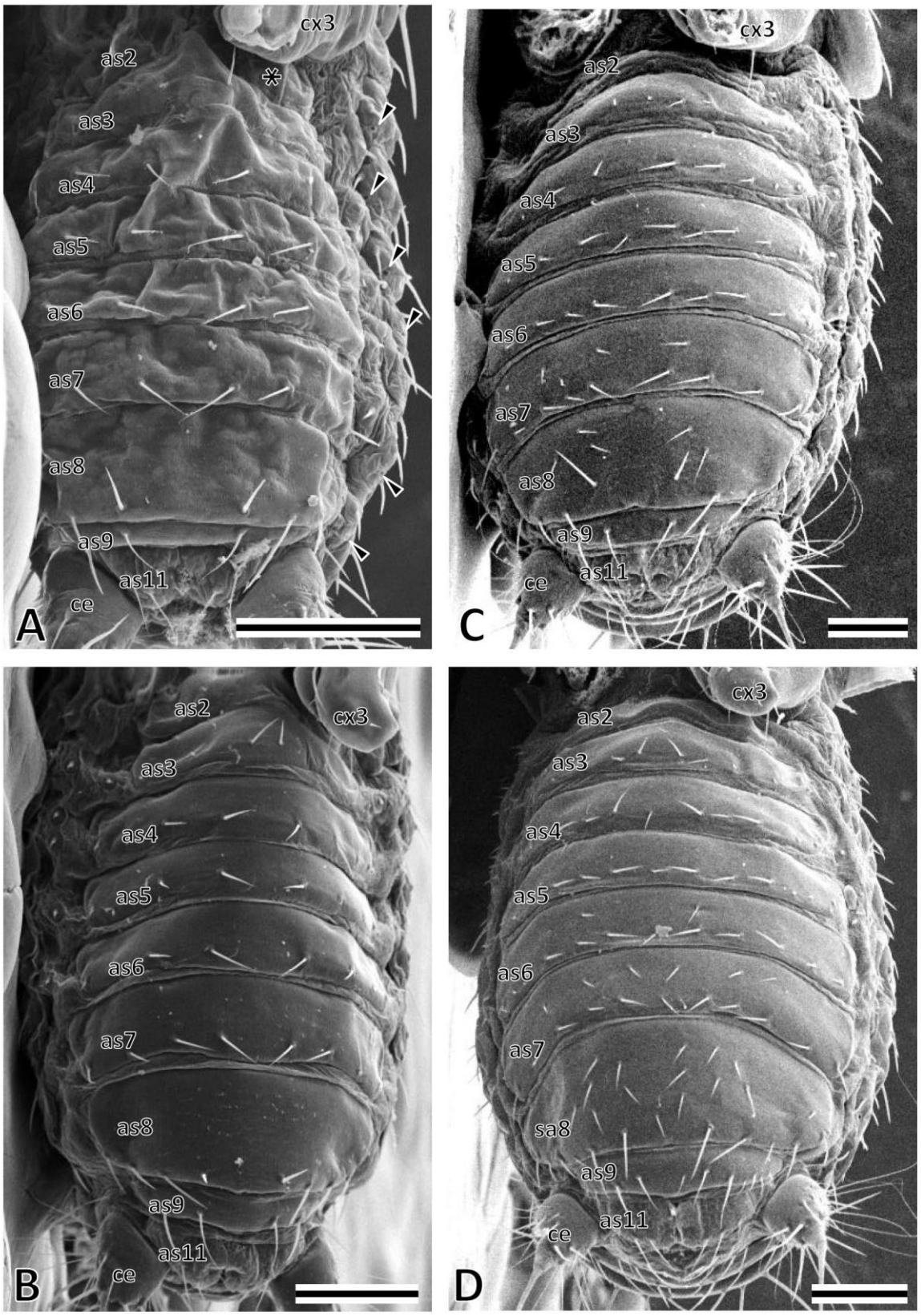
cx3
as2
as3
as4
as5
as6
as7
as8
as9
as11
ce
A
C
B
D
sa8

Fig. 31. Diagrammatic representations showing blastokinesis during the prekatatrepsis period in hemimetabolous insects, lateral view, anterior to the top, ventral to the left. A: Polyneoptera, immersed type. B: Polyneoptera, superficial Type. C: Acercaria and Palaeoptera. D: Zoraptera.

am, amnion; asf, amnioserosal fold; em, embryo; pce, protocephalon; pco, protocorm; se, serosa; y, yolk.

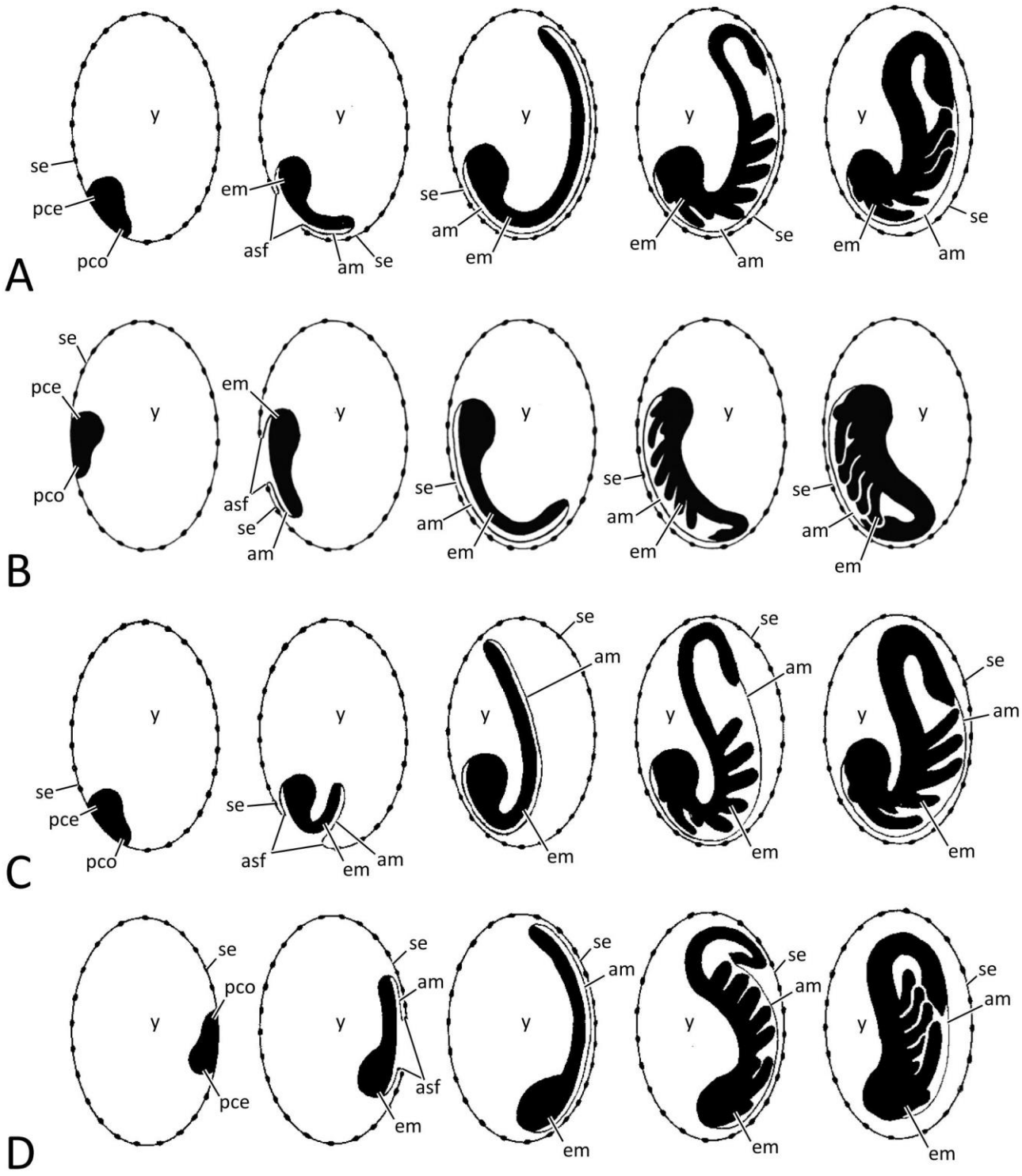
A
B
C
D
y
se
pce
pco
em
asf
am

Fig. 32. Proposed affinities of Zoraptera and Eukinolabia based on comparative embryological evidence (see Discussion 10).

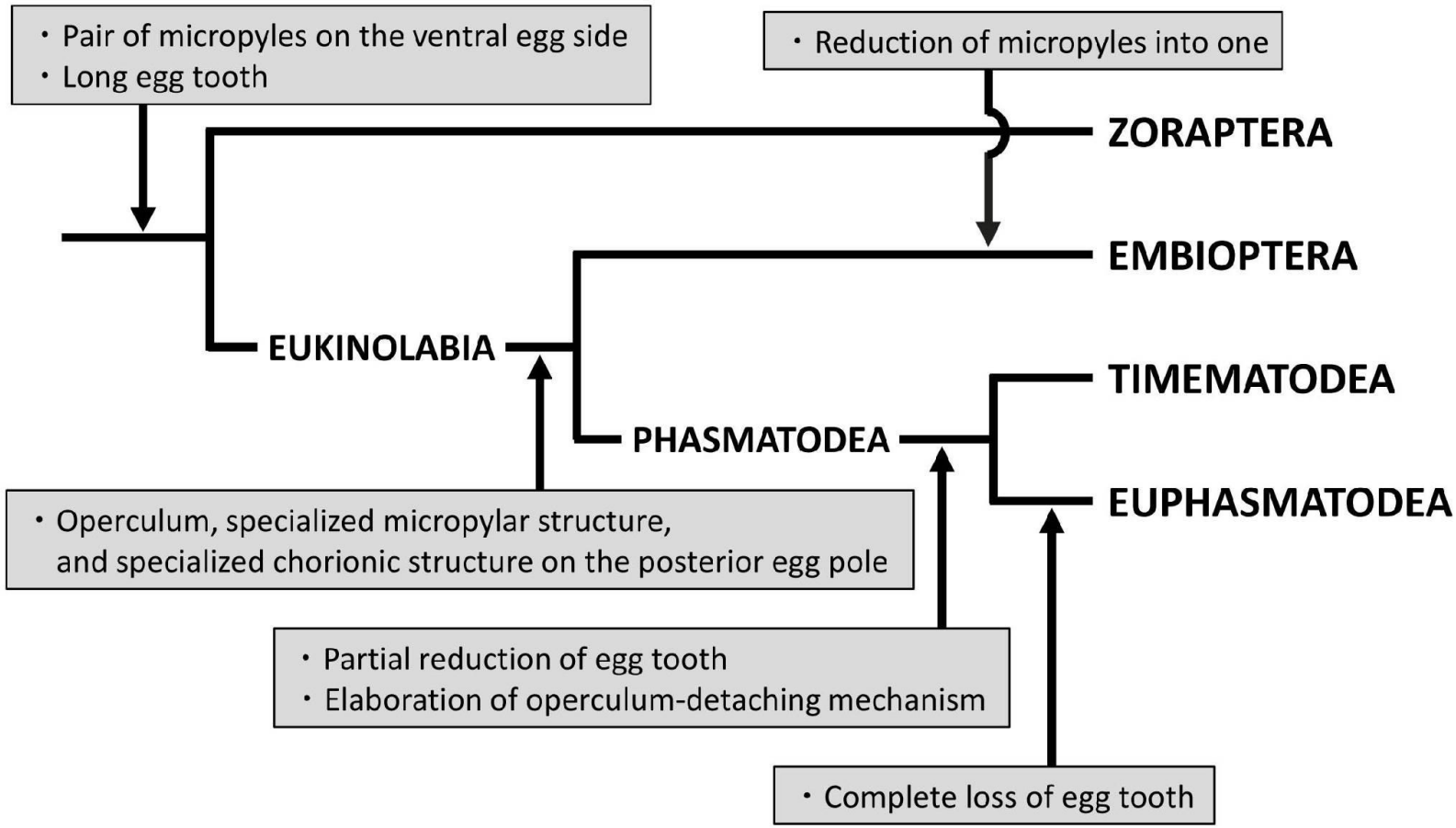
・Pair of micropyles on the ventral egg side
・Long egg tooth
・Reduction of micropyles into one
ZORAPTERA
EMBIOPTERA
EUKINOLABIA
TIMEMATODEA
PHASMATODEA
EUPHASMATODEA
・Operculum, specialized micropylar structure,
and specialized chorionic structure on the posterior egg pole
・Partial reduction of egg tooth
・Elaboration of operculum-detaching mechanism
・Complete loss of egg tooth